Spring 1-1-2010

Modeling the Penetration of Multi-Species Aggressive Chemicals into Concrete Structures

Nattapong Damrongwiriyanupap
University of Colorado at Boulder, damrongw@colorado.edu

MODELING THE PENETRATION OF MULTI-SPECIES AGGRESSIVE CHEMICALS INTO CONCRETE STRUCTURES

By

NATTAPONG DAMRONGWIRIYANUPAP

B.Eng., Civil Engineering, Chiang Mai University, Thailand, 1998

M.Eng., Civil Engineering, Chiang Mai University, Thailand, 2001

A thesis submitted to the

Faculty of the Graduate school of the

University of Colorado in partial fulfillment

of the requirement for the degree of

Doctor of Philosophy

Department of Civil, Environmental, and Architectural Engineering

2010

This thesis entitled:

Modeling the Penetration of Multi-Species Aggressive Chemicals

into Concrete Structures

written by Nattapong Damrongwiriyanupap

has been approved for the Department of

Civil, Environmental, and Architectural Engineering

_____

Yunping Xi

_____

Victor Saouma

_____

George Hearn

_____

Sivaselvan Mettupalayam

_____

Kevin Rens

Date_____

The final copy of this thesis has been examined by the signatories, and we find that

Both the content and the form meet acceptable presentation standards of scholarly

Work in the above mentioned discipline.

Damrongwiriyanupap, Nattapong (Ph.D., Civil, Environmental, and Architectural Engineering)

Modeling the Penetration of Multi-Species Aggressive Chemicals into Concrete Structures

Thesis directed by Professor Yunping Xi

Chloride is one of the aggressive chemicals that can threat to reinforced concrete structures. This threat is aggravated by damage due to corrosion of reinforcing steel. Over the years, there have been several models related to chloride diffusion in concrete for predicting the service life of reinforced concrete structures subjected to chloride attack. These can be mathematically characterized by diffusion equation based on Fick's law and by sophisticated transport theory, the Nernst-Planck equation. In this thesis, statistical, theoretical, and experimental studies were conducted on the penetration of deicing salts into concrete structures mainly focused on chloride-induced corrosion of reinforcement.

A statistical study presented an analytic method based on a simple solution of one-dimensional diffusion equation, Fick's law, for predicting the probabilistic features of corrosion initiation time of reinforcement in concrete structures subjected to chloride environments. A theoretical modeling was conducted to investigate ion transport in concrete described based on the physical model, the Nernst-Planck equation, which included diffusion mechanism due to ionic concentration gradient and migration process due to electrostatic potential gradient. The model considered the transport of not only chloride ion but also other chemical species involved in the concrete pore solution such as hydroxyl, sodium, potassium, and calcium ions. Then, the model was extended to study the effect of moisture and temperature on the transport of these ions. The two coupled effects of moisture diffusion and chloride penetration; and heat flow and chloride penetration were incorporated in the mathematical model. Several numerical examples

were simulated and solved by the proposed models and the obtained results agreed very well with the available test data. The results also showed the basic trends of ion transport in concrete with various initial and boundary conditions. An experimental study on multi-species aggressive chemicals diffusion in concrete was performed based on chloride ponding test. The penetration rate of different chloride-based solutions related to deicers used for ice and snow control was selected as a focus of this task. The experimental results obtained from this study showed that chloride ingress into concrete is dependent on the cations associated in solutions.

DEDICATION

To my father and my mother

Kukiat and Bualee Damrongwiriyanupap

To my lovely wife and son

Anyamanee and Promkoon N. Damrongwiriyanupap

To the Damrongwiriyanupap family

To my teachers and professors

To all researchers

ACKNOWLEDGEMENTS

I would like to express my deepest appreciation and sincerest thanks to my advisor, Professor Yunping Xi, for his guidance, support, mentorship, and encouragement during my study in the University of Colorado at Boulder. His knowledge, conscientious advice, and hearty help have given me invaluable experience and professional development.

Appreciation and grateful acknowledgement is extended to Professors Kaspar Willam, Victor Saouma, George Hearn, Sivaselvan Mettupalayam, and Kevin Rens for serving on my committee, reviewing this work, and providing suggestions and comments. Also, I would like to thank Prof. Richard Regueiro for a discussion on computational techniques for finite element simulation.

I am thankful to my parents and the Damrongwiriyanupap family for their unconditional support, encouragement, and love. I cannot forget my wife who is the most important person of the last four years of my study and life in Boulder, Colorado. She has been with and enabled me to stand up throughout every difficult moment along this long road of achievement. It is your endless love, unconditional support and patience that has sustained me throughout this long journey. I would also like to thank you for the biggest present that you gave me for my birthday this year, our little angel. He is the most precious present that I have ever received in my life.

I truly thank Prof. Nipon Rattanawangcharoen at the University of Manitoba, Canada, for giving me an opportunity to study abroad. Without you, I would not have received the scholarship from the Royal Thai government. I would also like to express my appreciation for Associate Professor Chesada Kasemset, Professor Mondhol Sanguansermsri, Dr. Apiwat

Oranratnachai, Dr. Kumpon Subsomboon, and Dr. Panu Puttawong for their help and recommendations.

My sincere thanks to my colleagues and friends Dr. Soontaree Tanaraksiritavorn, Dr. Suchart Limkatanyu, Okpin Na, Dr. Keun Kwang Lee, Dr. Daehung Kang, Dr. Suwito, Dr. Wiwat Puatatsananon, Pania Meshgin, Dr. Weiping Zhang, Dr. Ayman Ababneh, Yu-Chang Liang, Moad Isteita, Ali Kosarvi, Lindsay Nataniel, Renee Koller, Marty Bucher, Dr. Jirapa and Ray Trochim, Dr. Tanarit Sakulyanonvittaya, Dr. Wasin Mallikamas, Wacharapong Ratisukpimol, Nuttachai Sirihongthong, Ratiya, Scott, Pim, and Niel Edfors, Bobbi and Todd King, Kosol and Pranom Kiatreungwattana, Amnuay, Rob, and Annika Winter, Gary and Khambot Smith, Siranee, Mark, and Nicole Thompson, Natthavuth Tamang, Elizabeth and the Howard family, as well as the Winkenbach family for their support, encouragement, and friendship.

Finally, the financial support from the Royal Thai Government and under NSF grant CMMI-0727749 to the University of Colorado and the University of New Hampshire are gratefully acknowledged.

CONTENTS

LIST OF TABLES

LIST OF FIGURES

CHAPTER 1

INTRODUCTION

1.1 Background Information

Over the last a few decades, there has been much research in the field of mass transport devoted to several areas of studies such as physics, physical chemistry, pharmacy, biological engineering, chemical engineering, and civil and structural engineering. The mass transport processes can be mathematically characterized and numerically modeled by diffusion equations based on Fick's law and/or Nernst-Planck equation depending on the degree of complexity. For example, the basic diffusion equations can be applied to concrete to solve the heat transfer problem in reinforced concrete structures under high temperatures which is one of the major causes for the collapse of two towers of World Trade Center; the penetration of chloride-contaminated groundwater into reinforced concrete tunnel (Buenfeld, 2003) which is the severe problem of long-term durability of concrete structures; the swelling of clays caused by ion exchange in their interlayer spaces (Dormieux, et al., 1995). Another important example is the failure of levee in New Orleans when Katrina struck which is predominantly controlled by water penetration into the levee.

The particular problem we are interested in this study is the penetration of aggressive chemicals such as deicing salts into non-saturated concrete structures. This is an important problem because chloride ion from the deicers is one of the major causes of the degradation in reinforced concrete structures due to steel corrosion. This is a difficult and complex problem

encountered in the field of civil engineering. For non-saturated concrete structures, more than one diffusion mechanism, i.e. moisture and ionic-species gradients, act simultaneously resulting in a coupled system of equations. In addition, the electrochemical effect considering electric balance in the ionic solution must be used together with the diffusion equations to form a closed system that can be solved by a numerical method. In this study, finite element method is employed to solve the mathematical model of coupled equations of moisture and multi-species diffusion in concrete based on the Nernst-Planck equation. The prediction models to be developed in the present study will be useful for long-term durability design and evaluation of reinforced concrete structures. On the other hand, the prediction model can also be used in practice for by management agency of infrastructure systems.

In the U.S., deicing salts are used in highways and runways approximately 15.4 million tons per year (Basu, et al., 1999). The most commonly used deicing salts are sodium chloride (NaCl), calcium chloride ($CaCl_2$), and magnesium chloride ($MgCl_2$). The use of deicing salts can cause rust out of automobile and the corrosion of reinforcing steel in concrete structures of highway roads and bridges. The other types of deicing salts alternatively used for roadways and bridge decks are calcium magnesium acetate (CMA) and potassium acetate (KAC). These are considered as the best deicers because they have the advantages of being less harmful to the environment and much less corrosive to concrete pavements, bridge decks, and automobiles (Basu, et al., 1999). However, they are more expensive than chloride-based salts, i.e. sodium chloride, calcium chloride, and magnesium chloride.

In reality, different types of deicers are used on roadways and bridges in the same time. For example, magnesium chloride solution is used before a snow storm for ice control, and calcium chloride solid salt is used during the snow storm for snow control. Sometimes, deicing

salts are mixtures of sodium chloride and calcium chloride (Mindess, et al., 2003). As a result, multiple species, Na^+, Cl^-, and Ca^{2+}, coexist on the surface of concrete and ingress into concrete simultaneously. Among them, calcium chloride has more influence on the corrosion process than sodium chloride does since it can consume hydroxyl ion (OH^-) in cement paste thus reducing the pH value of pore solution in concrete, leading to early corrosion of embedded steel in concrete.

The motivations of this research work are to study diffusion mechanisms of multi-components aggressive chemicals in saturated and non-saturated concrete, and to develop reliable prediction models for the diffusion processes and for the corrosion initiation time of embedded steels in concrete structures.

1.2 Thesis Objectives

The objectives of the thesis are to develop several prediction models for multi-species diffusions in saturated and non-saturated concrete structures; and to conduct a systematic experimental study to verify the prediction models. The prediction models developed in this study include an analytical model and several numerical models. The analytical model is derived based on an one-dimensional nonlinear chloride diffusion equation. The random variations involved in the diffusion process are considered. Both the mean and standard deviation of the corrosion initiation time are calculated by taking into account the statistic variations in the thickness of concrete cover, water-to-cement ratio, and chloride threshold value.

The numerical models developed for multiple species diffusion in concrete are based on the Nernst-Planck equation which is related to transport mechanisms of multi-components of aggressive chemicals in concrete. The Nernst-Planck equation takes into account the diffusion processes due to the concentration gradient, the ionic interactions, and moisture effect on ionic

diffusion. The state equations are developed based on a set of Nernst-Planck and electroneutrality equation. Several material models for the transport parameters related to the diffusion of chloride and moisture in concrete are incorporated in the analytical and numerical models. The governing equations and applied boundary and initial conditions are numerically solved by the finite element method. Finally, an experimental study was performed to obtain ionic concentration profiles in the concrete that are then used to verify the numerical simulation.

1.3 Thesis Organization

This thesis has 8 chapters. This chapter is an introduction describing background information of the transport processes related to chloride and multi-species diffusion in concrete structures and the content of the thesis. The remaining chapters are organized as follows:

Chapter 2 presents detailed background information and extensive literature review of transport mechanisms of chloride ions and chloride-induced corrosion in concrete structures. A detailed background of statistical analysis on chloride penetration into concrete is described. Then, the penetration of chloride ions and multi-species aggressive chemicals into concrete is presented. The corrosion mechanism of embedded steel in concrete is briefly described which is one of the long term durability of reinforced concrete structures.

Chapter 3 presents an analytic method for predicting the probabilistic features of corrosion initiation time of reinforcement in concrete structures subjected to chloride environments. By using the analytic solution of nonlinear chloride diffusion equation, and using statistic data for thickness of concrete cover, water-to-cement ratio, curing time, chloride diffusion coefficient, surface chloride concentration and chloride threshold value, both the mean and standard deviation of the corrosion initiation time can be calculated analytically.

Chapter 4 describes the diffusion mechanism of multiple components of aggressive chemicals in saturated concrete structures. This process is related to the different types of deicing salts used on highway pavements and bridges for snow and ice controls. Not only is diffusion mechanism considered but ionic interaction is also taken into account in governing equations. The mathematical model is developed based on the Nernst-Planck equation. The numerical simulations are performed by using finite element method.

Chapter 5 presents the coupling effect of multi-species deicing salts and moisture diffusion in non-saturated concrete structures. This can be numerically modeled by taking into account the coupled terms of moisture and ions in governing equations based on the Nernst-Planck equation. Then, the solutions are solved numerically by the finite element method.

Chapter 6 presents the modeling of temperature effect on multi-species deicing salts ingress into saturated concrete structures. A theoretical and computational model of multi-ions diffusion in non-isothermal concrete is proposed by accounting for the influence of temperature. The Nernst-Planck equation is modified by incorporating the coupling term due to the temperature effect on ion transport in the model. Then, the governing equations are solved numerically by using the finite element method.

Chapter 7 describes an experimental study on the effect of different types of chloride-based deicing salts penetration into concrete structures. This chapter introduces some information of deicing salts commonly used for highway pavements and bridges in the U.S. The concentration profiles of various ions were measured; the effect of different cations on the diffusion rate of chloride ion into concrete was systematically studied; and then the experimental results were used to calibrate and verify the numerical models developed in the present study.

Chapter 8 contains conclusions and recommendations for future research.

CHAPTER 2

LITERATURE REVIEW

2.1 Chloride Ions Penetration into Concrete

Chloride-induced corrosion of reinforcement is one of the deterioration mechanisms that affect the long-term durability of reinforced concrete structures. Chlorides stay in concrete internal structure in three forms. The first one is called “chemically bound chloride” which is found in the hydration products of cement paste. The second one is absorbed on the surface of gel pores which is called “physically bound chloride”. The other is known as “free chloride” which can diffuse freely through concrete pore networks. The amount of free chloride ions in concrete materials are approximately 20% - 50% of the total chloride ions (Neville, 2002). Many studies have been shown that only free chloride can affect the corrosion mechanism of reinforcement not the total chloride content.

2.1.1 Chloride-Induced Steel Reinforcement Corrosion

The corrosion of reinforcing steel is one of the severe problems which can reduce the service life of concrete structures, especially in the chloride-rich environments such as marine structures, roadways, and bridge deck subjected to deicing salts. The rust of steel bar results in cracking, spalling, and delamination of embedded steel and concrete as shown in Fig. (2.1).

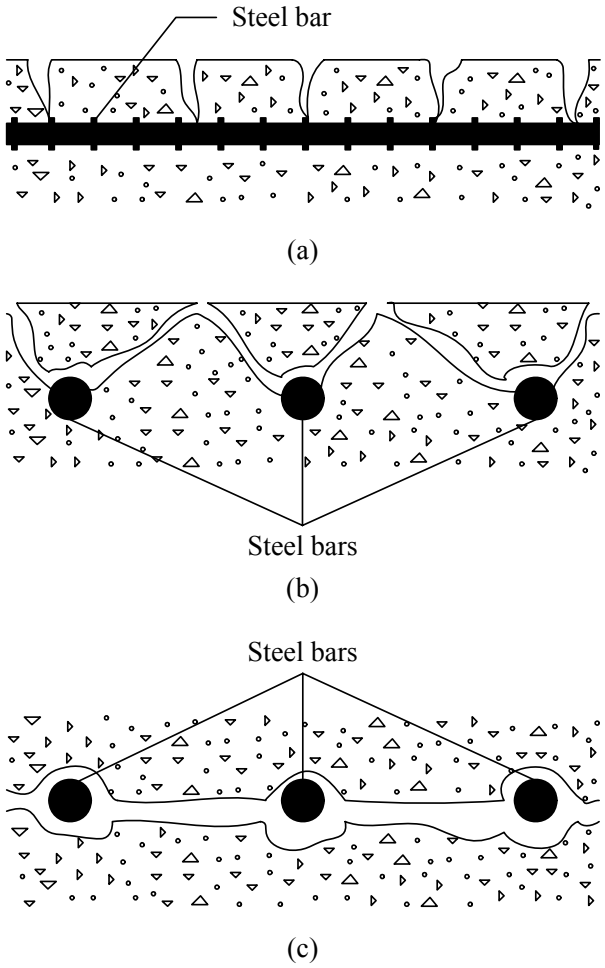

Fig. 2.1 Deterioration process of reinforced concrete structure due to corrosion of steel bars (a) cracking, (b) spalling, and (c) delamination

The deterioration process of reinforced concrete structures due to steel corrosion can be divided in three stages (Ababneh, 2002). The first stage occurs when chloride ions ingress into concrete and reach the critical value. As a result, the corrosion of steel bar starts. The second stage is dominated by the rust expansion: the volume of the rust is larger than the volume of the steel when it turns into the rust. The accumulation of rust can lead to a large volume expansion. The third stage is associated with concrete cracking. The propagation of cracks causes spalling

and delamination of the surrounding concrete. The damage of steel corrosion can affect the serviceability and load-bearing capacity of concrete structures by a reduction of cross-sectional area of steel bar and a weakness of bond strength between rebar and concrete.

Generally, the first stage may probably take place in the longest time, 15 to 20 years. The period of the second stage is dependent on the porosity of the interfacial transition zone around steel bars and it is generally shorter than the first one. The third process is the shortest one among the three stages because cracks forming around interface between rebar and concrete develop through the concrete cover in a much faster rate (Ababneh, 2002).

2.1.2 Corrosion Mechanism of Steel Reinforcement

The corrosion process starts when chloride ions reach the threshold value and then destroy the protective passivity layer. This layer forms on the surface of reinforcing steel bars during the hydration process of cement paste which is a thin protective layer of oxide. In addition, it can protect the steel bar from reacting with oxygen and water thereby preventing steel bars from formation of rust or corrosion (Neville, 2002). As the passivity of the protective layer is destroyed the electrochemical reaction of steel bars starts resulting in the damage process of the corrosion mechanism.

Anodic reaction (oxidation) of iron takes place at the anode and produces the positively charged ferrous ions (Fe^{++}) as shown in the following equation.

$$Fe \rightarrow Fe^{++} + 2e^{-} \qquad (2.1)$$

Then the ferrous ions transport into pore solution surrounding the steel bars and the free electrons, e^-, are involved in a reaction for the formation of hydroxyl ions (OH^-) that takes place at the cathode by the reaction of free electron with moisture and oxygen as described in Eq. (2.2).

$$2H_2O + O_2 + 4e^- \rightarrow 4OH^- \tag{2.2}$$

The hydroxyl ions can combine with ferrous ions to form ferrous hydroxide ($Fe(OH)_2$) as shown in the Eq. (2.3).

$$Fe^{++} + 2OH \rightarrow Fe(OH)_2 \tag{2.3}$$

A further oxidation process of ferrous hydroxide turn into the ferric hydroxide or rust:

$$4Fe(OH)_2 + 2H_2O + O_2 \rightarrow 4Fe(OH)_3 \tag{2.4}$$

The mechanism of corrosion of steel reinforcement can be depicted by Fig. (2.2).

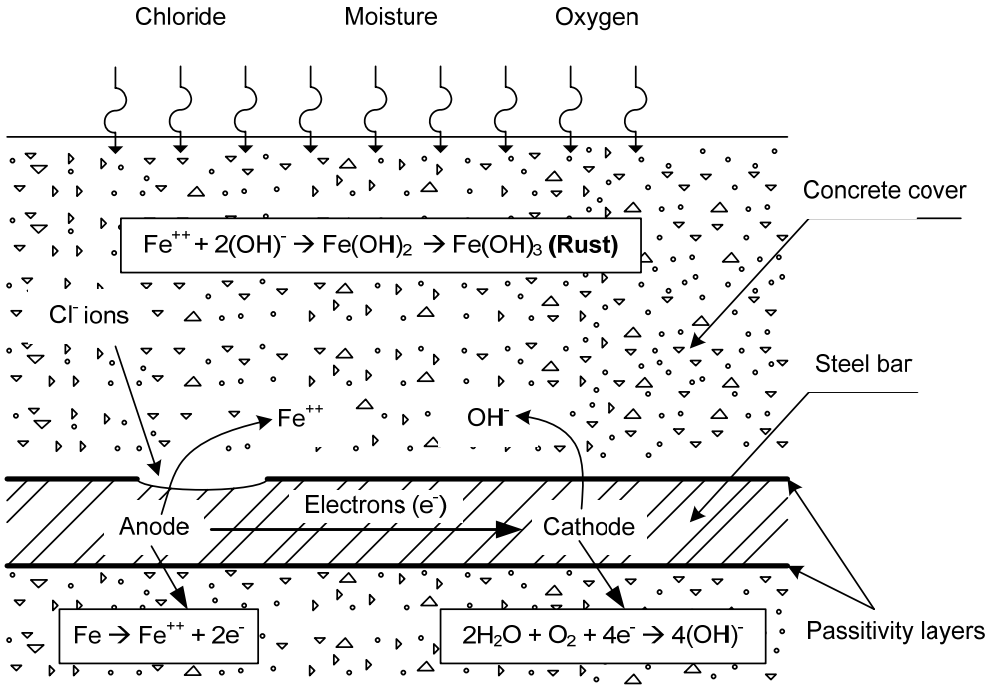

Fig. 2.2 Mechanism of chloride-induced steel bar corrosion

2.1.3 Chloride Threshold Value

The chloride threshold value can be defined as the minimum value of chloride concentration that can destroy the passivity layer of embedded steel bars. On the other hand, it can be simply described as the chloride concentration initiates the corrosion mechanism. This value can be considered in two different ways, i.e. in terms of total chloride and free chloride. Many researchers have proposed the different values of chloride threshold value as summarized in Table 2.1. The chloride threshold values shown in Table 2.1 are given in different units so there is a need to convert them to the unified unit. Based on AASHTO T 259 and AASHTO T 260, the unit of chloride content is expressed as gram of chloride per gram of concrete (g/g). Therefore, in this present study, we decided to use this unit (g/g) for numerical simulations.

The following examples are some unit calculation of chloride content in concrete. Hansson (1988) found the critical chloride content of 0.6% - 1.4% by weight of cement used in concrete. By assuming a cubic meter of concrete contains cement 300 kg; 0.6% - 1.4% of 300 kg cement is 1.8 – 4.2 kg; and then using 2,400 kg/m^3 as the density of conventional concrete, thus the critical value is 0.075% - 0.175%. Berke (1986) obtained the critical value of 0.9 – 1.0 kg of chloride per a cubic meter of concrete. As the density of concrete is 2,400 kg/m^3, then the critical chloride content in gram of chloride per gram of concrete (g/g) is 0.039% - 0.043%. The chloride threshold values in unit of gram of chloride per gram of concrete obtained by different researchers are given in the fourth column of Table 2.1.

Table 2.1 The chloride threshold values obtained from different researchers

Researchers	**Threshold values (gm of chloride / gm of cement)**	**Type of measured chloride ion**	**Threshold values (gm of chloride / gm of concrete)**
Alonson et al. (2000)	1.24% - 3.08%	Total chloride	0.155% - 0.385%
Alonso et al. (2000)	0.39% - 1.16%	Free chloride	0.049% - 0.145%
Hussain et al. (1995)	0.14% - 0.22%	Free chloride	0.0175% - 0.0275%
Thomas et al. (1990)	0.5%	Total chloride	0.0625%
Hansson (1988)	0.6% - 1.4%	Total chloride	0.075% - 0.175%
Hope and Ip (1987)	0.097% - 0.19%	Total chloride	0.012% - 0.024%
Gouda (1970)	0.6%	Total chloride	0.075%

2.2 Statistical Analysis of Chloride Penetration into Concrete Structures

Probabilistic and statistical analyses can be applied to several aspects of engineering disciplines such as risk analysis related to decision making, uncertainty conditions of design process, and the development of design procedures associated with significant factors of uncertainty (Ang and Tang, 2007). With a proper probabilistic and/or a statistical method, the performance of an engineering system can be evaluated under the influences of uncertainties. This is beneficial to our problem of chloride penetration into concrete that there are several uncertainty factors and/or random variables affecting the long-term performance of concrete structures exposed to deicing chemical. Therefore, reliable model based on statistical analysis can be employed to predict the performance and to determine the time for maintenance and rehabilitation of reinforced concrete structures subjected to chloride-rich environments.

In recent years, there are some researches devoted to probabilistic models for simulating chloride ingress into concrete. Most of these researches are based on the association of statistical chloride diffusion coefficient and surface chloride concentration incorporated in deterministic diffusion models taking into account some of uncertainty values. Kirkpatrick et al. (2002) developed a statistic model to predict the corrosion initiation time of concrete bridge deck exposed to chloride deicing salts by including the effect of statistical nature in the corrosion mechanism. The re-sampling techniques based on observed field data were implemented to the deterministic model to determine the first time to repair and rehabilitation. The collected field data were focused on surface chloride concentration, diffusion coefficient, and cover depth of 10 sample bridge decks in Virginia. To validate this model, the researchers used the collected data of historical service life of such bridge deck samples compared with their model. Furthermore, they conducted a study on the effect of changes in the specification which is one of causes

affecting the corrosion process in bridge decks. Engelund and Sorensen (1998) proposed a probabilistic model to determine the corrosion initiation of reinforced concrete structures by taking into account the parameters based on sample measurements. These parameters are concrete mix proportion, surface concentration, cover thickness, critical value of chloride concentration, and propagation of corrosion. The mean values and random variables of these factors are incorporated in the model. Another significant factor which affects the corrosion of steel bars in reinforced concrete structures was incorporated in the study by Martin-Perez et al. (2000). Their model included the effect of chloride concentration due to chloride binding capacity. Williamson et al. (2008) developed a model called "service-life model" that takes into account the probabilistic nature of significant factors of chloride diffusion by using Monte Carlo technique. This model was validated by the collected data for bridge decks constructed in Virginia from 1965 to 1968. Bentz (2003) proposed the simplified probabilistic model based on a linearized analysis method to predict the service life of concrete structures exposed to chloride chemical. Several significant factors; chloride diffusion coefficient at 28 days, relationship of diffusion coefficient and time, maximum surface chloride level, chloride threshold value, cover thickness, and propagation time period. The model was verified by modified Monte Carlo technique.

The review of the available probabilistic models show that several factors affecting the chloride penetration into concrete are incorporated in these models based on different methods of analysis. This study presents an analytic method for predicting the probabilistic features of corrosion initiation time of reinforcement in concrete structures subjected to chloride environments. By using the analytic solution of nonlinear chloride diffusion equation, and using statistic data for thickness of concrete cover, water-to-cement ratio, curing time, chloride

diffusion coefficient, surface chloride concentration, and chloride threshold value. Both the mean and standard deviation of the corrosion initiation time can be calculated analytically.

2.3 Multi-Ions Diffusion in Concrete Structures

Concrete structures subjected to aggressive chemicals can undergo various types of deterioration mechanisms. One of such aggressive chemical is sulfate solutions. Sulfate-induced damages result in swelling, spalling, and cracking in concrete (Marchand, et al., 2002). The other chemical is chloride. Deicing salts are the sources of chloride and there are many types of deicing salts commonly used for highway pavements and bridges, for example, sodium chloride (NaCl), calcium chloride ($CaCl_2$), and magnesium chloride ($MgCl_2$). Frequently, these salts are used in the same roads for ice and snow control. As a result, not only chloride ions (Cl^-) ingress into concrete, but also the others such as sodium (Na^+), calcium (Ca^{2+}), and magnesium (Mg^{2+}) can penetrate into concrete simultaneously.

In the past few years, there have been many researches on chloride penetration into reinforced concrete structures related to two types of mathematical models. The first one is empirical models based on a simple solution of one-dimensional diffusion equation. The second one is physical models related to physical and chemical transport theories (Nilsson, 2006). To prevent concrete structures from corrosion, one can improve the concrete property in penetration resistance which is related to porosity. One can also predict the corrosion initiation time by mathematical models. The prediction models can provide useful information for the structure owners and management agencies such that a proper decision can be made for repair and rehabilitation. Therefore, there is a pressing need to develop reliable prediction model.

The empirical models can be described by Fick's second law which is based on the assumption that the diffusion process of chloride ions into concrete is driven by the concentration gradient of the chloride, and it can be expressed as:

$$\frac{\partial C(x,t)}{\partial t} = D_a \frac{\partial^2 C(x,t)}{\partial x^2} \tag{2.5}$$

in which x is the depth of concrete measured from the surface, t is the exposure time, $C(x,t)$ is the chloride concentration at depth x and time t, and D_a is the apparent diffusion coefficient. If D_a is a constant, Eq. (2.5) can be solved by the simplest solution (Nilsson, 2006) with conditions of constant surface chloride concentration (C_0) and zero initial chloride content inside the sample for a one-dimensional infinite depth, which is

$$C(x,t) = C_0\left(1 - erf\frac{x}{2\sqrt{D_a t}}\right) \tag{2.6}$$

where C_0 is the surface chloride concentration and *erf (.)* is the error function. If the surface chloride concentration, apparent diffusion coefficient, and the depth of steel bar are known the chloride concentration at steel bar level at any time of exposure can be calculated by using Eq. (2.6).

The limitation of Eq. (2.6) is that the apparent diffusion coefficient, D_a, is not constant; and it is time dependent (Nilsson, 2006) and depends on many factors (Vu and Stewart, 2000; Daigle, et al., 2004). To solve this problem, some comprehensive models have been developed based on physical and chemical theories of multi-ions transport in porous media (Li and Page, 1998, 2000; Nguyen and Baroghel-Bouny, 2006; Samson and Marchand, 2007; Snyder and

Marchand, 2001; Wang, et al., 2005). According to the models, the flux of each ion in the solution can be characterized by Nernst-Planck equation in Eq. (2.7).

$$J_i = -D_i\left(\frac{\partial C_i}{\partial x} + \frac{z_i F}{RT}\frac{\partial \phi}{\partial x}C_i\right) \tag{2.7}$$

These models include the ionic interaction and chemical avtivity between ions and consider not only chloride ions but also other chemical components involved in the concrete pore solution such as OH^-, Na^+, K^+, and Ca^{2+} ions. Different from the Fick's second law models, these model involve diffusion due to ionic concentration gradient, migration mechanism due to electrstatic potential gradient, and hydrostatic pressure gradient. This can be matehmatically described as:

$$\frac{\partial C_i}{\partial t} = \frac{\partial}{\partial x}\left(D_i\frac{\partial C_i}{\partial x} + z_i D_i\frac{F}{RT}\frac{\partial \phi}{\partial x}C_i - vC_i\right), \quad (i = 1, 2, ...) \tag{2.8}$$

where C_i is the concentration, D_i is the diffusion coefficient, z_i is the charge number, F is the Faraday's constant, R is the gas constant, T is the temperature, Φ is the electrostatic potential, v is the velocity of bulk solution, and index i represents for the *i-th* species.

To solve Eq. (2.8), another relation accounted for electrostatic potential is needed. Various assumptions of electrostatic potential have been proposed. Li and Page (2000), Truc et al. (2000), and Wang et al. (2005) presented the electrostatic potential equation based on nil current in that there is no net current flow within the concrete pore solution expressed as Eq. (2.9). While, Samson and Marchand (1999, 2007) calculated the electrostatic potential by using Poisson's equation as shown in Eq. (2.10). Nguyen and Baroghel-Bouny found that electrostatic potential can be evaluated in terms of electroneutrality which can simplify the numerical simulation written as Eq. (2.11).

$$\sum_{i=1}^{n} z_i J_i = 0 \tag{2.9}$$

$$\frac{\partial^2 \phi}{\partial x^2} + \frac{F}{\varepsilon}\left(\sum_{i=1}^{n} z_i C_i + w\right) = 0 \tag{2.10}$$

$$\sum_{i=1}^{n} z_i C_i = 0 \tag{2.11}$$

In which z_i is the charge number, J_i is the flux, Φ is the electrostatic potential, ε is the permittivity of the medium, and w is a source of charge density.

Later on, Eq. (2.7) has been extended by taking into account the effect of chemical activity in the Nernst-Planck equation which is related to non-ideal solution in concrete pores. The extended Nernst-Planck equation (Samson and Marchand, 1999) can be express as:

$$J_i = -D_i\left(\frac{\partial C_i}{\partial x} + \frac{z_i F}{RT}\frac{\partial \phi}{\partial x}C_i + \frac{\partial(\ln \gamma_i)}{\partial x}C_i\right) \tag{2.12}$$

where γ_i is the chemical activity coefficient. Thus, the mass balance equation of each ionic species with an advection term can be written as:

$$\frac{\partial C_i}{\partial t} = \frac{\partial}{\partial x}\left(D_i \frac{\partial C_i}{\partial x} + z_i D_i \frac{F}{RT}\frac{\partial \phi}{\partial x}C_i + \frac{\partial(\ln \gamma_i)}{\partial x}C_i - vC_i\right), \tag{2.13}$$

$(i = 1, 2, ...)$

The multi-ionic species transport in concrete structures can be solved by coding Eq. (2.8) or Eq. (2.13) into computational model. Numerical simulations can be performed by using finite element model. In contrast to the empirical models, the comprehensive models, based on Nernst-Planck or extended Nernst-Planck equation, consider the electrochemical interaction of different ionic species, the variations of initial and boundary conditions, and material parameters can be incorporated into these models. These models have less variability than empirical models and are closer to the real conditions of concrete structures subjected to chloride environments. Therefore, these can be used to simulate and predict the chloride ingress into reinforced concrete structures more satisfactorily.

CHAPTER 3

A PROBABILISTIC PREDICTION MODEL FOR THE CORROSION INITIATION TIME OF STEEL REINFORCEMENT IN CONCRETE STRUCTURES

3.1 Introduction

Reinforced concrete structures exposed to deicing salts or coastal/marine conditions often exhibit premature deterioration and require unplanned maintenances or repairs. The major cause of the deterioration problems is chloride-induced corrosion of reinforcing steel which, because of the substantial volume increase that accompanies the transformation of iron to rust, can lead to cracking and spalling of the concrete cover. To prevent the corrosion damage, several methods have been developed including application of highly impenetrable concrete, application of waterproof membrane on the surface of concrete, and extraction chloride ions from the concrete pore solution before they reach the steel bar or before they reach the critical concentrations that can initiate the corrosion process. In order to evaluate the effectiveness of these techniques, quantitative information are needed about the factors affecting the rate of chloride penetration, the binding characteristics of chloride ions in concrete as well as factors affecting the relevant threshold concentrations.

The process of reinforcement corrosion may be divided into an initiation period, during which chloride ions are penetrating into concrete until they reach a critical or threshold level at the depth of the embedded steel; and a propagation period, during which the reinforcing steel bar is actively corroding. The initiation period is usually much longer than the propagation period.

Once the propagation period starts, it generally takes only a few years for concrete cover to crack and spall off. Hence, it is extremely important to know the length of the initiation period in order to predict the performance of a reinforced concrete structure and to schedule maintenance and repair activities of the structure.

To evaluate the corrosion initiation time of a reinforced concrete structure, the chloride penetration profile in the concrete must be predicted first. Once the chloride concentration at the depth of rebar level reaches the critical value, the initiation period can be considered as ended. There are two generic types of mathematical models that have been applied to predict chloride penetration in concrete (Nilsson, 2005), one is the chloride diffusion model based on a simple solution of the one-dimensional diffusion equation (Thomas and Jones, 1996; Boddy et al., 1999) and the other is the nonlinear transport model which considers multi-component ionic diffusion in concrete (Snyder and Marchand, 2001). Both types of models require large amount of information about boundary and initial conditions and more importantly the test data to validate material parameters in the prediction model. The initial and boundary conditions are related to the specific information of the structure, the service environment, and the concrete used in the structure. The test data normally consist of concrete mix design parameters, and measured chloride penetration profiles obtained from the structure in service or from laboratory specimens.

The initial and boundary condition and the material parameters in the prediction model are not constant but random variables, which can be affected by many factors including physical and chemical properties of concrete materials (cement, aggregate, water, and additives used in concrete) as well as the environmental conditions. The concrete mix design parameters vary depending on quality control methods used in the ready mix concrete company and the installation contractor on the construction site. The environmental conditions are random

variables with large fluctuations on a daily or hourly basis. The environmental conditions not only serve as boundary conditions for the prediction model but also affect properties of concrete significantly, this is because the hydration of Portland cement is a chemical process that continues after the structure is put into service and the hydration process depends on humidity level of the environment. This suggests that the outputs of prediction models used for corrosion initiation time of reinforced concrete structures are not deterministic but random in nature. Therefore, it is important to combine the deterministic prediction models with probability analysis based on statistical data. The combined analysis will be better than the deterministic analysis of just using single mean values of the random variables.

There have been some efforts to develop probabilistic models considering the random variables for predicting chloride penetration in concrete (Daigle et al., 2004; Engelund and Sorensen, 1998; Kirkpatrick et al., 2002; Bentz, 2003). Most of these models were simple extensions of the deterministic diffusion models based on the concepts of "statistical" chloride diffusion coefficient and "statistical" surface chloride concentration to take into account some of the modeling uncertainty. Such statistical models enabled the inclusion of uncertainties in the prediction model and material parameters, which lead to more reliable prediction of the chloride concentration in concrete when compared to conventional deterministic diffusion models.

In this study, we will re-formulate the chloride diffusion model based on the simple solution of one-dimensional diffusion equation to include (1) the binding capacity of chlorides; and (2) material models for chloride diffusion coefficient. When chloride ions enter porous concrete, some of them are bound on the pore wall, and others can diffuse in the pore structure. The chloride binding capacity is the ratio of bounded chloride to the total chloride. In the literature, it is evident that chloride binding capacity has significant influence on the chloride

penetration process in concrete (Martin-Perez, 2000; Li and Page, 2000). Similar to other material parameters involved in the process, chloride binding capacity exhibits randomness. One of the focuses of this paper is to develop a simple method which can be used to provide statistical features of the chloride binding capacity and their effect on the corrosion initiation period. The other focus is to express the chloride diffusion coefficient in terms of concrete mix design and processing parameters so that the effects of statistical variations of the mix design and processing parameters on the corrosion initiation period can be evaluated.

The statistical variation of corrosion initiation period will be analyzed based on the first and second order statistical information of the influential random variables (such as concrete mix design parameters, etc.) The distributions of the random variables are not involved in the analysis, which is advantageous in that most of statistical distributions of the random variables are not known in the practice. It is also important to point out that the simple one-dimensional diffusion equation is used in the present paper as an example to show the feasibility of the approach, because analytical solution is available for the one-dimensional problem. The same approach can definitely be used in nonlinear multiple dimensional diffusion analysis with a proper numerical simulation method.

3.2 Penetration of Chloride Ions in Concrete

If the chemical reactions of chloride ions with other ionic species in pore solution and pore surfaces are neglected, the concentration of chloride ions at any time and any location can be determined by using the equation of mass balance in the unit volume of concrete as follows,

$$\frac{\partial C_T}{\partial t} = -\nabla J \tag{3.1}$$

where C_T is the concentration of total chloride ions, t is the time, and J is the flux of free chloride ions in concrete pore solution. According to Fick's first law, the flux of free chloride ions can be expressed as follows,

$$J = -D_a \nabla C_f \tag{3.2}$$

where D_a is the so-called apparent diffusion coefficient of the free chloride ions and C_f is the concentration of free chloride ions in the pore solution. The concentration of total chloride ions is the sum of the free chlorides and bound chlorides. Based on experimentally obtained data the concentration of bound chlorides can be expressed in terms of the concentration of free chlorides as follows,

$$C_b = \frac{\alpha C_f}{w(1+\beta C_f)} \tag{3.3}$$

where $C_b = C_T - C_f$ is the concentration of bound chlorides, w is the content of moisture in which diffusion occurs expressed per unit weight of cement, α and β are the constants determined by experiments. Substituting Eqs. (3.2) and (3.3) into (3.1), yields,

$$\frac{\partial}{\partial t}\left[C_f + \frac{\alpha C_f}{w(1+\beta C_f)} \right] = D_a \nabla^2 C_f \tag{3.4}$$

Let

$$t = \tau \left[1 + \frac{\alpha}{w(1+\beta C_f)} \right] \tag{3.5}$$

where τ is a new time variable. Using Eq. (3.5), Eq. (3.4) can be approximately expressed as,

$$\frac{\partial C_f}{\partial \tau} = D_a \nabla^2 C_f \tag{3.6}$$

The solution of Eq. (3.6) for a one-dimensional problem of infinite depth can be expressed as,

$$C_f(x,\tau) = C_o erfc\left(\frac{x}{2\sqrt{D_a \tau}}\right) \tag{3.7}$$

where C_o is the concentration of chloride ions at the surface (x = 0) and *erfc*(.) is the complementary error function. Using Eq. (3.5), Eq. (3.7) can be expressed as,

$$C_f(x,t) = C_o erfc\left(\frac{x}{2\sqrt{D_a t}}\sqrt{1+\frac{\alpha}{w(1+\beta C_f)}}\right) \tag{3.8}$$

The analytical solution, Eq. (3.7), would be accurate if the modified time, τ, in Eq. (3.6) were independent of the concentration C_f. However, in the present problem, the modified time, τ, is dependent on C_f, which can be seen from Eq. (3.5). Therefore, Eq. (3.8) is not the exact solution of Eq. (3.4), but an approximation of the solution of Eq. (3.4). In order to examine the accuracy of the approximate solution, we used a numerical method (Crank-Nicolson finite difference method) to solve for Eq. (3.4) and then compare the solution of the numerical method with the approximate method, Eq. (3.8). Fig. 3.1 graphically shows the comparisons between the numerical solution and the approximate solution for two different diffusion coefficients at three different times. It is evident from the figure that the present approximate solution is well

acceptable. It is important to point out that Eq. (3.8) is valuable in the present study because it is an analytic solution and it can be used in later sections for deriving analytic probabilistic solutions of the corrosion initiation time.

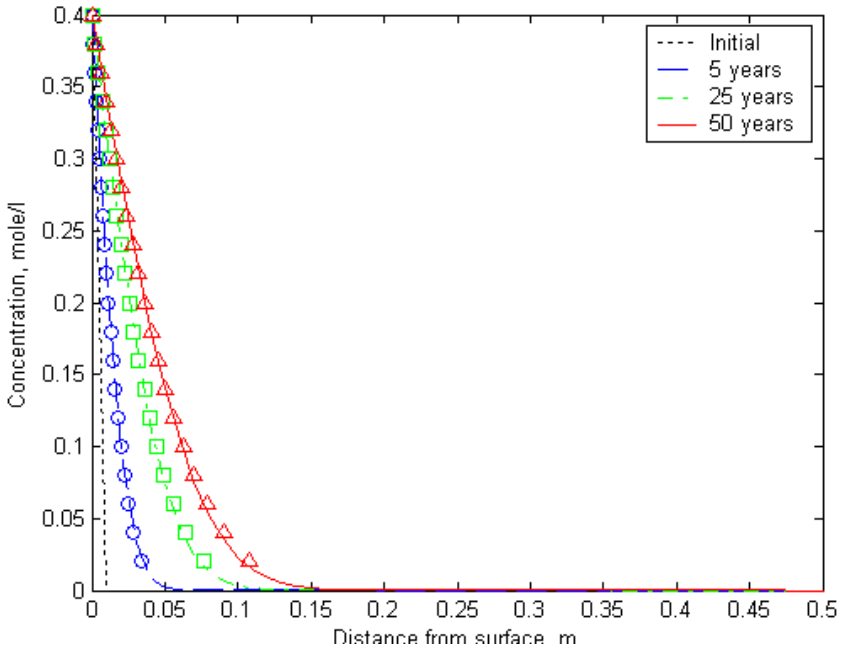

(a)

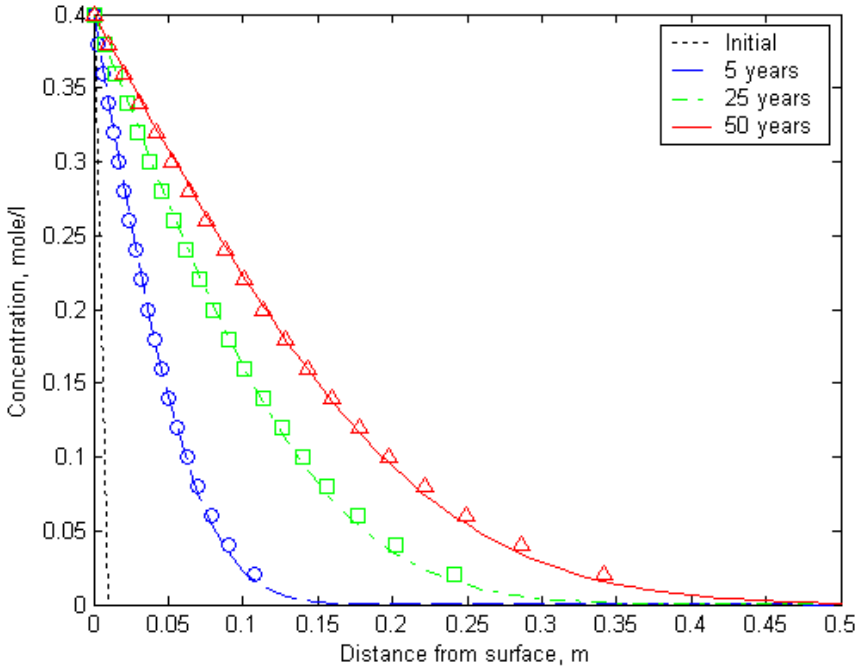

(b)

Fig. 3.1 Comparison of chloride concentration profiles obtained from numerical solution of Eq. (3.4) given by lines and simplified solution of Eq. (3.8) given by symbols at three times (w = 0.3, α = 0.42, β = 0.8 l/mole, C_s = 0.4 mole/l). (a) $D_a = 2.0\text{x}10^{-12}$ m^2/s and (b) $D_a = 20\text{x}10^{-12}$ m^2/s

Note that both sides of Eq. (3.8) involve C_f. In the practice, in order to obtain a C_f at a certain depth x and time t, one has to solve the nonlinear Eq. (3.8). However, the corrosion of reinforcing steel is initiated when the concentration of free chloride ions at the depth of steel exceeds a threshold value, thus the corrosion initiation time can be obtained by letting $x = d$ and $C_f = C_{f,th}$ in Eq. (3.8), that yields,

$$t_{corr} = \frac{d^2\left[1+\dfrac{\alpha}{w(1+\beta C_{f,th})}\right]}{4D_a\left[erfc^{-1}\left(\dfrac{C_{f,th}}{C_o}\right)\right]^2} = \frac{d^2\left(1+\dfrac{C_{b,th}}{C_{f,th}}\right)}{4D_a\left[erfc^{-1}\left(\dfrac{C_{f,th}}{C_o}\right)\right]^2} \tag{3.9}$$

where d is the depth of the concrete cover, and $C_{f,th}$ is the critical concentration of free chloride ions, $C_{b,th}$ is the concentration of bound chloride ions corresponding to $C_{f,th}$. For given values of d, D_a, $C_{b,th}/C_{f,th}$ and $C_{f,th}/C_o$, one can use Eq. (3.9) to calculate the time when the corrosion of reinforcement is initiated. As an example, Fig. 2 plots the curves of the corrosion initiation time against the concrete cover when the values of the other parameters are given. The figure shows that, the thicker of the concrete cover, the smaller the diffusion coefficient, the more the chlorides are bounded and the longer the corrosion initiation time.

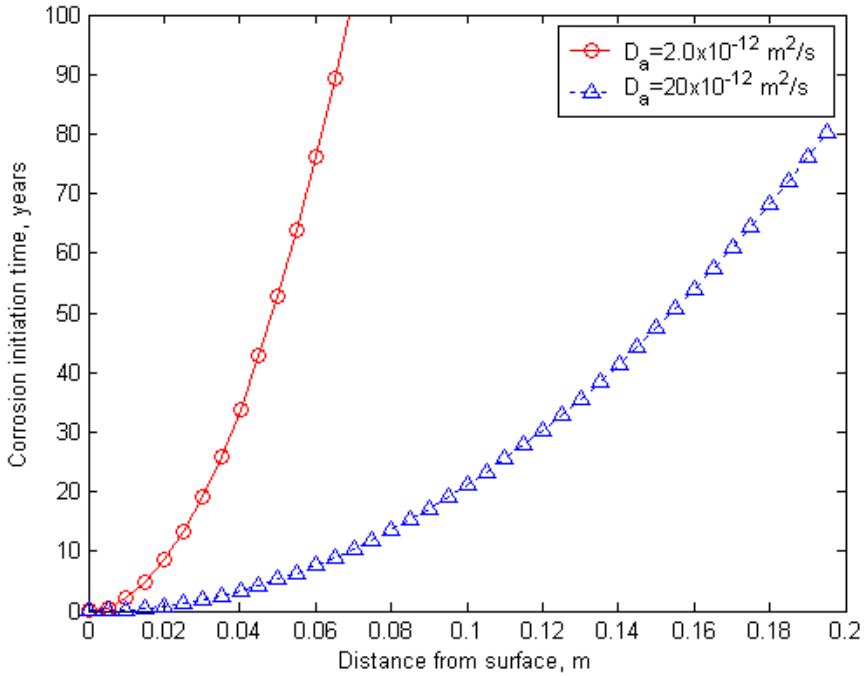

(a)

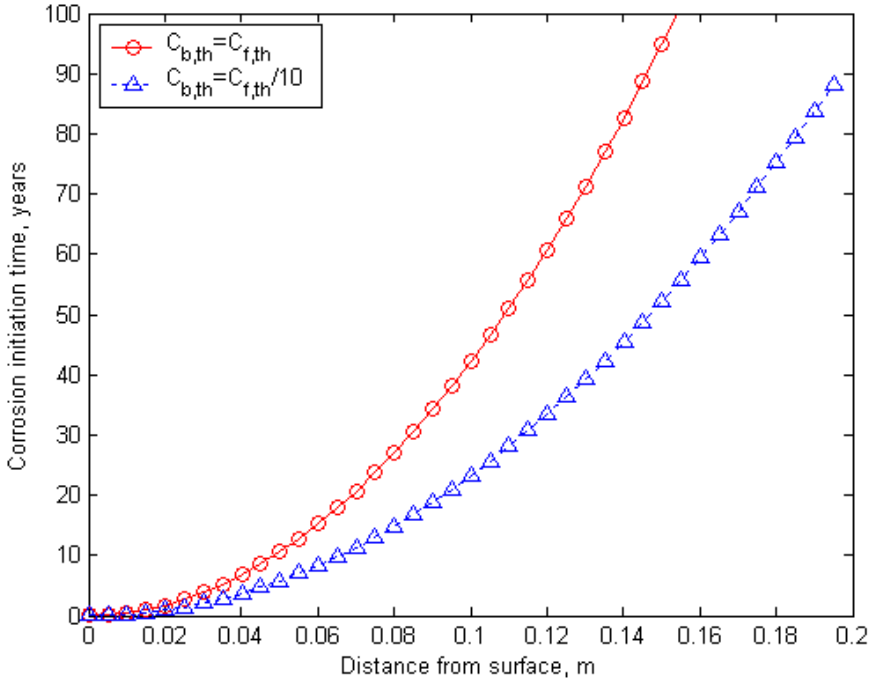

(b)

Fig. 3.2 Prediction of corrosion initiation time: (a) $C_{f,th}$ = 1.35 kg/m^3, $C_{b,th}$ = 1.35 kg/m^3, C_o = 3.5 kg/m^3. (b) $C_{f,th}$ = 1.35 kg/m^3, C_o = 3.5 kg/m^3, D_a = 10x10^{-12} m^2/s

The apparent diffusion coefficient of the free chloride ions, D_a, in Eq. (3.9) can be obtained from a model developed by Xi and Bazant (1999),

$$D_a = \left\{\left[\frac{1}{4}+\frac{28-t_0}{300}\right](w/c)^{6.55}+\frac{(28-t_0)}{62,500}\right\}.\frac{2\left[1-(V_p-V_p^c)\right]}{S^2}\left(V_p-V_p^c\right)^f\left[1-k_{ion}(C_f)^m\right] \tag{3.10}$$

where t_0 = curing time; w/c = water-to-cement ratio; m = 0.5; k_{ion} = $\sqrt{70}$; f = 4.2; V_p^c = 3%; S = internal surface area of cement paste which can be estimated by the monolayer capacity V_m of

adsorption isotherm of cement paste since V_m is proportional to S (Xi et al., 1994a); V_p = porosity of cement paste and can be approximately estimated by using the adsorption isotherm at saturation. Eq. (3.10) shows the general effects of various parameters on the diffusion coefficient. For example, when w/c increases, the diffusion coefficient increases; with a longer curing time, the diffusion process is slower; and when the concentration of free chloride is higher the diffusion coefficient is lower (called concentration effect).

From Fig. 3, one can see that the effect of water-to-cement ratio (*w/c*) and curing times (t_0) on apparent diffusion coefficient. The higher *w/c*, the higher apparent diffusion coefficient. This is because porosity of cement paste goes up with increasing *w/c*, and the rate of chloride penetration depends on the porosity. One can also see from the figure that at a constant *w/c*, the longer curing time, the lower apparent diffusion coefficient. This is due to the fact that degree of hydration is a function of time. With a longer during time, the maturity of the microstructure of cement paste is higher, and thus the diffusion coefficient of the concrete is lower.

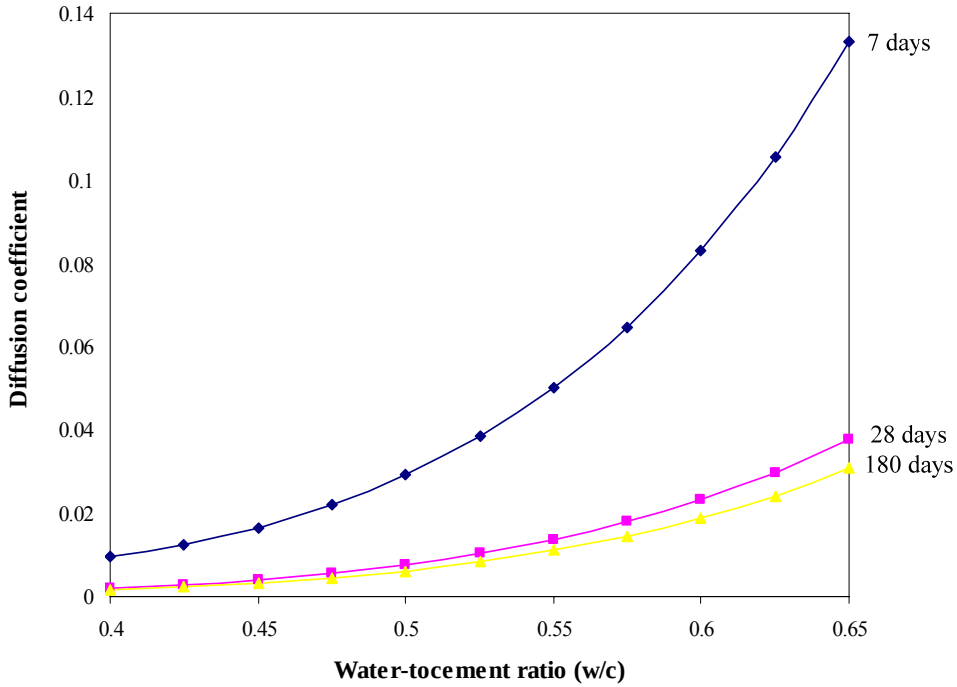

Fig. 3.3 Diffusion coefficient of concrete at various water-to-cement ratio and curing times

Substituting Eq. (3.10) into Eq. (3.9) yields

$$t_{corr} = \frac{d^2\left(1+\frac{C_{b,th}}{C_{f,th}}\right)}{4\left\{\left[\frac{1}{4}+\frac{28-t_0}{300}\right](w/c)^{6.55}+\frac{(28-t_0)}{62,500}\right\}.\frac{2\left[1-(V_p-V_p^c)\right]}{S^2}\left(V_p-V_p^c\right)^f\left[1-k_{ion}(C_f)^m\right].\left[erfc^{-1}\left(\frac{C_{f,th}}{C_0}\right)\right]^2} \tag{3.11}$$

Eq. (3.11) shows the general effects of various parameters on the corrosion initiation time. Fig. 3.4 shows the effect of *w/c* and the penetration time on chloride concentration at the depth of 2 cm. For example, for a concrete with w/c = 0.55 and 28 days of curing, the chloride concentration at 2 cm depth is about 10g/L (in the pore solution) after 500 days of penetration. The influence of curing time (t_0) on chloride concentration is shown in Fig. 3.5. This figure

shows the variation of chloride concentration at different curing times. It is shown that the longer curing time, the lower chloride concentration at a fixed depth. As discussed earlier, this is due to the continued hydration reactions between cement and water, which make the microstructure of cement paste more mature and thus the resistance to the chloride penetration is higher.

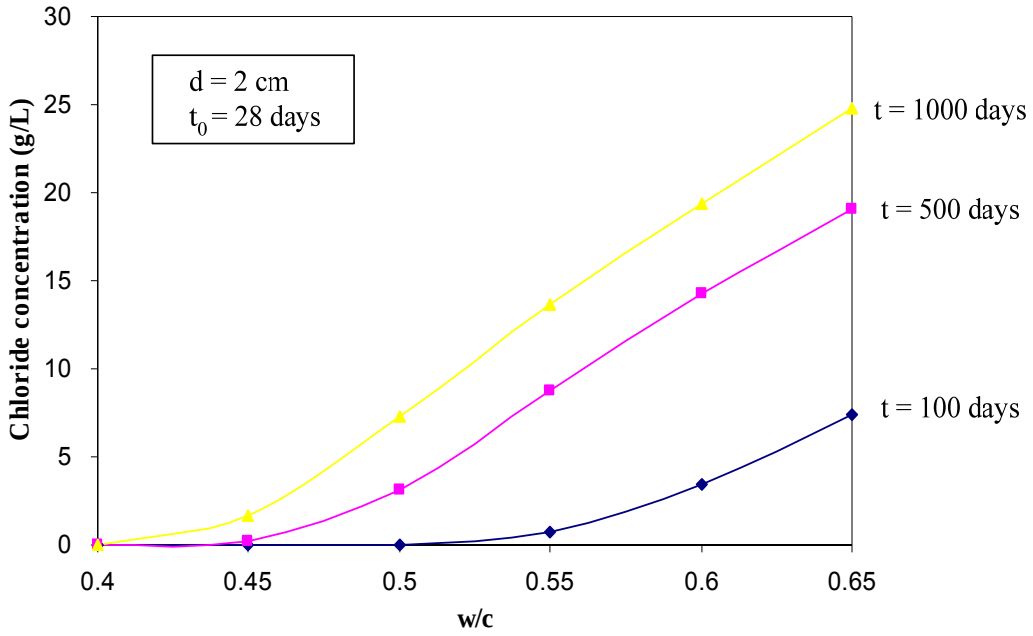

Fig. 3.4 Effect of w/c and penetration time on chloride concentration at depth d = 2 cm

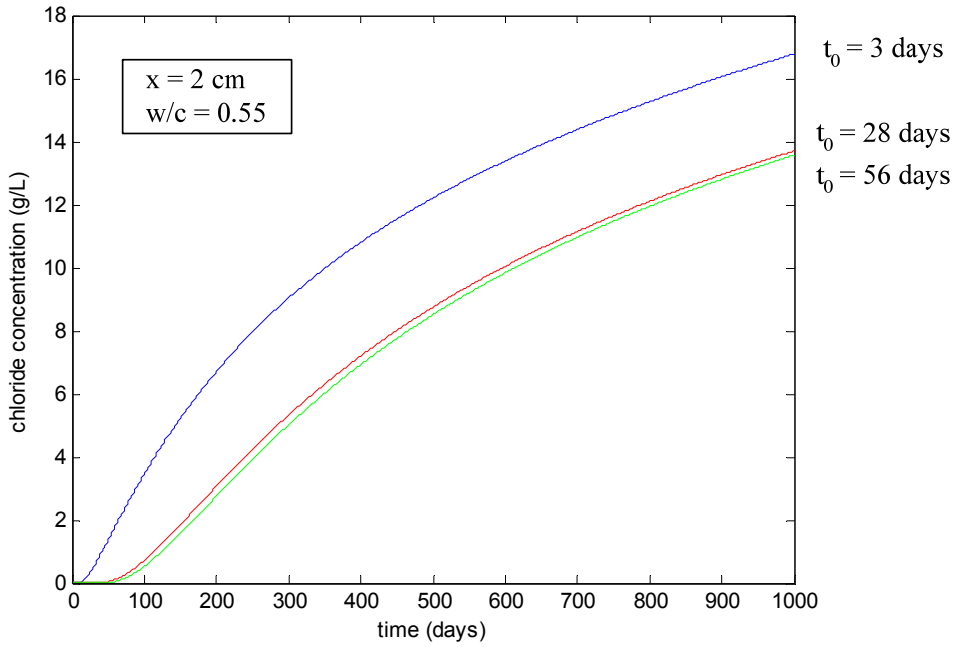

Fig. 3.5 Effect of curing time (t_0) on chloride concentration at depth d = 2 cm

3.3 Probabilistic Analysis of the Corrosion Initiation Time

The parameters, d, D_a, w/c, t_0, $C_{b,th}/C_{f,th}$ and $C_{f,th}/C_o$ in Eq. (3.11) are random variables. To predict the variation in service life of a structure due to variations in material characteristics, cover depth and the aggressiveness of environments, one has to consider random variations of these parameters (Li and Page, 2000; Duprat, 2007; Engelund et al., 1995). This can be done in three different ways. The first one is to consider the Eq. (3.4) as a stochastic partial differential equation with both random coefficients, and random initial and boundary conditions. The second one is to use Eq. (3.9) or (3.11) to assess the random variation of corrosion initiation time with the random variables d, D_a, w/c, t_0, $C_{b,th}/C_{f,th}$ and $C_{f,th}/C_o$. This method is feasible only when the statistical distributions of the random variables are available. The third one is to evaluate the

mean value and standard deviation of the corrosion initiation time based on the mean values and standard deviations of the random variables. In our case, the distributions of the random variables d, D_a, w/c, t_0, $C_{b,th}/C_{f,th}$ and $C_{f,th}/C_o$ are not available (or not all of them are available), therefore, only the third method is employed in this study.

According to Eq. (3.9), the standard deviation of the corrosion initiation time is a function of four random variables: d, D_a, $C_1 = C_{b,th}/C_{f,th}$ and $C_2 = C_{f,th}/C_o$. Among the four variable, d is related to the geometry of the structure; D_a is a transport property of concrete; $C_1 = C_{b,th}/C_{f,th}$ depends on the ratio of the free and bound chloride in concrete; and $C_2 = C_{f,th}/C_o$ represents the threshold free chloride content in the concrete and the initial chloride content (mainly from the mixing water used for the concrete). It should be pointed out that, $C_{b,th}$, $C_{f,th}$, and C_o are not three independent random variables. The bound chlorides come from the free chlorides, and the critical chloride concentration is obtained only when there is a surface chloride concentration. Thus, these three variables are treated as two ratios, and the two ratios may be considered as independent. Together, the four parameters d, D_a, C_1 and C_2 are considered as interdependent random variables, then the standard deviation of the corrosion initiation time can be calculated as follows (Benjamin and Cornell, 1970; Clifton, 1993; Kirkpatrick et al., 2002),

$$\sigma_t^2 = \left(\frac{\partial t_{corr}}{\partial d}\sigma_d\right)^2 + \left(\frac{\partial t_{corr}}{\partial D_a}\sigma_D\right)^2 + \left(\frac{\partial t_{corr}}{\partial C_1}\sigma_{C_1}\right)^2 + \left(\frac{\partial t_{corr}}{\partial C_2}\sigma_{C_2}\right)^2 \qquad (3.12)$$

in which σ_k is the standard deviation of the parameter k, and all partial derivatives can be obtained from Eq. (3.9). This equation shows the effect of the four random variables on the corrosion initiation time. Furthermore, the transport parameter D_a is a function of concrete material parameter, w/c, and curing condition, t_0, as shown in Eqs. (3.10) and (3.11). To take

into account the effect of water-to-cement ratio and curing time on the diffusion coefficient, Eq. (3.12) can be further expanded as,

$$\sigma_t^2 = \left(\frac{\partial t_{corr}}{\partial d}\sigma_d\right)^2 + \left(\frac{\partial t_{corr}}{\partial (w/c)}\sigma_{(w/c)}\right)^2 + \left(\frac{\partial t_{corr}}{\partial t_0}\sigma_{t_0}\right)^2 + \left(\frac{\partial t_{corr}}{\partial C_1}\sigma_{C_1}\right)^2 + \left(\frac{\partial t_{corr}}{\partial C_2}\sigma_{C_2}\right)^2 \qquad (3.13)$$

The mutual independency among water-to-cement ratio, curing time, and the other four variables are considered as valid for Eq. (3.13). All partial differentials of t_{corr} with respect to individual random parameter are given as follows (see appendix A for the derivation of Eq. (3.16), and appendix B for the derivation of Eqs. (3.18) and (3.19)). This equation shows the effect of the five random variables on the corrosion initiation time.

$$\frac{\partial t_{corr}}{\partial d} = \frac{2t_{corr}}{d} \qquad (3.14)$$

$$\frac{\partial t_{corr}}{\partial C_1} = \frac{t_{corr}}{1+C_1} \qquad (3.15)$$

$$\frac{\partial t_{corr}}{\partial C_2} = \frac{\sqrt{\pi} t_{corr}}{erfc^{-1}(C_2)} \exp\left[\left(erfc^{-1}(C_2)\right)^2\right] \qquad (3.16)$$

$$\frac{\partial t_{corr}}{\partial D_a} = -\frac{t_{corr}}{D_a} \qquad (3.17)$$

$$\frac{\partial t_{corr}}{\partial (w/c)} = \frac{-6.55 t_{corr} (w/c)^{5.55} \left[\frac{1}{4} + \frac{(28 - t_0)}{300} \right]}{\left\{ \left[\frac{1}{4} + \frac{(28 - t_0)}{300} \right] (w/c)^{6.55} + \frac{(28 - t_0)}{62,500} \right\}} \tag{3.18}$$

$$\frac{\partial t_{corr}}{\partial t_0} = \frac{t_{corr} \left[\frac{1}{62,500} + \frac{(w/c)^{6.55}}{300} \right]}{\left\{ \left[\frac{1}{4} + \frac{(28 - t_0)}{300} \right] (w/c)^{6.55} + \frac{(28 - t_0)}{62,500} \right\}} \tag{3.19}$$

It is obvious that if the mean and standard deviation of each parameter are known then the mean and standard deviation of the corrosion initiation time can be determined directly using Eq. (3.12) for the four random variables or Eq. (3.13) for the five random variables.

Table 3.1 shows the results of two examples using Eq. (3.12). The mean values and standard deviations for concrete cover and diffusion coefficient are similar to those published in literature (Kirkpatrick et al., 2002), while for $C_{b,th}/C_{f,th}$ and $C_{f,th}/C_o$ they are assumed based on the analysis of available data. One can see that small variations in the input random variables lead to large variation of the corrosion initiation time. Table 3.2 shows the results of two examples using Eq. (3.13). One can see that small variations in the input random variables lead to even larger variation of the corrosion initiation time comparing with Table 3.1. This is because the water-cement ratio (w/c) has very strong effect on transport properties of concrete.

In order to find which random variable has the dominant effect on corrosion initiation time, the effects of these random variables on corrosion initiation time are evaluated individually in that only one single parameter is considered as a random variable and the others are fixed (as the mean values). Fig. 3.6 shows that the influence of the five random variables (d, D_a, w/c, t_0,

$C_{b,th}/C_{f,th}$ and $C_{f,th}/C_o$) on the standard deviation of the corrosion initial time. Uncertainty values of the parameters are provided in Table 3.3.

Table 3.1 Mean values and standard deviations of the four parameters and corrosion initiation time

Parameter	Example 1		Example 2	
	Mean	Standard deviation	Mean	Standard deviation
d, mm	40	5.0	50	7.0
$\underline{\underline{D_a}}$, mm^2/year	12	8.0	50	20
$C_{b,th}$ / $C_{f,th}$	1.0	0.3	0.8	0.4
$C_{f,th}$ / C_o	0.2	0.1	0.30	0.2
t_{corr}, years	81	83	42	94.6

Table 3.2 Mean values and standard deviations of the five parameters and corrosion initiation time

Parameter	Example 1		Example 2	
	Mean	Standard deviation	Mean	Standard deviation
d, mm	40	5.0	50	7.0
$C_{b,th}$ / $C_{f,th}$	1.0	0.3	0.8	0.4
$C_{f,th}$ / C_o	0.2	0.1	0.30	0.2
w/c	0.5	0.2	0.5	0.15
t_0	28	4	28	7
t_{corr}, years	81	221.5	42	124.6

The results shown in Fig. 3.6 indicated that the standard deviation of the corrosion initiation time is mainly controlled by the variations of the water-to-cement ratio (w/c) and the ratio of critical free chloride concentration to surface chloride concentration ($C_{f,th}/C_o$). On the other hand, the variations of curing time (t_0), the depth of the concrete cover (d), and the ratio of critical bound chloride to critical free chloride ($C_{b,th}/C_{f,th}$) have relatively smaller influence on the standard deviation of the corrosion initiation time.

Table 3.3 The data of uncertainty values of each parameter

Parameter	Reference value	Uncertainty value
σ_d	7	+ (1% - 10%)
$\sigma_{(w/c)}$	0.15	+ (1% - 10%)
σ_{t_0}	7	+ (1% - 10%)
σ_{C_1}	0.4	+ (1% - 10%)
σ_{C_2}	0.2	+ (1% - 10%)
d	7	constant
w/c	0.5	constant
t_0	28	constant
$C_{b,th}$ / $C_{f,th}$	0.8	constant
$C_{f,th}$ / C_o	0.3	constant

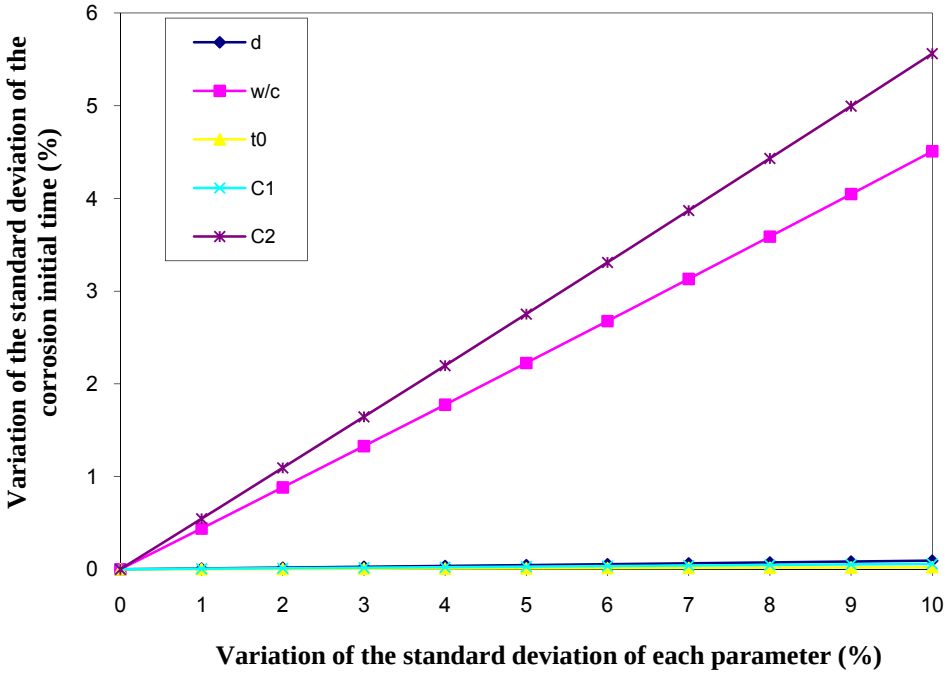

Fig. 3.6 Effect of uncertainty values of each parameter on the standard deviation of the corrosion initial time

3.4 Conclusions

1. A nonlinear diffusion model is presented for predicting the corrosion initiation time of reinforcement in concrete structures subjected to chloride environments. The total chloride content in concrete is divided into bound chloride and free chloride. Only the free chloride can diffuse in concrete.

2. By considering the random variables involved in the nonlinear diffusion model to be independent, an analytical probabilistic solution is derived for calculating the mean and standard deviation of the corrosion imitation time based on the means and standard deviations of the

random variable, which include concrete cover, water-to-cement ratio of concrete, curing time of concrete, surface chloride concentration, and chloride threshold value.

3. Among all random variables considered, the water-to-cement ratio of concrete and the ratio of critical chloride concentration to surface chloride concentration play more important roles than other variables in terms of the variation of corrosion initiation time.

4. Compared to various existing probabilistic models, the present method has several advantages: all equations are based on analytical solutions, there are no numerical simulations needed, and the method is very simple and thus very easy for practical applications.

CHAPTER 4

MULTI-IONIC SPECIES DIFFUSION IN SATURATED CONCRETE

4.1 Introduction

Chloride-induced corrosion in concrete is one of severe problems affecting the durability of concrete structures as the corrosion takes place when chloride ions reach the critical value and the passivity layer is destroyed. The rust deposit around the interface between embedded steel and surrounding concrete has larger volume than the steel consumed to form the rust. The volume expansion leads to cracking, spalling, and delamination of concrete cover in the reinforced concrete structures. In addition, the corrosion damage may significantly reduce the load-bearing capacity of the reinforced concrete structure by a reduction of cross-sectional area of steel bar. In order to understand the mechanisms of the chloride-induced corrosion and to predict the long-term performance of the structure, mathematical models characterizing the deterioration process need to be developed. As described earlier, chloride penetration into concrete is the first and the longest stage among the three stages of the deterioration process. Therefore, it is important to understand the penetration mechanisms of the chloride in concrete. On the other hand, chloride is not the only ions that diffuse in concrete, and it is important to understand the effect of other ions on the penetration of the chloride. In this chapter, a prediction model for simulating chloride ingress into concrete structures based on multi-ions transport theory will be presented.

Deicing salts are major sources of chloride ions. Sodium chloride, calcium chloride, and magnesium chloride are the types of deicing salts commonly used for highway roads and bridges. Frequently, different types of deicers are applied to the same area for ice and snow control. For example, magnesium chloride solution is used before a snow storm for ice control, and calcium chloride solid salt is used during the snow storm for snow control. As a result, multiple components of salts co-exist on the surface and ingress into concrete simultaneously. Therefore, the penetration rate of chloride is dominant not only by diffusion mechanism due to concentration gradient of the chloride ions but also by the ionic interaction among the chloride and other ions. In addition to the other ions co-exist in deicers with chloride ions, this study also takes into account the ions exist in the concrete pore solution prior to the presence of deicers, i.e. hydroxyl ions (OH^-), sodium ions (Na^+), and potassium ions (K^+).

In recent years, many researchers have investigated the penetration of chloride into concrete structures. There have been two ways for formulating the mathematical models of chloride penetration into concrete. One is based on empirical model, i.e. Fick's second law (Saetta et al., 1993; Frey et al., 1994; Wee et al., 1997; Swaddiwudhipong et al., 2000). The other is based on the transport theory of multi-ions that is Nernst-Planck equation taking into account the physical and chemical factors related to chloride and other ions in electrolyte diffusion in concrete. Mathematical models developed based on this approach can be used to describe and simulate the transport mechanism of multiple ions in cement-based materials. These include the diffusion, electrical migration, and chemical activity of chloride ions and ions in concrete pore solution.

Nguyen and Baroghel-Bouny (2006) developed a mathematical and numerical model based on Nernst-Planck equation to predict the chloride ingress into saturated concrete. Their model included the experimental study to determine the chloride diffusion coefficients and chloride binding capacity. The electroneutrality assumption was employed to calculate the balance of ionic interaction between ions in concrete pore solution. Then, the numerical results were validated by test data obtained from concrete samples under different exposure conditions. Li and Page (2000) and Wang et al. (2000) proposed a finite element model of chloride removal from concrete. This model was developed based on the Nernst-Planck equation related to the ionic interaction of multi-ions in concrete pore solution and the adsorption and desorption of ions between the solid and liquid phases. The study of influences of boundary conditions, porosity, and tortuosity of concrete were incorporated in the model. Later on, Wang et al. (2005) developed their previous mathematical model by incorporating the convection of pore solution in the model to predict the chloride penetration into concrete. The electrostatic potential is calculated by using the nil current assumption. Numerical results were compared with the solution obtained from Fick's second law. Samson et al. (1999) presented the mathematical model of ions diffusion in porous media. This model was developed based on Nernst-Planck equation. Poisson's equation was used to evaluate the electrical coupling between ions. These ions were assumed in an ideal solution (no chemical activity effects were considered). The numerical results were obtained by using 1D finite element method. Then, Samson and Marchand (1999) extended the model to account for the chemical activity effects by considering ions in non-ideal solution. The mathematical model was formulated by taking into account the chemical activity terms in the governing equation. Lately, Samson and Marchand (2007) proposed the transport model of ions in unsaturated cement-based materials related to external

sulfate or calcium and hydroxide leaching. The mathematical model was developed based on the set of Nernst-Planck/Poisson equation by taking into account the diffusion, electrical coupling, chemical activity, and advection mechanisms. The model was studied in the isothermal condition. The numerical simulations were performed by using 1D finite element method.

In this chapter, a comprehensive model of chloride penetration into saturated concrete is developed. The mathematical model is formulated based on Nernst-Planck equation and then nil current assumption is presented to determine the interaction between ions that is induced electrostatic potential. This is assumed that there is no current for electrical coupling between ions. The physical and chemical factors related to chloride and other ions ingress into concrete are taken into account. These material parameters include binding capacity of chloride and calcium ions; and the diffusion coefficient of chloride ions developed by Xi and Bazant (1999). Different types of deicing salts, calcium chloride and sodium chloride, are applied as boundary conditions of a concrete structure and ions in concrete pore solution, hydroxyl, sodium, and potassium ions, are accounted for the mathematical model. Finally, the numerical simulations are performed by using finite element method.

4.2 Basic Formulation of Governing Equations

The flux of each ions transport in an ideal solution in porous media based on the Nernst-Planck equation without considering the chemical activity effects can be described as:

$$J_i = -D_i \nabla C_i - z_i D_i \left(\frac{F}{RT} \nabla \phi \right) C_i \qquad (4.1)$$

where J_i is the flux, D_i is the diffusion coefficient, C_i is the concentration, z_i is the charge number, F is the Faraday's constant, R is the gas constant, T is the temperature, Φ is the electrostatic potential, and index i represents *i-th* species. The mass balance equations for each ionic species can be expressed as:

$$\frac{\partial C_i}{\partial t} = -\nabla J_i \tag{4.2}$$

By substituting Eq. (4.1) into Eq. (4.2), we have

$$\frac{\partial C_i}{\partial t} = \nabla\left(D_i \nabla C_i + z_i D_i \left(\frac{F}{RT} \nabla \phi \right) C_i \right) \tag{4.3}$$

Eq. (4.3) describes the transport mechanism of each ion in an ideal solution. This can be presented in terms of the diffusion due to concentration gradient, the first term in right hand side, and the migration or the electrical coupling between ions in the second term in right hand side. It is noticed from Eq. (4.3) that, in order to solve the Nernst-Planck equation, another relation accounted for electrostatic potential induced by ionic interaction is required. The electrostatic potential can be determined based on three different assumptions. Samson and Marchand (2007) solved the electrostatic potential for ions transport in cement-based materials by using Poisson's equation described as Eq. (4.4). As mentioned by Samson et al. (1999), the Poisson' equation can be used in more general cases. The nil current assumption has been used by Wang et al. (2005) to describe the electrostatic potential. This assumption is based on the fact that there is no net current flow within the concrete pore solution given by Eq. (4.5). Differing from those

researchers, in this study, the electroneutrality approach is selected to determine the electrostatic potential. This can be expressed as Eq. (4.7).

$$\nabla^2\phi + \frac{F\left(\sum z_i C_i + w\right)}{\varepsilon} = 0 \tag{4.4}$$

$$I = F\sum_{i=1}^{n} z_i J_i \tag{4.5}$$

$$\sum_{i=1}^{n} C_i z_i = 0 \tag{4.7}$$

in which w is the fixed charge density, ε is the dielectric constant of the surrounding medium, I is the external current density, and J_i is the flux.

The main advantages of using electroneutrality condition rather than Poisson's equation are to simplify the governing equations, and thus reduce time consuming computation, and more importantly avoid a difficulty in computational schemes caused by the very large number, $\frac{F}{\varepsilon} \approx 10^{16}$ (Wang et al., 2005; and Nguyen et al., 2006). The comparison among nil current, Poisson's equation, and electroneutrality condition used in modeling of chloride penetration into concrete was investigated by Nguyen et al. (2006). The studies showed a good agreement of concentration profiles of ions with very little errors. In order to compare the results obtained by using these three different methods, in this present study, the ionic concentration profiles of concrete sample exposed to 1 mol/l of NaCl are plotted as Fig. 4.1. As noticed from Fig. 4.1, the distribution

profiles of chloride, sodium, and ions in concrete pore solution, potassium, and hydroxyl, obtained based on these three assumptions have a very good agreement.

It can be seen from Eq. (4.7) that the electrostatic potential is dependent on charge number and concentration of all ions in electrolyte. Therefore, numerical models can be performed by incorporating the mass balance equation, Eq. (4.3), and the relation of electrostatic potential, Eq. (4.7), in the mathematical model.

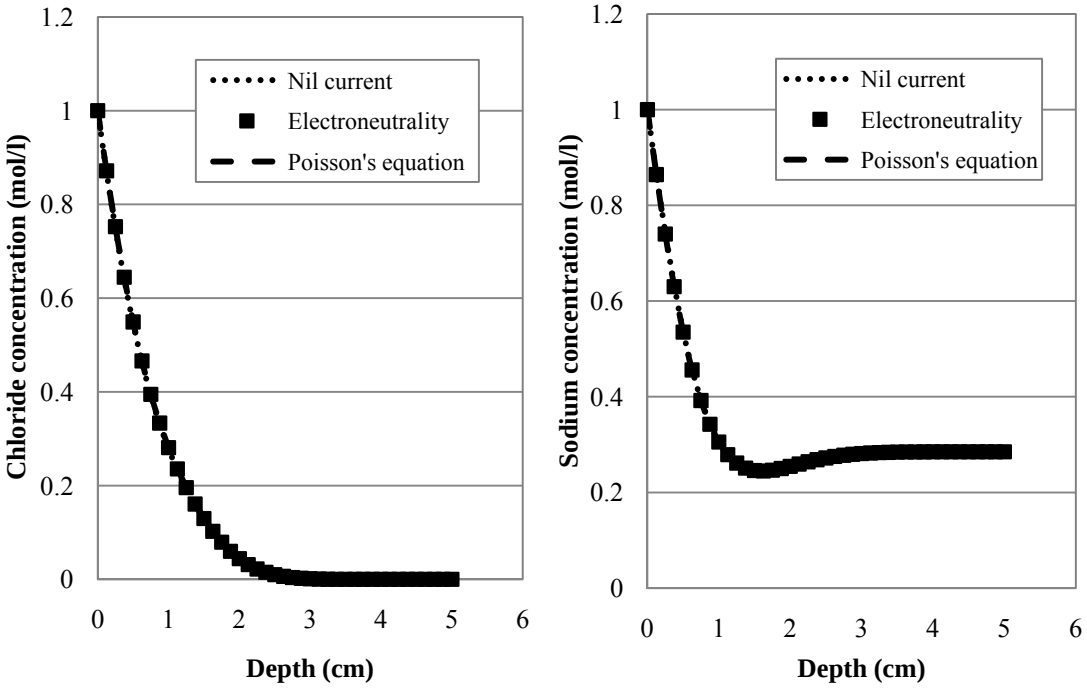

(a) Cl (b) Na

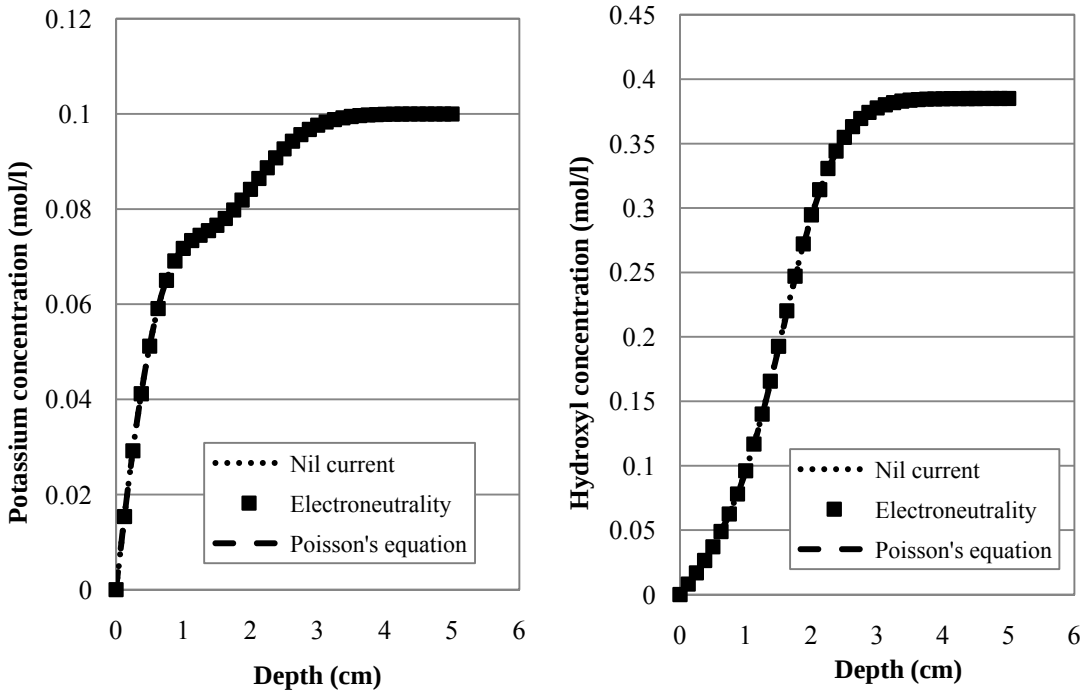

(c) K (d) OH

Fig. 4.1 Concentration profiles of four ionic species with three different approaches

4.3 Material Parameters

In order to perform numerical simulations and obtain the numerical results from governing equations, Eqs. (4.3) and (4.7), the material parameters involved in the equations have to be defined. These parameters are chloride diffusion coefficient (D_{Cl}) and chloride binding capacity $(\partial C_{lf} / \partial C_{lt})$. As mentioned in chapter 2, when chloride ions ingress into concrete, some of them will be bound to concrete pore called bound chloride. The others called free chloride can diffuse freely through concrete pore. The chloride diffusion coefficient and the chloride binding capacity will be discussed in this chapter.

4.3.1 Chloride Diffusion Coefficient

The diffusion coefficient of chloride ions in concrete can be estimated using the multifactor method as follows:

$$D_{Cl} = f_1 f_2(g_i) f_3(H) f_4(T) f_5(C_f) \tag{4.8}$$

in which f_1 is a factor accounting for the influence of water-to-cement ratio (w/c) and curing time of concrete (t_0). A formulation for f_1 was proposed by Xi and Bazant (1999):

$$f_1 = \frac{28 - t_0}{62{,}500} + \left(\frac{1}{4} + \frac{(28 - t_0)}{300}\right)\left(\frac{w}{c}\right)^{6.55} \tag{4.9}$$

The second factor, $f_2(g_i)$, is considered for the effect of composite action of the aggregates and the cement paste on the diffusivity of concrete. This factor can be calculated by using the three phase composite model developed by Christensen (1979):

$$f_2(g_i) = D_{cp}\left(1 + \frac{g_i}{(1-g_i)/3 + 1/\left(\left(D_{agg}/D_{cp}\right)-1\right)}\right) \tag{4.10}$$

where g_i is the volume fraction of aggregates in concrete, and D_{agg} and D_{cp} are the diffusivities of aggregates and cement paste, respectively. These two parameters can be determined by using the model proposed by Martys et al. (1994):

$$D = \frac{2\left(1-\left(V_p - V_p^c\right)\right)}{S^2}\left(V_p - V_p^c\right)^{4.2} \tag{4.11}$$

in which V_p is the porosity, S is the surface area, and V_p^c is the critical porosity (the porosity at which the pore space is first percolated). When Eq. (4.11) is used for diffusivity of cement paste, D_{cp}, V_p, S, and V_p^c are considered as the parameters for cement paste. The critical porosity may be taken as 3% for cement paste (Martys et al. 1994). Based on the study proposed by Xi et al. (1994a), the surface ares of cement paste, *S*, can be estimated by the monolayer capacity, V_m, of adsorption isotherm of concrete which is proportional to *S*. The porosity, V_p, can be estimated by adsorption isotherm, $n(H,T) = W_{sol}/W_{conc}$ at saturation ($H=1$). W_{sol} and W_{conc} are the weight of pore solution and concrete, respectively. More detail on adsorption isotherm can be found in Xi et al. (1994a, b). The diffusivity of aggregates, D_{agg}, can also be taken as a constant, and a proposed value is $1\text{x}10^{-12}$ cm/s.

The third factor, $f_3(H)$, is accounted for the effect of relative humidity on the chloride diffusion coefficient. A model proposed by Bazant and Najjar (1972) can be applied to this study. This factor is assumed that the chloride diffusion can be estimated by moisture diffusion:

$$f_3(H) = \left(1 + \frac{(1-H)^4}{(1-H_C)^4}\right)^{-1} \tag{4.12}$$

In which H_C is the critical humidity level at which the diffusion coefficient drops halfway between its maximum and minimum values (H_C = 0.75). Eq. (4.12) is very important in terms of influencing on the coupling between the moisture and chloride diffusion.

The fourth factor, $f_4(T)$, is taken the effect of temperature on the diffusion coefficient of concrete into account. This can be calculated by using Arrhenius' law:

$$f_4(T) = \exp\left[\frac{U}{R}\left(\frac{1}{T_0} - \frac{1}{T}\right)\right] \tag{4.13}$$

in which U is the activation energy of the diffusion process, R is the gas constant (8.314 J mol^{-1} K^{-1}), T and T_0 are the current and reference temperatures, respectively, in Kelvin (T_0 = 296 K). According to Page et al. (1981) and Collepurdi et al. (1972) studies, the activation energy of the diffusion process depends on water-to-cement ratio, *w/c*, and cement type which can be found in Table 4.1.

Table 4.1 Activation energies for various cement paste

w/c	Ordinary Portland cement (KJ/mol)	Cement with pozzolans (KJ/mol)
0.4	41.8 ± 4.0	-
0.5	41.8 ± 4.0	4.18
0.6	41.8 ± 4.0	-

The fifth factor, $f_5(C_f)$, is to account for the dependence of the chloride diffusion coefficient on the free chloride concentration which can be expressed as follows:

$$f_5(C_f) = 1 - k_{ion}(C_f)^m \tag{4.14}$$

where k_{ion} and m are two constants, 8.333 and 0.5, respectively. k_{ion} and m were obtained by Xi and Bazant study (1999)

4.3.2 Chloride Binding Capacity

The total chloride concentration represents in terms of the summation of free chloride, C_f, and bound chloride, C_b, that is

$$C_t = C_f + C_b \tag{4.15}$$

The chloride binding capacity is defined as the ratio between the change of free chloride content and total chloride content. The chloride binding capacity can be expressed as:

$$\frac{dC_f}{dC_t} = \frac{1}{1 + \frac{dC_b}{dC_f}} \tag{4.16}$$

The term dC_b / dC_t can be obtained experimentally. By using the model recently developed by Xi and Bazant (1999), chloride binding capacity can be expressed as:

$$\frac{dC_f}{dC_t} = \frac{1}{1 + \frac{A10^B \beta_{C-S-H}}{35{,}450\beta_{sol}} \left(\frac{C_f}{35.45\beta_{sol}} \right)^{A-1}} \tag{4.17}$$

where A and B are two material constants related to chloride adsorption and equal to 0.3788 and 1.14, respectively (Tang and Nilson 1993). The binding capacity depends on the two parameters, β_{sol} and β_{C-S-H}. More information on these two parameters will be discussed.

The parameter β_{sol} is described as the relationship between pore solution and concrete (*L/g*). This parameter is related to the effect of the structure of hydration products and can be expressed as:

$$\beta_{sol} = \frac{V_{sol}}{w_{conc}} = \frac{w_{sol}}{\rho_{sol} w_{conc}} = \frac{n(H,T)}{\rho_{sol}} \tag{4.18}$$

where V_{sol} is the volume of pore solution, w_{sol} is the weight of pore solution, w_{conc} is the weight of concrete, ρ_{sol} is the density of the pore solution (*g/L*) and is dependent on chloride concentration. To simplify the calculation, the parameter ρ_{sol} can be estimated by using the density of pore water. The weight ratio of pore solution to concrete (w_{sol}/w_{conc}) represents chloride adsorption isotherm which is related to relative humidity, *H*, temperature, *T*, and pore structure of concrete. Due to a lack of test data on chloride isotherm, *n(H,T)* may define as the isotherm of water adsorption instead of chloride isotherm. The adsorption isotherm of concrete can be described in terms of adsorption isotherm of cement paste and aggregate as follows:

$$n(H,T) = f_{cp} n_{cp}(H,T) + f_{agg} n_{agg}(H,T) \tag{4.19}$$

in which f_{cp} and f_{agg} are the weight percentages of cement paste and aggregates, and $n_{cp}(H,T)$ and $n_{agg}(H,T)$ are the water adsorption isotherms of cement paste and aggregate.

The parameter β_{C-S-H} can be explained as the weight ration of C-S-H gel to concrete (g/g). This factor is used to determine the effect of the cement composition and age of concrete on the volume fraction of C-S-H gel which is written as:

$$\beta_{C-S-H} = \frac{w_{C-S-H}}{w_{total}} \tag{4.20}$$

where w_{C-S-H} and w_{total} are the weight of C-S-H gel and the total weight of concrete. The details of parameters *n(H,T)* and β_{C-S-H} can be found in the paper by Xi (1995a.).

The limitation of binding capacity based on the Freundlich isotherm, Eq. (4.17), is that the term $\partial C_f / \partial C_t = 0$ when the free chloride concentration, C_f, is zero because of $A < 1$. As a result, $\partial C_f / \partial C_t = 0$ leads to $\partial C_f / \partial t = 0$. This can be concluded that C_f is a constant at all time steps and equals to initial free chloride concentration. Thus, chloride diffusion never starts. To solve this problem, Tang and Nilsson (1993) suggested that the Freundlich isotherm can be used when C_f is large (> 0.01 mol/l), and the Langmuir isotherm is employed when C_f is small (< 0.05 mol/l). For these reasons, in this present study, the chloride binding capacity the Langmuir isotherm is used for initial free chloride concentration ($C_f = 0$) while free chloride concentration is more than zero ($C_f > 0$) the chloride binding capacity can be determined by Eq. (4.17) based on Freundlich isotherm. The Langmuir isotherm is expressed as:

$$\frac{1}{C_b^{'}} = \frac{1}{k^{'} C_{bm}} \frac{1}{C_f^{'}} + \frac{1}{C_{bm}} \tag{4.21}$$

where $k^{'}$ is an adsorption constant, and C_{bm} is the bound chloride content at saturated monolayer adsorption (Tang and Nilsson, 1993). Based on adsorption test data, $k^{'}$ and C_{bm} can be obtained by curve fitting. However, $C_b^{'}$ and $C_f^{'}$ are the bound and free chloride contents used in Eq. (4.21). The units of these two parameters are in milligrams of bound chloride per gram of calcium silicate hydrate gel (mg/g) and in free chloride per liter of pore solution (mol/l), respectively, which is different from C_b and C_f. In the numerical simulation, it is necessary to use the consistent unit. Therefore, $C_b^{'}$ and $C_f^{'}$ can be converted and correlated to the unit of C_b and C_f as follows:

$$C_b^{'} = \frac{1{,}000\, C_b}{\beta_{C-S-H}} \tag{4.22}$$

$$C_f^{'} = \frac{C_f}{35.45 \beta_{sol}} \tag{4.23}$$

Substituting Eqs. (4.22) and (4.23) into Eq. (4.21), yields

$$\frac{1}{C_b} = \frac{1{,}000}{\beta_{C-S-H}} \left[\frac{35.45 \beta_{sol}}{k^{'} C_{bm}} \frac{1}{C_f} + \frac{1}{C_{bm}} \right] \tag{4.24}$$

Eq. (4.24) can be re-expressed in a simple form as

$$C_b = \frac{1}{\beta + \frac{1}{\alpha C_f}} \tag{4.25}$$

in which,

$$\alpha = \frac{k' C_{bm} \beta_{C-S-H}}{35{,}450 \beta_{sol}} \tag{4.26}$$

$$\beta = \frac{1{,}000}{\beta_{C-S-H} C_{bm}} \tag{4.27}$$

Derivative of Eq. (4.25) with respect to C_f yields

$$\frac{dC_b}{dC_f} = \frac{1}{\alpha (C_f)^2 \left(\beta + \frac{1}{\alpha C_f} \right)^2} \tag{4.28}$$

By substituting Eq. (4.28) into Eq. (4.16), then the binding capacity based on Langmuir isotherm can be expressed as:

$$\frac{dC_f}{dC_t} = \frac{1}{1 + \frac{dC_b}{dC_f}} = \frac{1}{1 + \frac{1}{\alpha \left(\beta C_f + \frac{1}{\alpha} \right)^2}} \tag{4.29}$$

The Eq. (4.29) is used to calculate the binding capacity when free chloride concentration tends to zero, then the binding capacity is $1/(1+\alpha)$. The parameter α can be calculated by using Eq. (4.26) and is dependent on many factors. As a result, α is definitely a non-zero number. The parameters in chloride binding capacity based on Langmuir isotherm can be obtained from Tang and Nilsson (1993) paper that is $1/C_{bm} = 0.1849$, $1/(k^{'}C_{bm}) = 0.002438$, $k^{'} = 75.841$, and $C_{bm} = 5.4083$.

4.4 Numerical Model

Numerical simulations are performed and the governing equations, Eqs. (4.3) and (4.7), can be solved by using finite element method. The finite element formulation will be briefly introduced in this chapter. For more details on finite element formulation, it can be found in appendix A. The continuous variables, ionic species, in the system are spatially discretized over the space domain, Ω. The domain discretization can be described as:

$$\Omega = \bigcup_{e=1}^{nel} \Omega^e \tag{4.30}$$

in which *nel* is the total number of elements in space domain and Ω_e is a subdomain or an element. It is also defined $\partial\Omega$ as the boundary of space domain and $\partial\Omega^e$ the boundary of subdomain. By using isoparametric elements, the concentration of each species is defined in terms of nodal values, that is,

$$C_i = \lfloor \mathbf{N} \rfloor \{\mathbf{C}\}_i \tag{4.31}$$

where $\lfloor \mathbf{N} \rfloor$ is the element shape function. The notations $\lfloor \ \rfloor$ and $\{ \}$ are row and column vectors, respectively. The element shape functions are expressed as:

$$\lfloor \mathbf{N} \rfloor = \lfloor N_1 \ \ N_2 \ldots \ N_n \rfloor \tag{4.32}$$

in which N_i is the shape function for node i and n is the total numbers of nodes in an element which is equal to 4 for isoparametric element. The vector of ionic species, $\{\mathbf{C}\}$, can be defined as:

$$\{\mathbf{C}\} = \lfloor C_1 \ \ C_2 \ldots \ C_n \rfloor \tag{4.33}$$

For the binding capacity of ions, the bound ion concentration is defined as S. In this study, the binding capacity is considered only for chloride ion so that the release rate of bound chlorides can be described in terms of the ratio of rates of the free to the bound chloride concentration, λ, as follows:

$$\dot{S}_i = \lambda \dot{C}_i \tag{4.34}$$

in which $\lambda = (\partial C_b / \partial C_f)$ which can be derived following Eq. (4.17). The nodal free ionic concentrations are solved by substituting into governing equations, Eqs. (4.3) and (4.7), and applying the Galerkin method to the weak forms of Eqs. (4.3) and (4.7), then the finite element matrix of transient mass diffusion can be obtained as follows:

$$(\mathbf{M_S} + \mathbf{M_C})\dot{\mathbf{d}} + \mathbf{Kd} = \mathbf{F} \tag{4.35}$$

in which,

$$\mathbf{M_S} = \int_{\Omega} \mathbf{N}^{\mathbf{T}} \lambda \ \mathbf{N} \, d\Omega \tag{4.36}$$

$$\mathbf{M_C} = \int_{\Omega} \mathbf{N}^{\mathbf{T}} \mathbf{N} \, d\Omega \tag{4.37}$$

$$\mathbf{K} = \int_{\Omega} \mathbf{B}^{\mathbf{T}} \mathbf{D} \mathbf{B} \, d\Omega \tag{4.38}$$

$$\mathbf{D} = \begin{bmatrix} D_i & \cdots & 0 \\ \vdots & \ddots & 0 \\ 0 & 0 & D_n \end{bmatrix} \tag{4.39}$$

(i = number of ionic species = 1, 2, …, n)

F = 0 = no external flux in this present study

4.5 Numerical Results and Discussion

4.5.1 Influence of Ionic Interaction

The numerical calculation based on the finite element formulation is performed to study the effect of ionic interaction on multi-species diffusion in a concrete slab shown in Fig. 4.3. In this case, we assume 1 mol/l of NaCl solution ingress from the top surface into a concrete sample so that there are two species, 1 mol/l of chloride ion and 1 mol/l of sodium ion, which have a negative charge and a positive charge, respectively. The diffusion coefficients of chloride and sodium ion taken from Wang et al. (2005) are 1.02×10^{-10} m^2/s and 2.7×10^{-11} m^2/s, respectively. Fig 4.2 shows the effect of ionic interaction between these two species. According to Fick's law, without considering ionic interaction, chloride ion will diffuse faster than sodium ion because chloride has diffusion coefficient higher than sodium. This can be seen from Fig. 4.2 that, at a fixed depth in the concrete slab, chloride has higher concentration than that of sodium. With considering the ionic interaction, the faster diffusing ion (i.e. the chloride ion) is slowed down by the electrostatic potential that is induced by the ionic interaction between the two species. On the other hand, the slower diffusing ion (i.e. the sodium ion) is accelerated. This is obviously noticeable from Fig. 4.2 that, at fixed depth, the chloride concentration is equal to sodium concentration. As a result, the chloride and sodium concentration profiles become overlapped with each other.

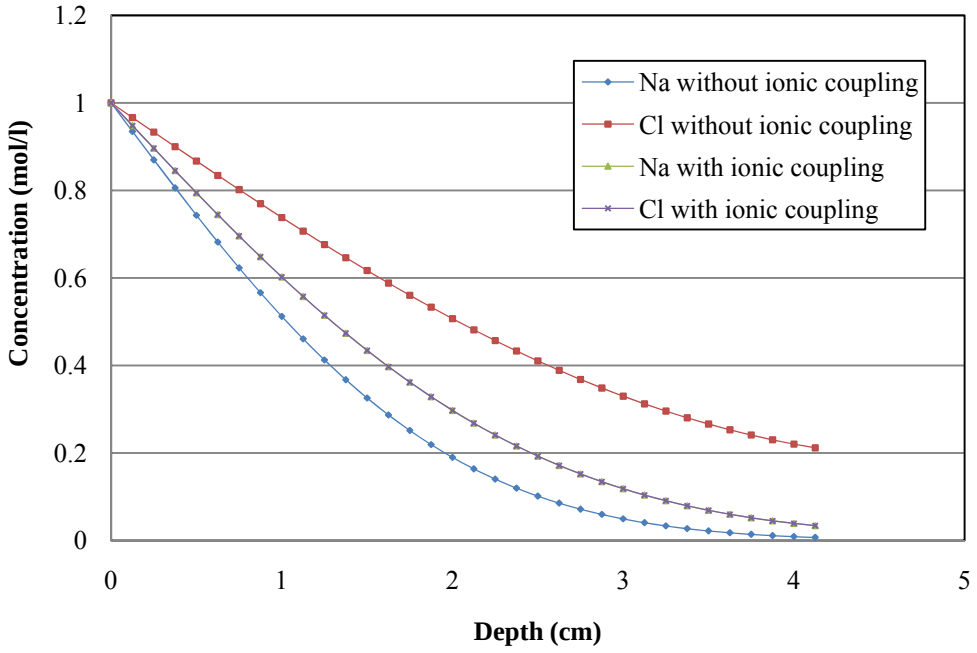

Fig. 4.2 Concentration profile of chloride and sodium with and without considering ionic interaction at 50 days of exposure

4.5.2 Multi-Species Diffusion in Saturated Concrete

Now we focus on two different types of deicing salts, NaCl and $CaCl_2$, penetrating into the concrete slab from the top surface. The ions in concrete pore solution, K^+, Na^+, and OH^-, are taken into account in the numerical analysis. The material parameters and input data for the numerical simulation related to the governing equations are shown in Table 4.2. These are diffusion coefficient, initial concentration at the top surface, and initial concentration of each ionic species in concrete pore solution, water-to-cement ratio, and volume fraction of aggregate. The numerical simulations are performed for the concrete under the saturated condition. This

means relative humidity inside and outside concrete sample is equal to 100%. As a result, there is no effect from moisture gradient on multi-ions diffusion in concrete.

The geometry of concrete sample used in numerical simulation is shown in Fig. 4.3. It is a 3 cm by 5 cm concrete slab. The concrete sample is exposed to 0.5 mol/l NaCl and 0.5 mol/l $CaCl_2$ solutions on the top surface. The other boundaries are assumed to be insulated. The concrete sample is divided into 400 elements and 451 nodes by using isoparametric elements for the finite element model.

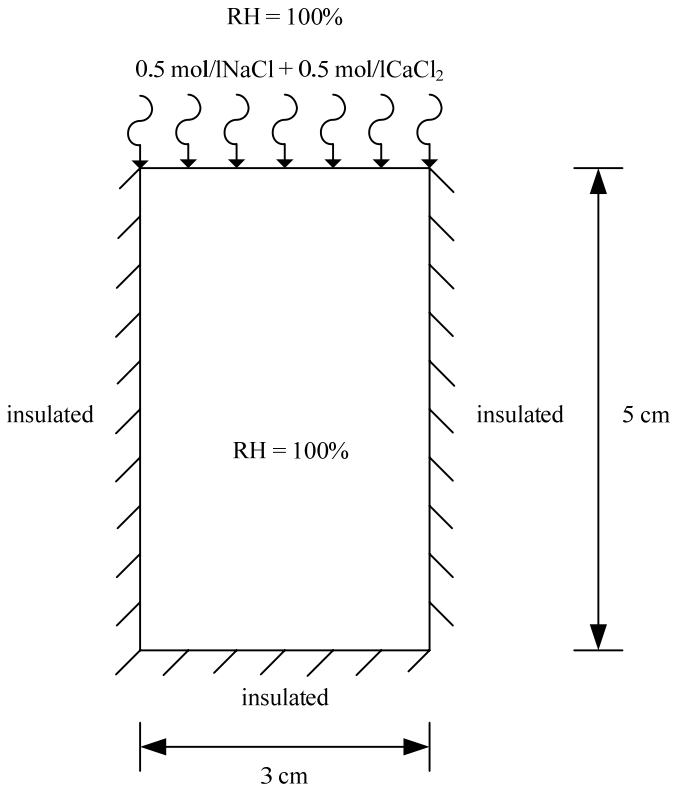

Fig. 4.3 The concrete sample used in the numerical model under saturated condition

Table 4.2 Material parameters and input data for the concrete sample

Species	K	Na	Cl	OH	Ca
Charge number	+1	+1	-1	-1	+2
Diffusion coefficient, D_{ci}	$0.40\text{x}10^{-10}$ (m^2/s)	$0.28\text{x}10^{-10}$ (m^2/s)	D_{Cl}	$5.30\text{x}10^{-10}$ (m^2/s)	$0.16\text{x}10^{-10}$ (m^2/s)
Initial condition at top surface of concrete sample	0	0.5 mol/l	1.5 mol/l	0	0.5 mol/l
Initial condition in pore solution	0.0995 (mol/l)	0.0389 (mol/l)	0	0.1384 (mol/l)	0
Water-to-cement ratio (w/c)	0.55				
Volume fraction of aggregate (g_i)	0.65				

The relation between free chloride concentration and the depth at different times of exposure is shown in Fig. 4.4. The depth of penetration is measured from the top surface of concrete sample. It can be seen from the Fig. 4.4 that the free chloride concentration decreases with increasing depth from the top surface. At a fixed depth, the longer exposure time, the higher the free chloride concentration.

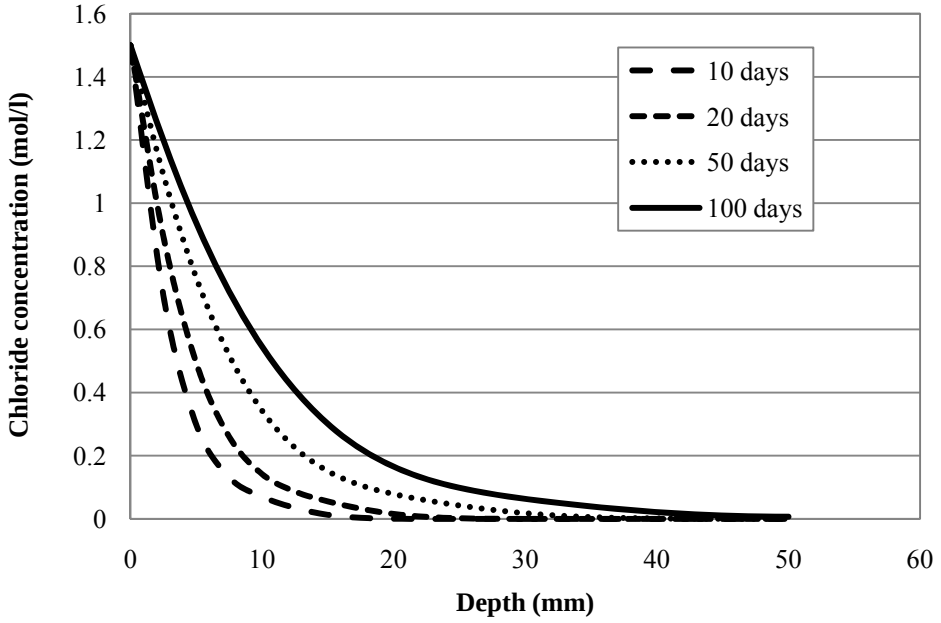

Fig. 4.4 The concentration profile of free chloride in saturated condition at different time of exposure

The trends of sodium and calcium concentration are similar to the free chloride concentration because they have the same initial conditions. The concentration gradients of chloride, sodium, and calcium are in the same direction, from the outside (the top) to inside concrete sample. The plots of sodium and calcium concentration with the depth at different times of exposure are shown in Figs. 4.6 and 4.7, respectively.

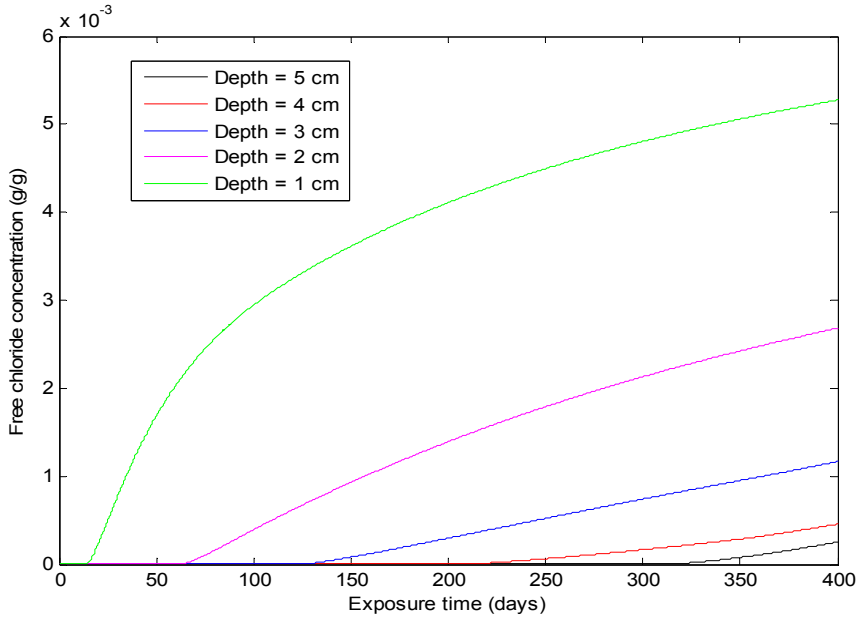

Fig. 4.5 The distribution of free chloride concentration in saturated condition at different depths from the exposed surface

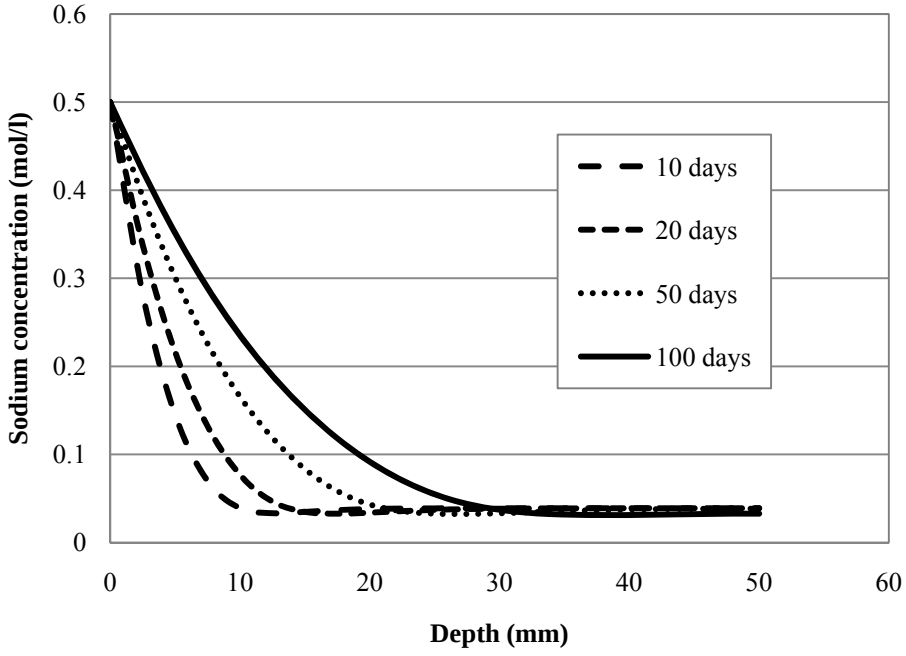

Fig. 4.6 The concentration profile of sodium in saturated condition at different times of exposure

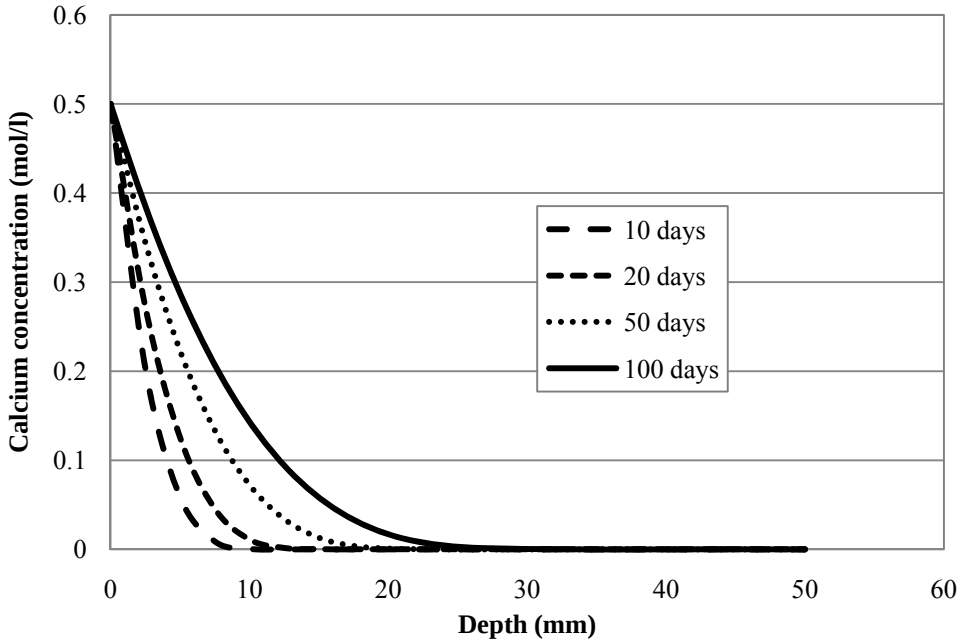

Fig. 4.7 The concentration profile of calcium in saturated condition at different times of exposure

In contrast to chloride, sodium, and calcium concentration profiles, the trends of concentration gradient of potassium and hydroxyl ions are from inside to outside of concrete sample because the inside concentrations of the ions are higher than the concentrations at the exposed surface, and in fact, there are no sources of potassium and hydroxyl ions at the top exposed surface. The variations of potassium and hydroxyl concentrations with depth at different times of exposure are shown in Figs. 4.8 and 4.9, respectively. As noticed, the concentrations of potassium and hydroxyl ion increase with the increase of depth from top surface.

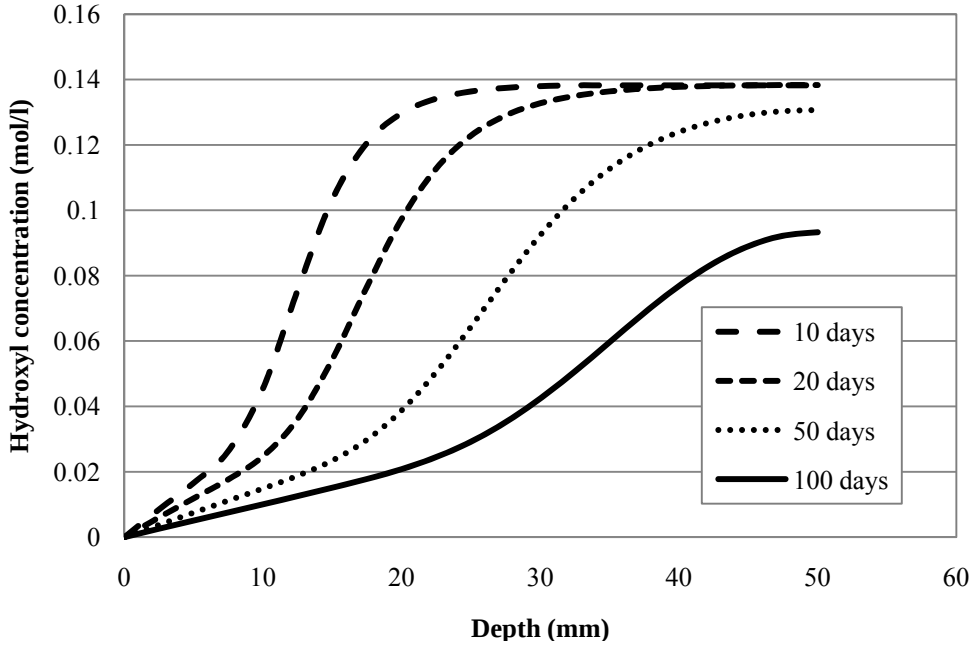

Fig. 4.8 The profile of hydroxyl concentration in saturated condition at different times of exposure

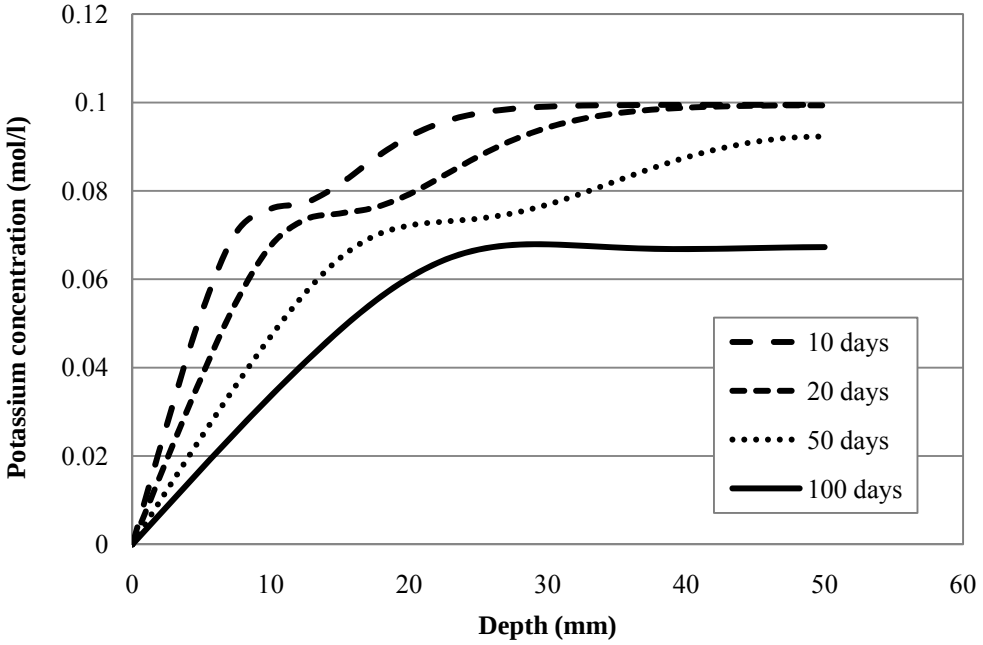

Fig. 4.9 The profile of potassium concentration in saturated condition at different times of exposure.

4.6 Conclusions

1. The mathematical model is developed based on the Nernst-Planck equation and the electroneutrality condition is incorporated in the model to solve electrostatic potential. The model is used to simulate the multi-species deicing salts penetration into saturated concrete structures. The material parameters related to chloride diffusion in concrete are taken into account. These parameters are chloride diffusion coefficient and chloride binding capacity.

2. The numerical results are solved by using the finite element method which is an effective tool and widely used for solving the partial differential equations of mass diffusion.

3. Compared to the empirical models, the present model is a robust mathematical model to characterize the sophisticated transport phenomena. It includes the ionic interaction between ions not only from exposed surface but also ions in concrete pore solution. This interaction induces the electrostatic potential which has significant effect on concentration profiles of each ionic species and cannot be considered negligible.

4. The present model can also be applied to simulate the saturated concrete structures subjected to other aggressive chemicals.

5. The framework of present model can be extended to simulate the multi-species deicing salts ingress into non-saturated concrete structures. This will be described in the next chapter.

CHAPTER 5

MULTI-IONIC SPECIES DIFFUSION IN NON-SATURATED CONCRETE

5.1 Introduction

The previous chapter is focused on multi-species deicing salts penetration into saturated concrete structures. However, in reality, concrete is frequently found in non-saturated condition rather than saturated condition. In non-saturated condition, chloride ions can penetrate into concrete by two driving forces, chloride and moisture gradients. The moisture diffusion is very important and has influence on chloride penetration in non-saturated concrete (Ababneh et al., 2003 and Abarr, 2005) by changing the chloride penetration rate. Therefore, to investigate the effect of moisture diffusion on multi-species penetration into concrete, the moisture gradient is incorporated in the governing equations. In the case of fully saturated concrete, ion penetration is dominated by the concentration gradient of each ion because pores inside concrete become completely filled with solution and thus there is no water movement. In contrast to non-saturated concrete, both the moisture and ion concentration gradients have strong influence on the ion penetration as well as on the moisture diffusion. This is considered as a two-way coupling process. As a result, moisture movement can carry not only chloride ions but also other species. On the other hand, the chloride movement due to the concentration gradient can also drive the moisture diffusion (Ababneh and Xi, 2002 and Abarr, 2005).

Many researchers have studied the chloride penetration into non-saturated concrete. Saetta et al. (1993) developed a numerical model for chloride penetration into partially saturated concrete by considering the effect of the relative humidity on the rate of chloride penetration. They modified the chloride diffusion and added coupling terms in the governing equations by taking into account the material parameters, environmental conditions, and the dependence of chloride diffusion and concrete mix parameters. The nonlinear and coupled partial differential equations were solved by using finite element method. Nilsson (2000) proposed a model for chloride penetration into concrete exposed to seawater splash or deicing salt. It was concluded that the chloride diffusion and convection could be described as function of the moisture content in concrete. Miller et al. (2004) investigated the chloride ingress into concrete exposed to saturated and wetting and drying conditions. The results showed the rate of chloride penetration depends on different exposure conditions. For wetting and drying environment, the chloride penetrates into concrete by sorption and diffusion processes while the diffusion is the dominant mechanism in saturated concrete. De Vega G. et al. (2007) conducted a test for evaluating chloride diffusion coefficients through partially saturated concrete. It was found that the lower humidity in concrete, the lower chloride diffusion coefficients. Boulifiza et al. (2003) proposed mathematical models and numerical simulations for moisture movement and chloride penetration in concrete based on diffusion and advection mechanisms. The study focused on cracked and uncracked concrete under saturated and non-saturated conditions. It showed that water movement at a crack is very sensitive to degree of saturation and chloride penetration is significantly influenced by existing cracks. Nielsen and Geiker (2003) developed a model, a combination of composite theory and Power's model for microstructural development, to predict the interaction between the chloride diffusion coefficient and degree of saturation in cementitious

material. The study concluded that the chloride diffusion coefficient depends on degree of saturation.

Ababneh and Xi (2002) conducted an experimental study to determine the influence of chloride penetration on moisture diffusion in concrete. The test results showed that the moisture diffusion is significantly affected by chloride penetration, and then there should be an additional term accounted for the coupling effect in governing equation. In addition, the results showed that the coupling parameter is not constant but depends on free chloride concentration. Abarr (2005) developed a test focusing on the effect of moisture diffusion on chloride penetration in concrete. The results showed that moisture diffusion has significant influence on chloride penetration in concrete by accelerating the rate of penetration. Similar to Ababneh and Xi (2002) study, the governing equation should be taken into account the coupling effect of moisture diffusion on chloride penetration. From this study, it was found that the coupling parameter depends on chloride concentration. The study concluded that chloride penetration and moisture diffusion are two fully coupled diffusion processes in non-saturated concrete. From these two studies, it can be concluded that there should be two coupling terms incorporated in the two governing equations for moisture and chloride diffusions, and the two coupling terms can be formulated by using two coupling parameters which are related to chloride concentration. As a result, the governing equations are not only fully coupled but also nonlinear.

Marchand (2000) proposed the numerical model of cement materials subjected to aggressive chemical environments called “STADIUM”. This model was developed base on the set of extended Nernst-Planck/Poisson equations. The model was accounted for the electrical interaction between ions in solution and chemical activity effect. The influence of moisture diffusion was considered in terms of capillary suction. This was performed by incorporating the

advection term into governing equations. The governing equations were also modified by taking into account the water content in pore solution. Then, Samson and Marchand (2007) used the STADIUM model to simulate the cement-based materials exposed to pure water and sulfate solution and compared with the test data. Wang et al. (2005) developed a mathematical model based on their previous model, a simulation model of electrochemical chloride removal (ECR), to predict chloride ions from saline environment penetration into concrete by incorporating the convection of pore solution in the model. The mathematical model was formulated based on Nernst-Planck equation and the electrostatic potential was evaluated by an assumption that there is no current flow within concrete pore solution. It was found that the ionic interaction and the convection flow of pore solution have significant effect on ionic concentration profiles. Lately, Nguyen et al. (2008) proposed a transport model of coupled ion and moisture in porous building materials. Moisture transport was considered in terms of the transport of liquid and vapor phases with aqueous electrolyte theory; and coupled with ion transport in unsaturated porous media. The model was developed based on the Nernst-Planck/electroneutrality set of equations and accounted for the crystallization phenomena on the transport properties. The model was compared with the experimental data obtained by Nuclear Magnetic Resonance (NMR) method. It was shown that the model can be used to simulate the ion transport in plaster/Bentheimer sandstone under various cases with unified ionic diffusivities successfully.

The purpose of this chapter is to investigate the effect of moisture diffusion on multi-species deicing salts penetration into non-saturated concrete. To perform this, the formulations of governing equations for multi-ions diffusion in concrete based on the set of Nernst-Planck/nil current equation and mass balance equations for ions and moisture diffusion in concrete are described theoretically and the coupling effects are taken into account. As a result, Nernst-Planck

equation is modified based on the studies as proposed by Abaneh and Xi (2002) and Abarr (2005). Then, several material parameters are incorporated in the numerical model and the solutions are solved by using finite element method.

5.2 Basic Formulation of Governing Equations

The flux of each ions transport in an ideal solution in porous media based on Nernst-Planck equation without considering the chemical activity effects can be described as follow:

$$J_i = -D_i \nabla C_i - z_i D_i \left(\frac{F}{RT} \nabla \phi \right) C_i \tag{5.1}$$

where J_i is the flux, D_i is the diffusion coefficient, C_i is the concentration, z_i is the charge number, F is the Faraday's constant, R is the gas constant, T is the temperature, Φ is the electrostatic potential, and index i represents for *i-th* species. As described in chapter 4, the electroneutrality is selected and incorporated in the model to solve the electrostatic potential.

The moisture content in concrete can be expressed by water content (w) or by pore relative humidity (H). In this study, pore relative humidity is used to represent the moisture content in concrete. Pore relative humidity is considered as a combined indicator of liquid water and water vapor (Bazant and Najjar, 1972). The moisture flux (J_H) can be described in terms of the gradient of pore relative humidity as follows:

$$J_H = -D_H \nabla H \tag{5.2}$$

in which D_H is the humidity diffusion coefficient and H is the pore relative humidity. As described previously, the governing equations between each ion and moisture are fully coupled

and then these coupled governing equations must be solved simultaneously. Therefore, the flux of each ion (J_i) in non-saturated concrete can be written in terms of free ion concentration gradient and moisture gradient as:

$$J_i = -D_i \nabla C_i - z_i D_i \left(\frac{F}{RT} \nabla \phi \right) C_i - D_{i-H} \nabla H \tag{5.3}$$

Similar to moisture flux, Eq. (5.2) can be modified by adding the coupling term, which is taken into account the influence of ion diffusion on moisture flux, expressed as:

$$J_H = -D_{H-i} \nabla C_i - D_H \nabla H \tag{5.4}$$

The mass balance equations of ionic species and moisture can be described as:

$$\frac{\partial C_i}{\partial t} = -\nabla J_i \tag{5.5}$$

$$\frac{\partial w}{\partial t} = -\nabla J_H \tag{5.6}$$

By substituting Eqs. (5.3) and (5.4) into, Eqs. (5.5) and (5.6), respectively, we obtain

$$\frac{\partial C_i}{\partial t} = \nabla \left(D_i \nabla C_i + z_i D_i \left(\frac{F}{RT} \nabla \phi \right) C_i + D_{i-H} \nabla H \right) \tag{5.7}$$

$$\frac{\partial w}{\partial t} = \frac{\partial w}{\partial H} \frac{\partial H}{\partial t} = \nabla \left(D_{H-i} \nabla C_i + D_H \nabla H \right) \tag{5.8}$$

where $(\partial w/\partial H)$ is the moisture capacity, $D_{i\text{-}H}$ and $D_{H\text{-}i}$ are the coupling parameters of the effect of moisture on ionic transport and the effect of ions on moisture diffusion, respectively.

5.3 Material Parameters

In order to solve the governing equations, Eqs. (5.7) and (5.8), the material parameters must be defined. The chloride diffusion coefficient and chloride binding capacity were introduced in chapter 4. In this chapter, the moisture capacity, moisture diffusion coefficient, and the coupling parameters will be discussed.

5.3.1 Moisture Capacity $(\partial w/\partial H)$

The moisture capacity of concrete can be determined by taking the average of the moisture capacities of cement paste and aggregate as proposed by Xi et al. (2000)

$$\frac{dw}{dH} = f_{agg}\left(\frac{dw}{dH}\right)_{agg} + f_{cp}\left(\frac{dw}{dH}\right)_{cp} \tag{5.9}$$

in which f_{agg} and f_{cp} are the weight percentages of the aggregate and cement paste, respectively; $\left(\frac{dw}{dH}\right)_{agg}$ and $\left(\frac{dw}{dH}\right)_{cp}$ are the moisture capacities of aggregate and cement paste, respectively, which can be calculated based on the model proposed by Xi et al. (1994a, b) and Xi (1995a, b).

5.3.2 Moisture Diffusion Coefficient (D_H)

The moisture diffusion coefficient of concrete based on composite theory derived by Christensen (1979) cab be expressed as

$$D_H = D_{H_{cp}} \left(1 + \frac{g_i}{\frac{[1-g_i]}{3} + \frac{1}{[(D_{H_{agg}} / D_{H\,cp}) - 1]}} \right) \tag{5.10}$$

where g_i is the aggregate volume fraction, $D_{H\,cp}$ is the humidity diffusivity of the cement paste and $D_{H_{agg}}$ is the humidity diffusivity of the aggregates. According to the fact that the pores in aggregates are discontinuous and dominated by cement paste, the humidity diffusivity of aggregates is very small as compared with the humidity diffusivity of cement paste. Thus, $D_{H_{agg}}$ in Eq. (33) can be negligible. The humidity diffusivity of cement paste can be calculated by the empirical formula as proposed by Xi et al. (1994b).

5.3.3 Coupling Parameters ($D_{i\text{-}H}$ and $D_{H\text{-}i}$)

So far, there has been no material models developed for the coupling parameters between ion transport and moisture diffusion in concrete. These can be described based on the previous research works of Ababneh and Xi (2002) and Abarr (2005). Ababneh and Xi (2002) conducted an experimental study on the effect of chloride penetration on moisture diffusion in concrete. The results from the experiment shows that the effect of chloride penetration on moisture diffusion is significant and it should be taken into account as the coupled effect on moisture

diffusion. It is also found that the coupling parameters, $D_{H\text{-}Cl}$, is not a constant but depends on chloride concentration. Similarly, Abarr (2005) performed a test to investigate the effect of moisture diffusion on chloride penetration in concrete. One can see from their results that $D_{Cl\text{-}H}$ increases with increasing of chloride concentration and $D_{Cl\text{-}H}$ decreases to zero when the free chloride concentration is small. Therefore, it can be concluded that $D_{Cl\text{-}H}$ is chloride concentration dependent.

According to Ababneh and Xi (2002) and Abarr (2005) studies, both coupling parameters, $D_{H\text{-}Cl}$ and $D_{Cl\text{-}H}$, are chloride concentration dependent and they can be expressed in terms of free chloride concentration as follows:

$$D_{Cl-H} = \varepsilon Cl_f \tag{5.11}$$

$$D_{H-Cl} = \delta Cl_f \tag{5.12}$$

in which ε and δ are two constants depending on concrete mix design. In order to obtain ε and δ, the results performed by numerical simulations of coupled chloride and moisture diffusion in concrete are plotted in Fig. 5.1 compared with the test data conducted by Abarr (2005). The constants ε and δ are obtained by the best fit between numerical results and experimental results. By the curve fitting, ε and δ are determined to be 0.19 and 0.52, respectively.

However, there are no experimental data or material models of coupling parameters for other species, Na, Ca, OH, and K. As the first approximation, the coupling parameters of these ionic species can be evaluated based on the previous research (Ababneh and Xi, 2002; Abarr, 2005). For example, the effect of moisture on ionic diffusions can be considered as the same

constant, ε, as used for chloride. This is a reasonable assumption due to the fact that the moisture movement can carry any other ions in the same way as it carries the chloride ions. So, Eq. (5.11) can be extended to

$$D_{i-H} = \varepsilon Cl_f = \varepsilon C_i \tag{5.13}$$

in which the subscript *i* represents all ions including chloride.

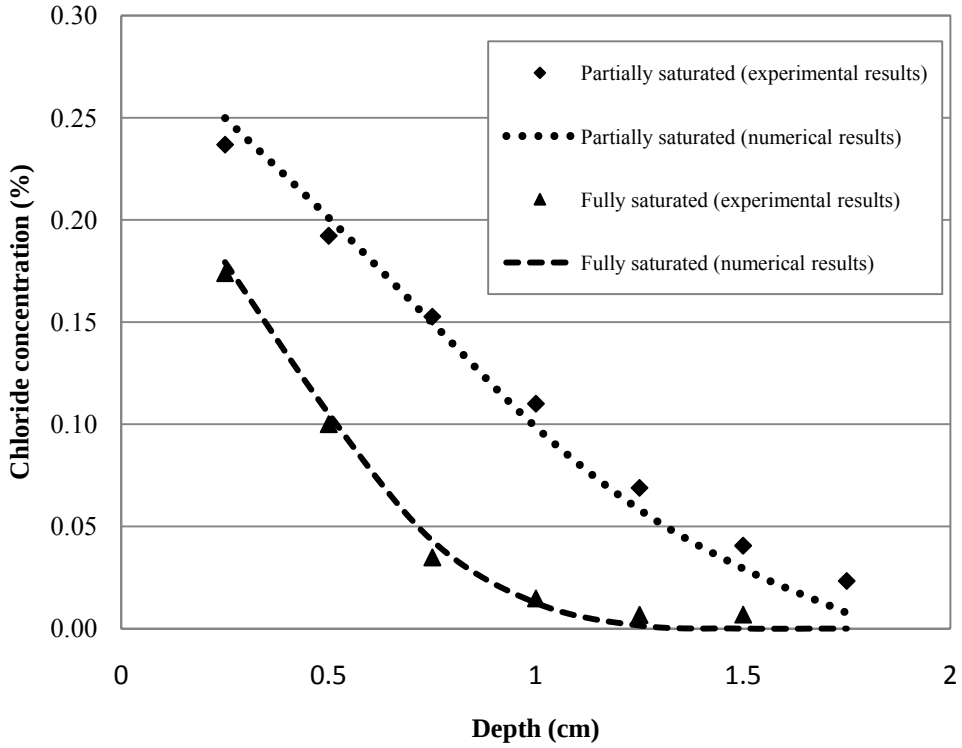

Fig. 5.1 The plot between numerical results and experimental results of coupled chloride and moisture diffusion in concrete

On the other hand, the effect of ionic diffusion on the moisture diffusion cannot be treated in the same way, that is, the coupling parameter, δ, cannot be considered as a constant for all different ions. This is because the effect of the diffusion of a specific ion on the moisture movement varies with the diffusion rate of the ion. Again, as the first approximation, the coupling parameter, δ, of each species can be estimated by the ratio between a specific ionic species and the chloride ion (i.e. the coupling parameter is proportional to the ratio of the diffusion coefficient of the ion and the diffusion coefficient of chloride):

$$\frac{D_i}{D_{Cl}} = \frac{D_{H-C_i}}{D_{H-Cl_f}} = \frac{\delta_i C_i}{\delta Cl_f} \tag{5.14}$$

5.4 Numerical Model

Numerical simulations are performed and the governing equations, Eqs. (5.7), (5.8), and electroneutrality condition, can be solved by using the finite element method. The finite element formulation will be briefly introduced here. The continuous variables, ionic species, in the system are spatially discretized over the space domain, Ω. The domain discretization can be described as:

$$\Omega = \bigcup_{e=1}^{nel} \Omega^e \tag{5.15}$$

in which *nel* is the total number of elements in space domain and Ω_e is a subdomain or an element. It is also defined $\partial\Omega$ as the boundary of space domain and $\partial\Omega^e$ the boundary of

subdomain. By using isoparametric elements, the concentration of each species is defined in terms of nodal values, that is,

$$C_i = \lfloor \mathbf{N} \rfloor \{\mathbf{C}\}_i \tag{5.16}$$

where $\lfloor \mathbf{N} \rfloor$ is the element shape function. The notations $\lfloor \ \rfloor$ and $\{\ \}$ are row and column vectors, respectively. The element shape functions are expressed as:

$$\lfloor \mathbf{N} \rfloor = \lfloor N_1 \ \ N_2 \ldots \ N_n \rfloor \tag{5.17}$$

in which N_i is the shape function for node i and n is the total numbers of nodes in an element which is equal to 4 for isoparametric element. The vector of ionic species, $\{\mathbf{C}\}$, can be defined as:

$$\{\mathbf{C}\} = \lfloor C_1 \ \ C_2 \ldots \ C_n \rfloor \tag{5.18}$$

For the binding capacity of ions, similar to Chapter 4, the bound ion concentration is defined as *S*. In this study, the binding capacity is considered only for chloride ion so that the release rate of bound chlorides can be described in terms of the ratio of the rates of free and bound chloride concentration, λ, as follows:

$$\dot{S}_i = \lambda \dot{C}_i \tag{5.19}$$

in which $\lambda = (\partial Cl_b / \partial Cl_f)$ which can be derived following Eq. (4.17). The nodal free ionic concentrations are solved by substituting into governing equations, Eqs. (5.7), (5.8), and electroneutrality condition expressed as Eq. (4.7). Then, by applying the Galerkin method to the weak forms of Eqs. (5.7), (5.8), and (4.7), the finite element matrix of transient mass diffusion can be obtained as follows:

$$(\mathbf{M_S} + \mathbf{M_C})\dot{\mathbf{d}} + \mathbf{Kd} = \mathbf{F} \tag{5.20}$$

in which,

$$\mathbf{M_S} = \int_{\Omega} \mathbf{N}^{\mathbf{T}} \lambda \ \mathbf{N} \, d\Omega \tag{5.21}$$

$$\mathbf{M_C} = \int_{\Omega} \mathbf{N}^{\mathbf{T}} \mathbf{N} \, d\Omega \tag{5.22}$$

$$\mathbf{K} = \int_{\Omega} \mathbf{B}^{\mathbf{T}} \mathbf{D} \mathbf{B} \, d\Omega \tag{5.23}$$

$$\mathbf{D} = \begin{bmatrix} D_H & D_{H-i} & \cdots & D_{H-n} \\ D_{i-H} & D_i & 0 & 0 \\ \vdots & 0 & \ddots & 0 \\ D_{n-H} & 0 & 0 & D_n \end{bmatrix} \tag{5.24}$$

(i = number of ionic species = 1, 2, …, n)

F = 0 = no external flux in this present study

5.5 Numerical Results and Discussion

The study focuses on two different types of deicing salts, NaCl and $CaCl_2$, penetrating into concrete sample from the top surface. The ions in concrete pore solution, K^+, Na^+, and OH^-, are also taken into account in the numerical analysis. The material parameters and input data for numerical simulations related to the governing equations are shown in Table 5.1. These are diffusion coefficient, initial concentration at the top surface, and initial concentration in concrete pore solution of each ionic species, water-to-cement ratio, volume fraction of aggregate, and pore relative humidity. The numerical simulations are performed in non-saturated condition. This means the moisture gradient is taken into account for its effect on the diffusion of ionic species in concrete. The relative humidity condition used in numerical simulation is RH = 50% inside and RH = 100% outside of concrete sample. Thus, the moisture gradient moves from external to internal concrete specimen.

The geometry of concrete sample used in numerical simulation is shown in Fig. 5.2. It is a 3 cm by 5 cm concrete slab. The concrete slab is exposed to 0.5 mol/l NaCl and 0.5 mol/l $CaCl_2$ solutions on the top surface. The other boundaries are assumed to be insulated. The concrete sample is divided into 400 elements and 451 nodes by using isoparametric elements for finite element model.

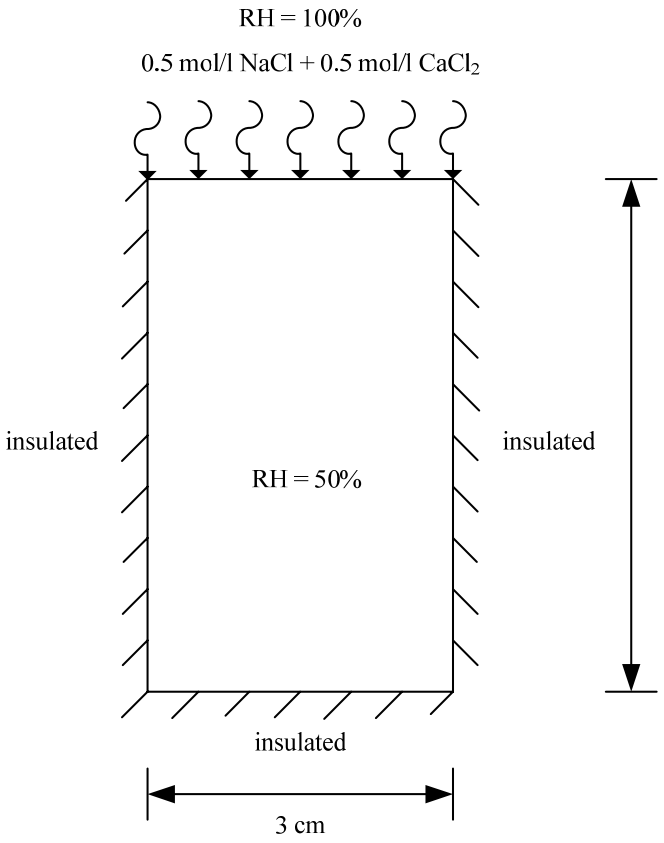

Fig. 5.2 Concrete sample used in the numerical model for non-saturated condition

Table 5.1 Material parameters and input data for concrete sample

Species	K	Na	Cl	OH	Ca
Charge number	+1	+1	-1	-1	+2
Diffusion coefficient, D_{ci}	$^{*}3.9\text{x}10^{-11}$ (m^2/s)	$^{*}2.7\text{x}10^{-11}$ (m^2/s)	D_{Cl} (Eq. 10)	$^{*}5.28\text{x}10^{-10}$ (m^2/s)	$^{\S}2.4\text{x}10^{-11}$ (m^2/s)
Initial condition at top surface of concrete sample	0	0.5 (mol/l)	1.5 (mol/l)	0	0.5 (mol/l)
Initial condition in pore solution	0.0995 (mol/l)	0.0389 (mol/l)	0	0.1384 (mol/l)	0
Water-to-cement ratio (w/c)	0.55				
Volume fraction of aggregate (g_i)	0.65				
Outside concrete sample	RH = 100%				
Inside concrete sample	RH = 50%				

The profile of free chloride concentration at different times of exposure is shown in Fig. 5.3. The depth of penetration is measured from the top surface of concrete sample. It can be seen from the Fig. 5.3 that the free chloride concentration decreases with increasing depth from the top surface. At the fixed depth, when the exposure time is longer the free chloride concentration is higher. Fig. 5.4 shows the distribution of total chloride with the time of exposure at different depths from the exposed surface. The trend of total chloride concentration increases with increasing time of exposure because free and bound chlorides tend to increase with longer times of exposure. At the fixed time of exposure, the total chloride concentration decreases with the increase of depth from top surface.

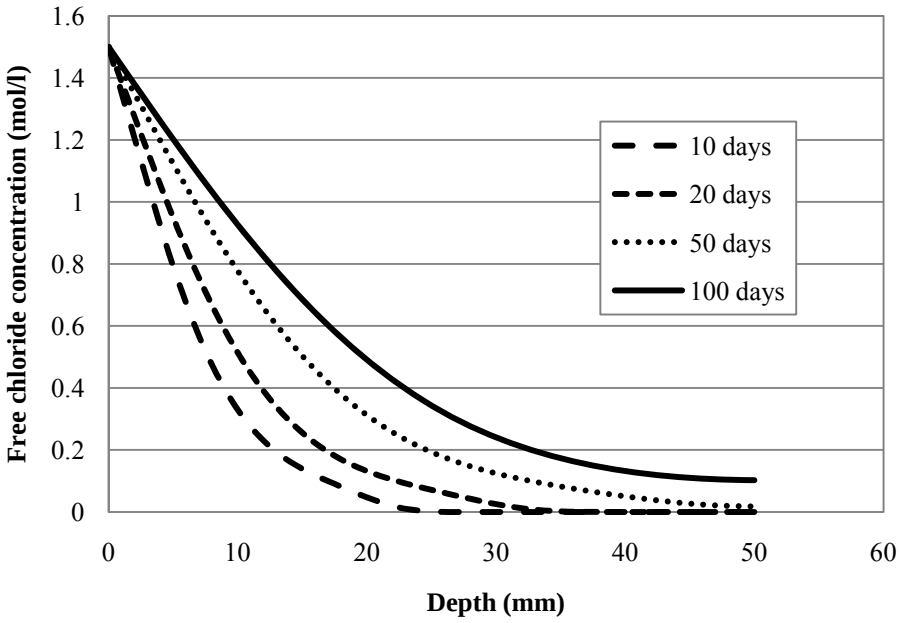

Fig. 5.3 Chloride profile at different time of exposure for non-saturated

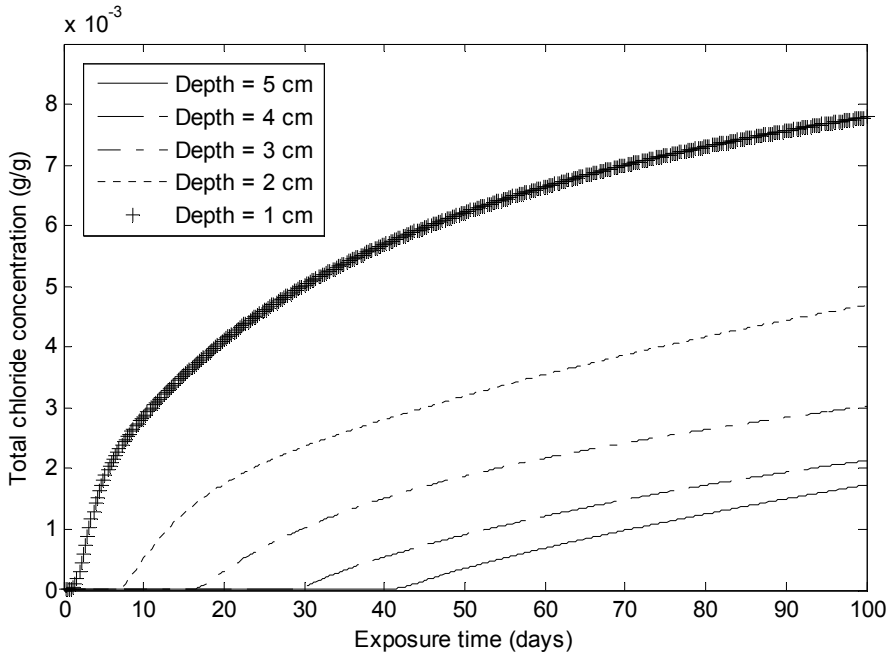

Fig. 5.4 The distribution of total chloride concentration with the exposure time at different depth from exposed surface for non-saturated condition

The trends of sodium and calcium concentration are similar to free chloride concentration because they have the same boundary conditions that the concentration at the exposed surface is higher than that inside of the specimen. This means the concentration gradients of chloride, sodium, and calcium are from outside to inside concrete sample. The plots of sodium and calcium concentration with the depth at different times of exposure are shown in Figs. 5.5 and 5.6, respectively.

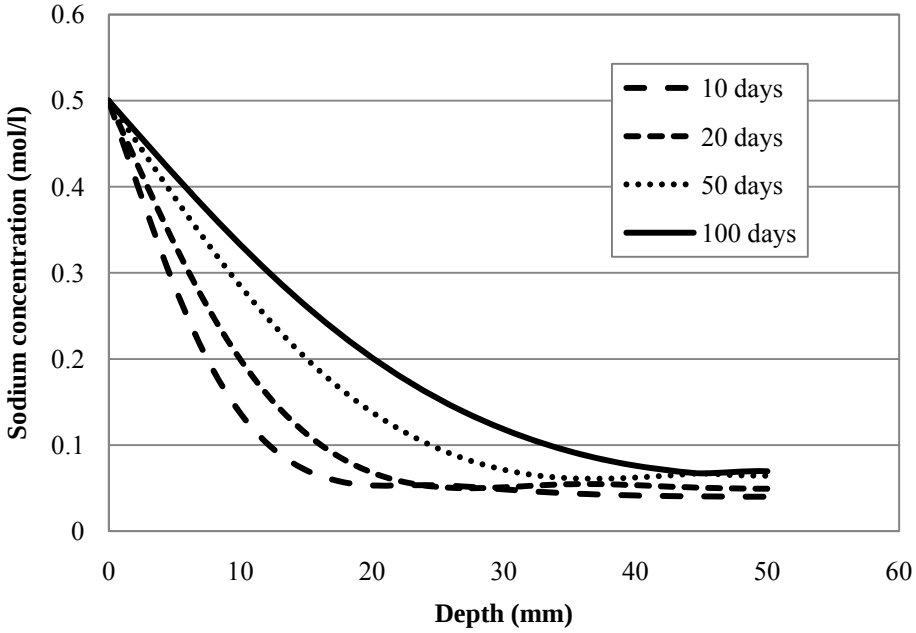

Fig. 5.5 Sodium profile at different time of exposure for non-saturated condition

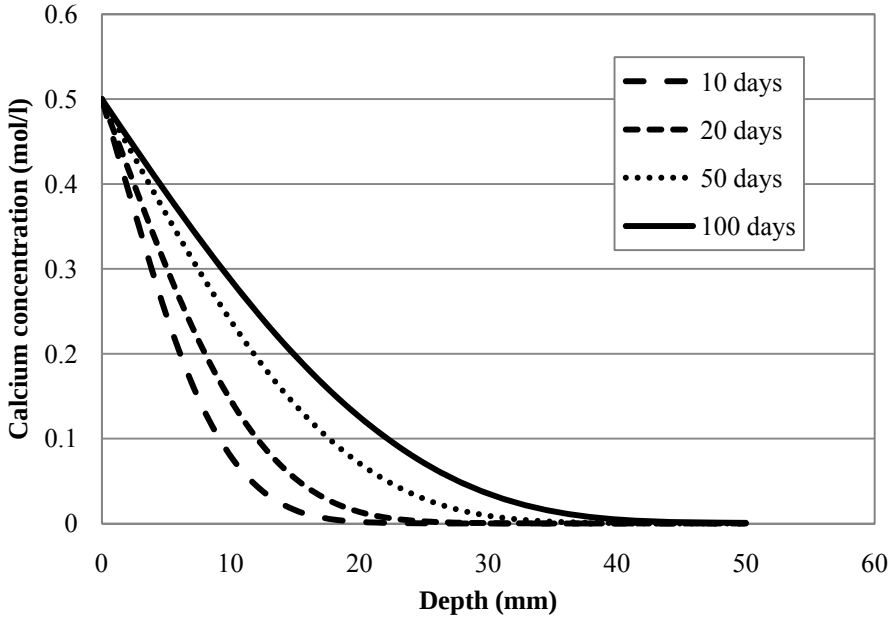

Fig. 5.6 Calcium profile at different time of exposure for non-saturated condition

In contrast to chloride, sodium, and calcium concentration profiles, the trends of concentration gradient of potassium and hydroxyl ion are from inside to outside of concrete sample because they have the inside concentration higher than that of the exposed surface, and there is no sources of potassium and hydroxyl solution on the top surface. The variations of potassium and hydroxyl concentration with depth at different times of exposure are shown in Figs. 5.7 and 5.8, respectively. It is noticed from Figs. 5.7 and 5.8 that the concentration of potassium and hydroxyl ions increase with the increase of depth from the top surface. The maximum values occur on the concentration profiles of these two ions due to the moisture effect. As seen, these values increase with increasing of exposure times. This is because the moisture gradient increase gradually when the time of exposure increases and accelerates the penetration rate of chloride, sodium, and calcium ions so that potassium and hydroxyl ions tend to diffuse to a certain depth, maximum concentration, to satisfy the electroneutrality condition. However, this value drops at 100 days of exposure because the moisture becomes saturated at 100 days which can be seen from the moisture profile in Fig. 5.9.

Fig. 5.9 shows the moisture profile at 10, 20, 50 and 100 days of exposure. It can be seen from the figures that moisture gradient moves from exposed surface to inside of concrete specimen. In fact, the moisture gradient can carry chloride, sodium, and calcium ions and diffuse simultaneously accelerating the penetration rate of these ions.

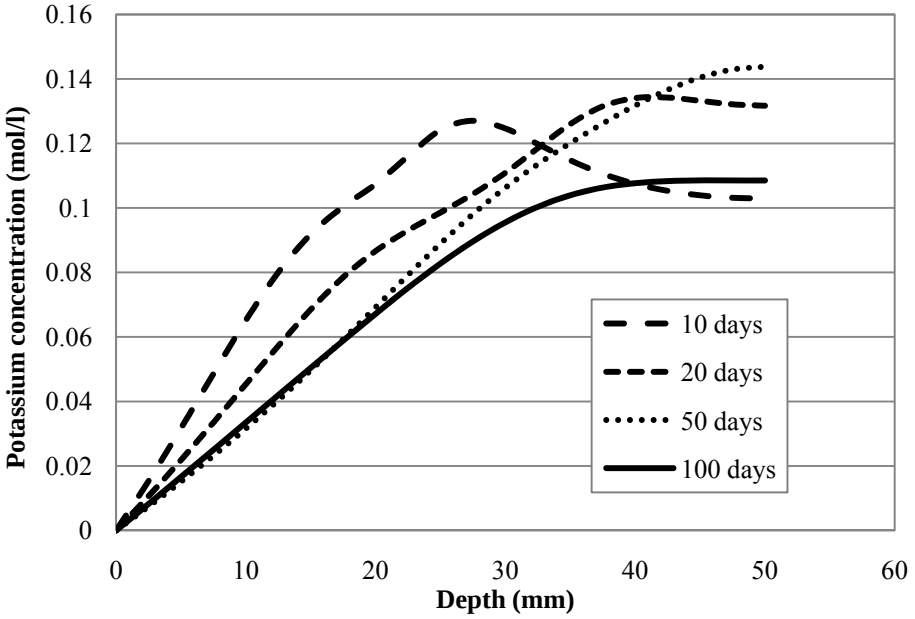

Fig. 5.7 Potassium profiles at different times of exposure in non-saturated concrete

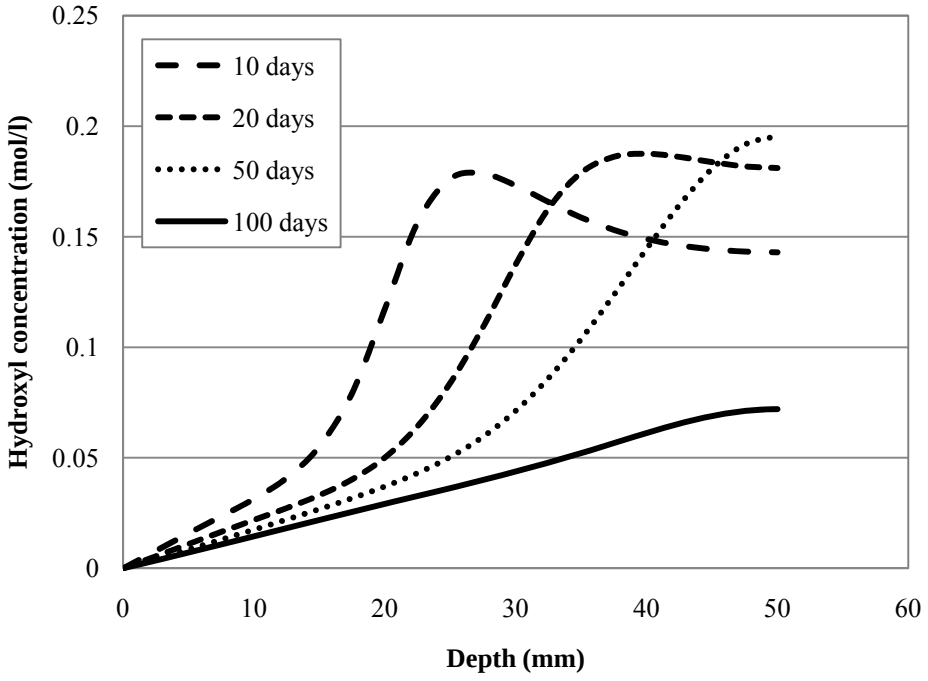

Fig. 5.8 Hydroxyl profiles at different times of exposure in non-saturated concrete

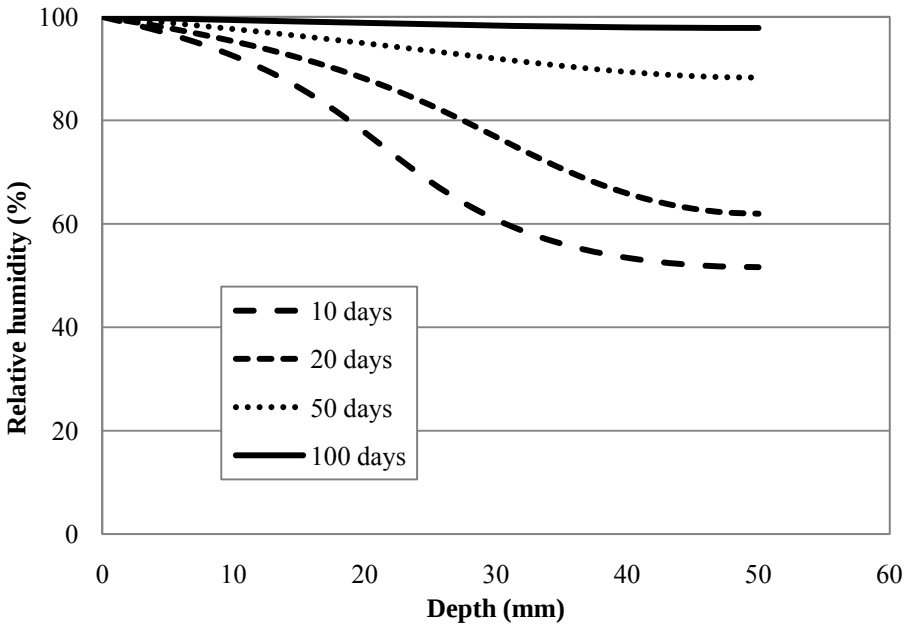

Fig. 5.9 Moisture profiles at different times of exposure in non-saturated concrete

Figs. 5.10, 5.11, 5.12, 5.13, and 5.14 show the chloride, sodium, calcium, potassium, and hydroxyl concentration at 10 days of exposure for non-saturated concrete compared with the saturated condition. It is noticed that moisture has influence on the diffusion of multi-ionic species in concrete by accelerating the penetration rate of chloride, sodium, and calcium. For potassium and hydroxyl ions, their diffusion rates are slowed down by moisture gradient at the depth close to the exposed surface so that the concentration of these two species is higher in the case of saturated condition. On the other hand, below this depth, the concentrations of potassium and hydroxyl for non-saturated concrete are higher than saturated condition because of electroneutrality condition.

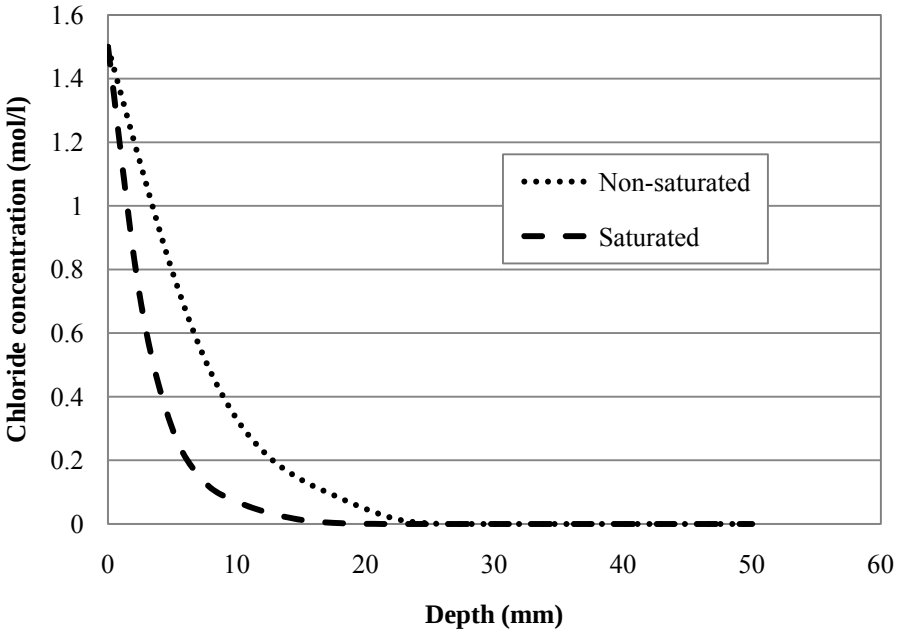

Fig. 5.10 Chloride profiles at 10 days of exposure

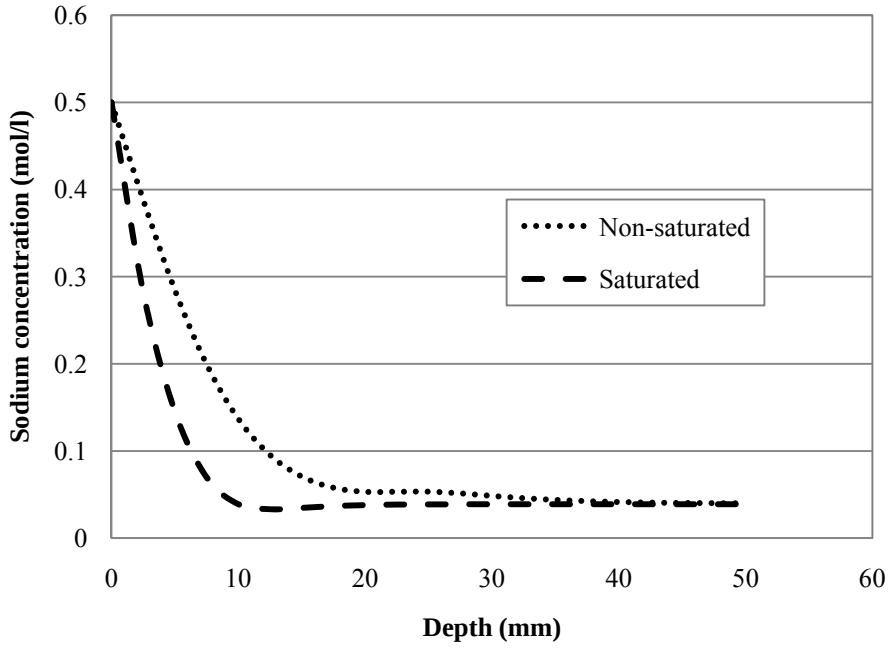

Fig. 5.11 Sodium profiles at 10 days of exposure

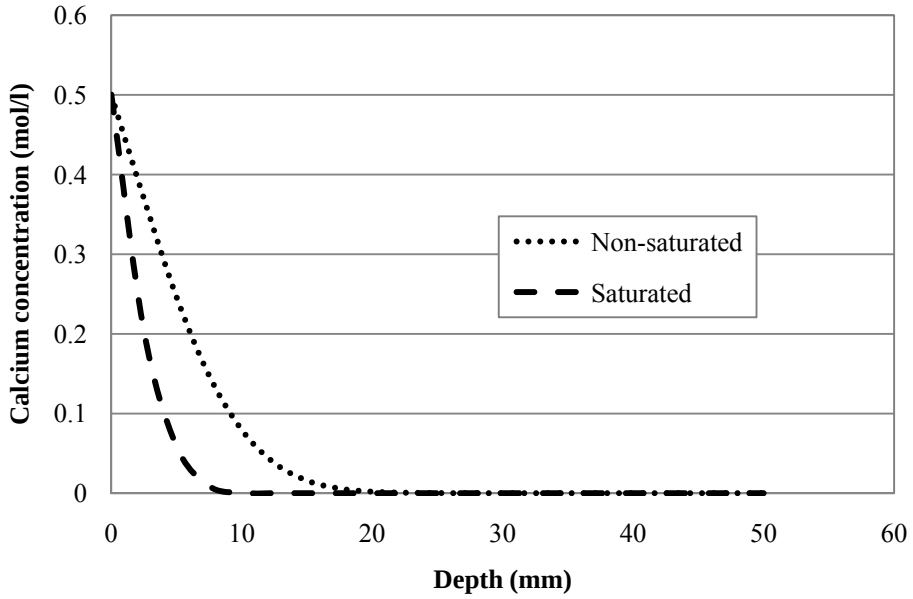

Fig. 5.12 Calcium profiles at 10 days of exposure

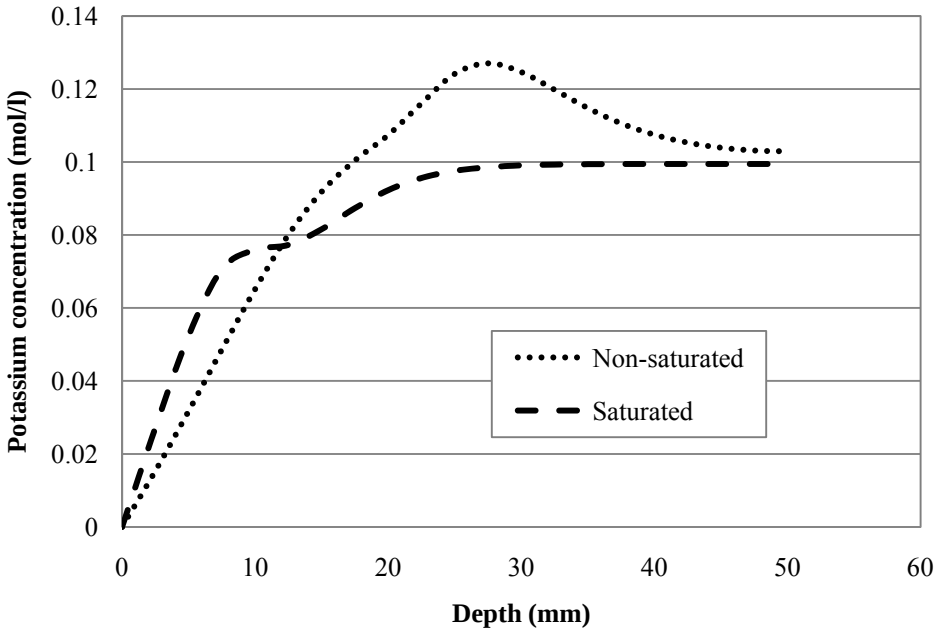

Fig. 5.13 Potassium profiles at 10 days of exposure

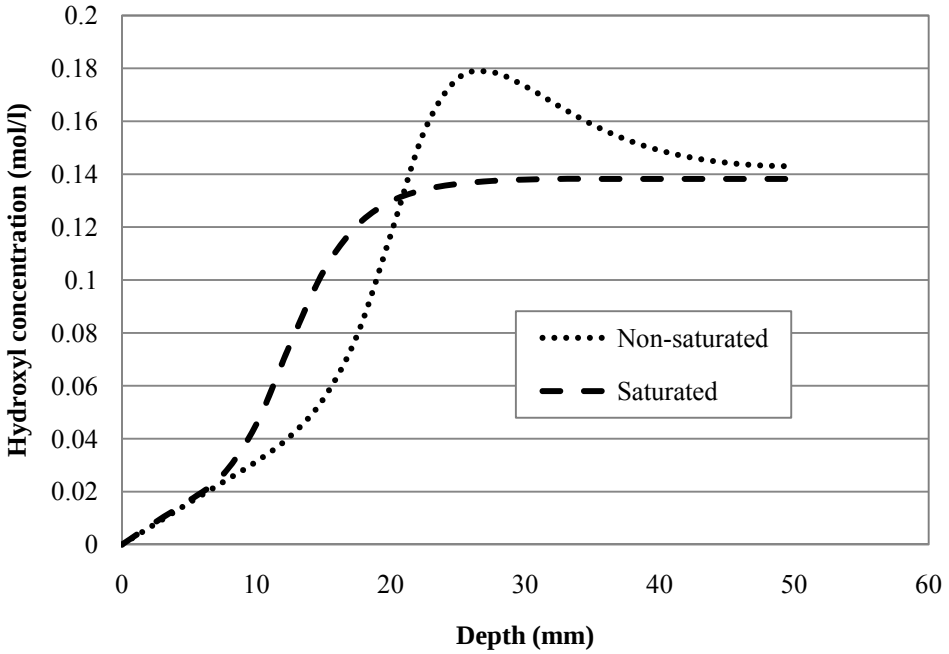

Fig. 5.14 Hydroxyl profiles at 10 days of exposure

For validation, the numerical results obtained from the present model are compared with the test data conducted by Andrade and Whiting (1996). The experimental results are the chloride concentration obtained from the 90-day ponding test of two types of concrete with different water-cement ratios, w/c = 0.4 and 0.6. A comparison is shown in Fig. 5.15. As illustrated, the total chloride concentration predicted by the present model is in very good agreement with test data.

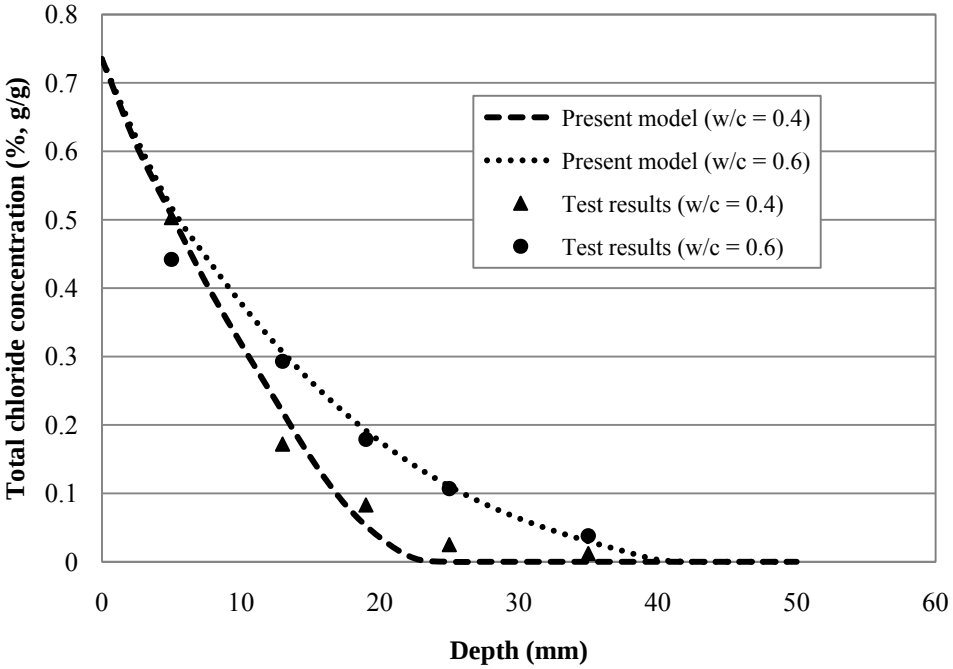

Fig. 5.15 A comparison between numerical results and test data

5.6 Conclusions

1. A mathematical model is developed based on the Nernst-Planck equation and electroneutrality condition to solve for the ionic-induced electrostatic potential. The model is then used to simulate the multi-species deicing salts penetration into non-saturated concrete structures by taking into account the moisture effect. The moisture diffusion is studied and simulated based on the material models of diffusion mechanisms in cement paste and aggregate.

2. The material parameters related to chloride and moisture diffusion in concrete are taken into account. These parameters are chloride diffusion coefficient, chloride binding capacity, moisture diffusion coefficient, moisture capacity, and coupling parameters between ions and moisture.

3. The model considers the two-way fully coupled moisture and ion diffusion, and the coupling parameters are introduced by incorporating in the governing equations as explicit terms.

4. Moisture diffusion has significant effect on penetration of deicing salts into concrete by accelerating the penetration rate of chloride, sodium, and calcium ions which are in the same direction as moisture gradient. However, hydroxyl and potassium ions are slowed down by the moisture gradient since the gradients of these two types of ions are in the opposite direction as the moisture gradient.

5. The difference due to the moisture effect can be observed from the concentration profiles of chloride, sodium, calcium, potassium, and hydroxyl ions in non-saturated condition when compared with saturated case.

6. The numerical simulations are performed using finite element method and the results are compared with an available chloride ponding test of 90-days to validate the model. It is found that the numerical results agree very well with the experimental results. Thus, the model can be used to predict satisfactorily the penetration of aggressive chemicals such as deicing salts into non-saturated condition. By using this model, the corrosion initiation time and the maintenance and/or rehabilitation time of reinforced concrete structure with chloride-induced corrosion damage can be estimated.

CHAPTER 6

TEMPERATURE EFFECT ON CHLORIDE PENETRATION INTO SATURATED CONCRETE STRUCTURES

6.1 Introduction

Chloride-induced corrosion of reinforcing steel is one of the major problems in long-term durability of concrete structures. The problem occurs particularly in reinforced concrete strutures subjected to chloride-rich environments such as marine structures in splash and tidal zones; bridge decks, and parking garages exposed to deicing salts. Chloride ions ingress into concrete through interconnected pore network. When chloride ions penetrate into concrete and reach the critical value the corrosion of reinforcement can start and eventually causes deterioration of reinforced concrete structures. Due to large volume expansion of rust formation, it may cause cracking, spelling, and determination of concrete cover. These damages can result in reducing load-bearing capacity of structures.

It is necessary to develop a mathematical model to predict chloride ions transport in concrete material. In saturated condition, Chloride penetration into concrete is mainly due to concentration gradients of the diffusing ions. However, in reality, reinforced concrete structures are often exposed to climate change conditions that means surrounding mositure and temperature is not constant. For nonsaturated condition, the moisture transport has a significant effect on the chloride diffusion in concrete (Ababneh, 2002; Abarr, 2005; Suwito, 2005). Similarly, moisture diffusion is influenced by chloride penetration by accerlating rate of moisture diffusion (Abaneh

and Xi, 2002). In the concrete, not only the moisture diffusion has an influence on the chloride diffusion, the temperature variation also has effect on the chloride penetration. This has been investigated by many researchers based on experimental and numerical studies.

Isteita (2009) conducted an experimental study on temperature effect on chloride diffusion in concrete. It was found that the thermal-coupled effect contributed significantly to chloride penetration mechanism. With increasing of temperature, rate of chloride penetration increased. A coupling parameter for the effect of temperature on the chloride diffusion was also developed in the study. Over the years, there have been mathematical and numerical models developed to investigate chloride ions transport in concrete. The formulation of mathematical model for diffusion mechanism can be performed following two approaches, One is basel on Fick's first and second laws which is related to the diffusion mechanism at macroscopic level (Saetta et at., 1993, 1995; Frey et at., 1994; Sergi et at., 1992; Berke and Hicks, 1994; Tang and Nilsson, 1992; wee et at., 1997; Ababneh, 2002; Xi and Bazant, 1999; Suwito, 2005). Lately, the other formulation of ion transport in concrete is derived based on the Nernst-Planck equation which is taken into account the electro-chemical phenomena.

The Nernst-Planck equation has been widely used by many researchers to simulate ion transport in concrete material. Yu and Page (1996), Li and Page (1998, 2000) developed the mathematical model to simulate electrochemical chloride removal (ECR) from concrete and then Wang et al. (2005) applied the ECR model to perform the simulation of the mechanism of chloride ingress into concrete. Samson et al. (1999) conducted a theoretical study on ion diffusion mechanisms in cement-based materials. Later on, Samson and Marchand (1999) presented the mathematical model of ion diffusion mechanisms in porous media based on the Nernst-Planck equation and Extended Nernst-Planck equation which is accounted for chemical

potential gradient. Recently, Marchand (2001) and Samson and Marchand (2007) developed a simulation model of multiionic transport in unsaturated cement-based materials exposed to aggressive chemical environments called STADIUM. The mechanism of chloride penetration into nonsaturated concrete was also investigated by Nguyen et at. (2006). The governing equations of the proposed model were derived based on the Nernst-Planck and electroneutrality equations. Then, the numerical results otbained from the model were compared with test data and a good agreement was observed.

As the actual condition of concrete structures exposed to chloride environments are most likely in non-isothermal condition rather than isothermal condition, the temperature variation may have significant effect on the transport properties and chemical reaction of ions. At one hand, the rate of penetration and chemical reaction of ions are slowed down with lowering the temperature. On the other hand, at higher temperature, the driving force due to temperature gradient can increase the transport rate and chemical reaction of ions (Samson and Marchand, 2007). This phenomena was investigated by Isteita (2009) and it was found that the rate of chloride penetration into concrete was accerlerated by increasing temperature.

In this study, we will develop a mathematical model to predict the influence of temperature on chloride penetration into saturated concrete structures. The moisture diffusion is not considered in the model. The governing equation of chloride ions is derived based on Nernst-Planck equation which takes into account the electrostatic coupling between chloride ions and ions in the concrete pore solution, Na^+, K^+, and OH^-. And, the governing equation of temperuture is described in terms of Fouries's law. Differing from those models proposed by saetta et al. (1993) and Martin-Perez et al. (2001), the present model takes into account the coupled effect of temperature on chloride diffusion by considering an explicit term in the ionic flux equations.

There is a coupling parameter in the term, and the parameter was obtained from Isteita study (2009). The governing equations are solved by the finite element method. The numerical results obtained from the model are compared with available test data. Then, the model can be applied to predict chloride penetration into saturated concrete structures in non-isothermal condition.

6.2 Basic Formulation

The formulation of chloride ions and other species in concrete pore solution, Na^+, K^+, and OH^-, is based on the Nernst-Planck equation. The governing equation of heat flow is described by the Fourier's law of heat conduction. The transport of all ionic species is associated with the coupled effect of temperature. The coupling parameter is proposed and then incorporated in the governing equations. In this study, we focus on the effect of temperature on chloride ingress into concrete in saturated condition.

The flux of each ionic species through a unit area of porous media depends on diffusion and migration mechanisms, the Nernst-Planck equation, can be expressed as:

$$J_i = -D_i \nabla C_i - z_i D_i \left(\frac{F}{RT} \nabla \phi \right) C_i \qquad (6.1)$$

where J_i is the flux of species i, D_i is the diffusion coefficient of species i, C_i is the concentration of species i in the solution, z_i is the charge number of species i, F is the Faraday constant, R is the gas constant, T is the temperature of material, and Φ is the electrostatic potential. The mass balance equation for each species can be written as:

$$\frac{\partial(C_i + S_i)}{\partial t} = -\nabla J_i \tag{6.2}$$

By substituting Eq. (6.1) into Eq. (6.2), it gives:

$$\frac{\partial(C_i + S_i)}{\partial t} = \nabla\left(D_i \nabla C_i + z_i D_i \left(\frac{F}{RT} \nabla \phi \right) C_i \right) \tag{6.3}$$

in which S_i is the concentration of bound ions of species *i*. The transport process of ions is described as Eq. (6.3) which comprises of two mechanisms. The first term on the right-hand side represents the diffusion mechanism due to ionic concentration gradient. The other is the migration mechanism of ionic species induced by electrostatic potential gradient (Wang et al., 2005).

The concentration of bound ions is applied to only chloride not for other species (Na^+, K^+, and OH^-). When chloride ions penetrate into concrete, some of them can have chemical reaction with cement components and attach to the pore wall called bound chloride. The others are free to move through interconnected pores in concrete which become free chloride. Thus, the mass balance equation of chloride ions can be formulated in terms of bound and free chloride concentration. The summation of bound and free chloride concentration is total chloride which can be defined and written as a form of chloride binding capacity as Eq. (6.4).

$$\frac{\partial C_t}{\partial C_f} \frac{\partial C_f}{\partial t} = \nabla\left(D_i \nabla C_i + z_i D_i \left(\frac{F}{RT} \nabla \phi \right) C_i \right) \tag{6.4}$$

where C_t is the total chloride concentration (in grams of total chloride per gram of concrete, g/g), C_f is free chloride concentration, and $\frac{\partial C_t}{\partial C_f}$ is the chloride binding capacity. Determination of chloride binding capacity will be discussed in the part of material model.

In order to solve the Nernst-Planck equation, another relation accounted for electrostatic potential induced by ionic interaction is required. The electrostatic potential can be determined based on three different assumptions. Samson and Marchand (2007) solved the electrostatic potential for ions transport in cement-based materials by using Poisson's equation. As mentioned by Samson et al. (1999), the Poisson's equation can be used in more general cases. Differing from those researchers, in this study, the elctroneutrality approach is employed to solve for the electrostatic potential. This can be expressed as:

$$\sum_{i=1}^{n} C_i z_i = 0 \qquad (6.5)$$

in which C_i is the concentration of species i, z_i is the charge number of species i, and n is the number of ionic species. The main advantages of using electroneutrality condition rather than Poisson's equation are to simplify the governing equations, reduce computational time, and avoid difficulty in computational schemes because it includes a very large number, $\frac{F}{\varepsilon} \approx 10^{16}$ (Wang et al., 2005; and Nguyen et al., 2006). The comparison among nil current, Poisson's equation, and electroneutrality condition used in modeling of chloride penetration into concrete was investigated in chapter 4. The study showed a good agreement of concentration profiles of ions with acceptable results.

For the heat flow in concrete material, the heat flux can be simply expressed as the well-known Fourier's law of heat conduction equation:

$$J_Q = -D_{T-T}\nabla T \tag{6.6}$$

in which J_Q is the heat flux, $D_{T\text{-}T}$ is the thermal diffusivity of concrete, and T is temperature. The mass balance equation of heat flow is written as:

$$\frac{\partial Q}{\partial t} = -\nabla J_Q \tag{6.7}$$

Combining Eqs. (6.6) and (6.7), and decoupling the heat capacity from the total heat, then the partial differential equation (PDE) governs the heat flow in concrete can be defined as:

$$\frac{\partial Q}{\partial t} = \frac{\partial Q}{\partial T}\frac{\partial T}{\partial t} = \nabla\left(D_{T-T}\nabla T\right) \tag{6.8}$$

where $\frac{\partial Q}{\partial T}$ is the heat capacity of concrete. One can see from the Eq. (6.8) that heat flow in concrete is temperature dependent. In order to take into account the temperature effect on the transport of ions in concrete, the mass balance equations of each ionic species need to be reformulated by incorporating the coupling parameter in the equations described as:

$$\frac{\partial(C_i + S_i)}{\partial t} = \nabla\left(D_i \nabla C_i + z_i D_i \left(\frac{F}{RT} \nabla \phi \right) C_i + D_{i-T} \nabla T \right) \tag{6.9}$$

in which $D_{i\text{-}T}$ is the coupling parameter due to influence of temperature on ions diffusion. This parameter was developed based on the experimental study of temperature effect on chloride penetration into saturated concrete by Isteita (2009). The results from the experiment showed that the parameter is not constant but depends on chloride concentration, the aging of concrete, and temperature. In order to simplify the numerical simulation, we apply the value of the coupling parameter obtained from Isteita study (2009) to all species.

6.3 Material Models

In order to solve the governing equations, Eqs. (6.8) and (6.9), the material parameters must be defined. The chloride diffusion coefficient and chloride binding capacity are introduced in chapter 4. In this chapter, the coupling parameters will be discussed.

6.3.1 Coupling Parameter ($D_{i\text{-}T}$)

The coupling parameter presented in this study was proposed by Isteita (2009). The parameter was evaluated based on the experimental study of temperature effect on chloride penetration into saturated concrete. The results from the experiment showed that effect of temperature on chloride diffusion is significant and it should be taken into account the coupled effect of temperature on chloride diffusion in concrete. The influence of temperature on ions diffusion is related to Soret effect, thermal diffusion phenomena, which is the occurrence of a diffusion flux due to the temperature gradient. Then, the coupling parameter was derived by using a multifactor approach. It was also found that the coupling parameter is not constant but

depends on chloride concentration, aging of concrete, and temperature. This can be obtained by curve fitting of the test data written as:

$$D_{Cl-T} = aC_f f_1(t) f_2(T) \tag{6.10}$$

where *a* is the constant which can be estimated by curve fitting at different ages of concrete and temperature conditions on exposed surface. The first factor, $f_1(t)$, is the factor accounting for the effect of the aging of concrete which is relevant to hydration reactions of cement paste. The second factor, $f_2(T)$, takes into account the influence of temperature which is described by the definition of Arrhenius's law. Based on the Soret effect, the heat flow in concrete can carry not only chloride ions but also other ions in concrete pore solution so that we may apply this coupling parameter to all ionic species (Cl^-, Na^+, K^+, and OH^-), it gives,

$$D_{i-T} = D_{Cl-T} = aC_f f_1(t) f_2(T) \tag{6.11}$$

in which D_{i-T} is the coupling parameter due to temperature effect on each ionic species *i*.

6.4 Numerical Simulation

Numerical simulations are performed to study the effect of temperature on chloride penetration into saturated concrete and to compare with the available test data. In order to obtain numerical results, the material models discussed in the previous sections are incorporated in the governing equations, Eqs. (6.8) and (6.9). In the present study, the finite element method is employed for solving partial differential equations of ions and temperature transport in concrete.

The study focuses on NaCl penetrating into concrete sample from the top surface. The ions in concrete pore solution, Na^+, K^+, and OH^-, are involved in the numerical analysis. The material parameters and input data for numerical simulations related to the governing equations are shown in Table 6.1. These are diffusion coefficients, initial concentration at the top surface, and initial concentration in concrete pore solution of each ionic species, water-to-cement ratio, and volume fraction of aggregate. The concentration of alkali ions in pore solution, Na^+ and K^+, are obtained from cement manufacturing company which provides the chemical composition of cement used in experimental study. The concentration of hydroxyl ion can be calculated by using electroneutrality condition which is equal to the summation of Na^+ and K^+. The numerical simulations are performed in saturated condition. This means relative humidity inside and outside concrete sample are equal to 100%. As a result, there is no effect from moisture gradient on multi-ions diffusion in the present study. The units of all ionic concentrations are in mol/l except for the total chloride which is in grams of chloride/gram of concrete weight (g/g) as mentioned in AASHTO T 259 and AASHTO T 260.

Table 6.1 Material parameters and input data

	Cl	Na	K	OH
Diffusion coefficient (m^2/s)	D_{Cl} (Eq. 10)	*$2.7x10^{-11}$	*$3.9x10^{-11}$	*$5.28x10^{-10}$
Initial pore solution concentration (mol/l)	0.0	0.0389	0.0995	0.1384
Heat capacity (J/kg ^oC)	§1,000			
Thermal diffusivity (W/m ^oC)	§2			
Chloride binding capacity	dC_b / dC_t (Chapter 4)			
Coupling parameter	$D_{i\text{-}T}$ (Eq. 6.11)			
Water-cement ratio	0.55			
Volume fraction of aggregate	0.65			
Cement type	I/II			

* The values are taken from Wang et al. (2005).

§ The values are taken from Isgor and Razaqpur (2004).

The geometry of concrete sample used in numerical simulation is shown in Fig. 6.1. It is a 3 cm by 5 cm concrete specimen. The concrete sample is exposed to 1 mol/l NaCl solution on the top surface. The other boundaries are assumed to be insulated. The moisture condition inside the concrete sample is assumed to be fully saturated, 100% RH. The concrete sample is divided into 400 elements and 451 nodes by using isoparametric elements for finite element analysis. In order to compare with available test data, the numerical simulations are studied in two cases accounted for two different temperature gradients as shown in Fig. 6.1. For Case 1, 2, and 3, the temperatures on the top surface of concrete samples are 50 ^{o}C, 35 ^{o}C, and 20 ^{o}C, respectively. And, the initial temperature inside specimens is specified as 20 ^{o}C. This means there is no temperature gradient for Case 3.

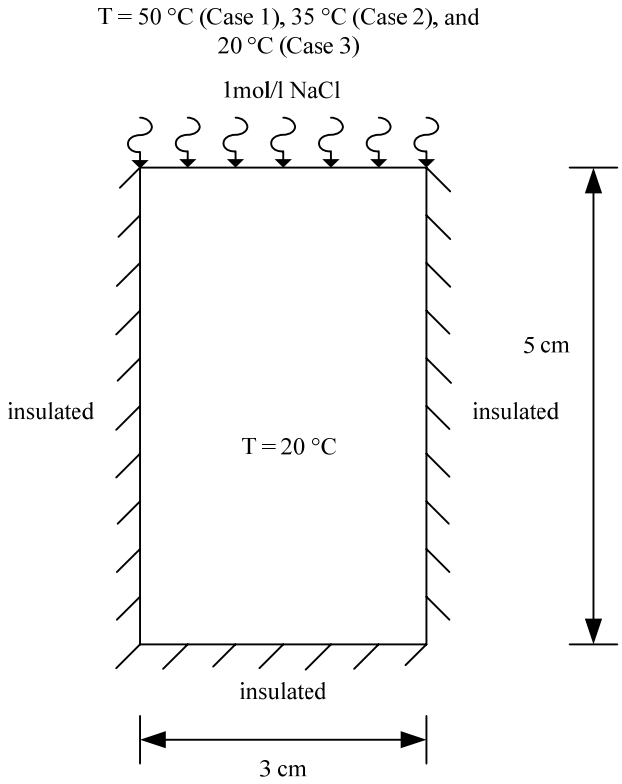

Fig. 6.1 Geometry and boundary conditions of concrete specimen used for numerical analysis

6.5 Numerical Results and Discussion

The concentration profiles of chloride, sodium, potassium, and hydroxyl ions exposed to 1 mol/l NaCl solution at different initial temperature conditions (T = 50 °C, 35 °C, and 20 °C) are shown in Figs. 6.2, through 6.13. At T = 50 °C, as shown in Figs. 6.2 through 6.5, the concentration of chloride is remarkably influenced by temperature, especially at the depth close to the exposed surface which can be seen as an instant increase from Fig. 6.2. After this point, the concentration decreases with increasing depth. Fig. 6.3 shows the concentration profile of sodium which decreases when the depth of penetration increases. This is because the concentration gradient of sodium and chloride move from the top to bottom surface.

For hydroxyl ions, the concentration increases when the depth of penetration increases, as shown in Fig. 6.4, due to the lower concentration at exposed surface than the internal concentration the concentration gradient of hydroxyl is in the reverse direction of chloride and sodium ions. The distribution profile of potassium starts from zero at the exposed surface and increases until reaching the peak, as shown in Fig. 6.5, which is the area adjacent to the exposed surface and then drops to the initial value of pore solution concentration. The main reason of this phenomenon is to balance the electroneutrality condition with negative charge ions, Cl^- and OH^-, which chloride has a very high concentration in this area, as mentioned in the previous.

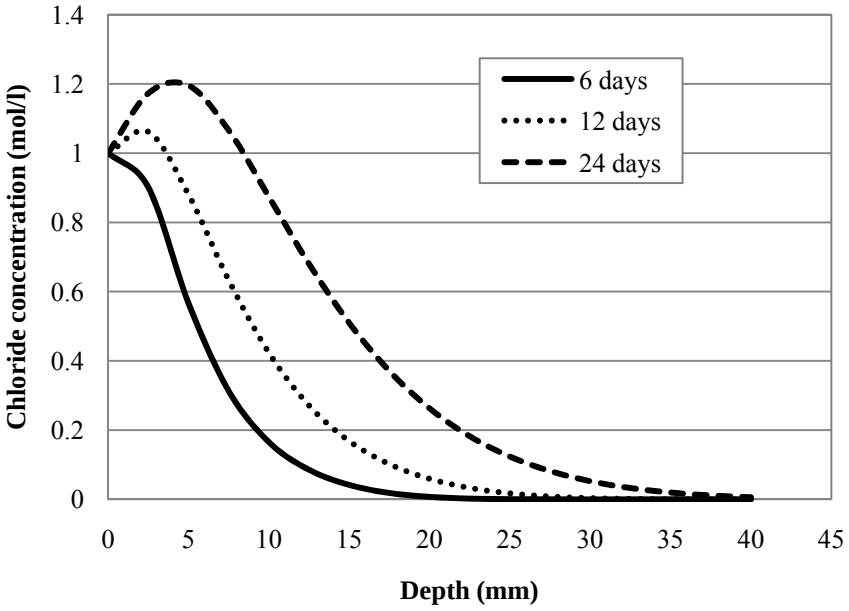

Fig. 6.2 Chloride concentration profiles at T = 50 °C

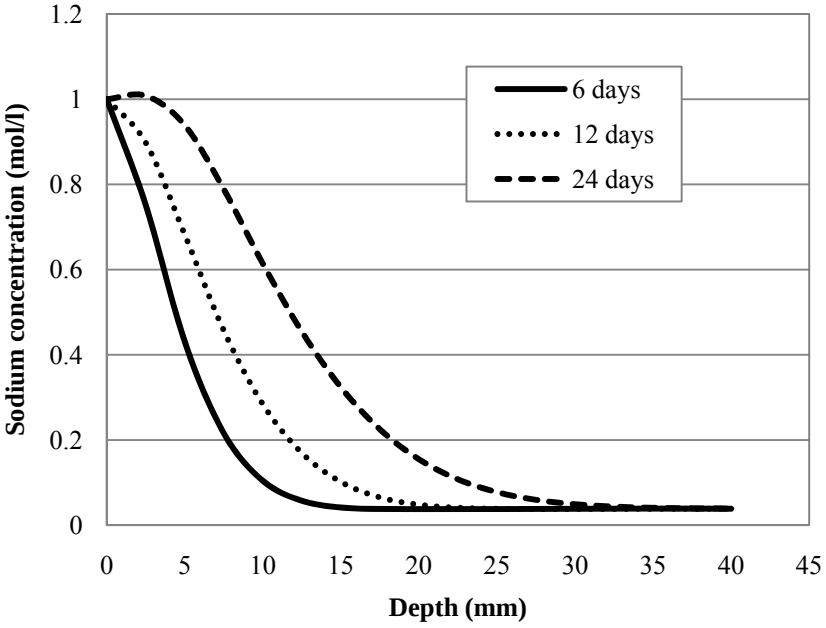

Fig. 6.3 Sodium concentration profiles at T = 50 °C

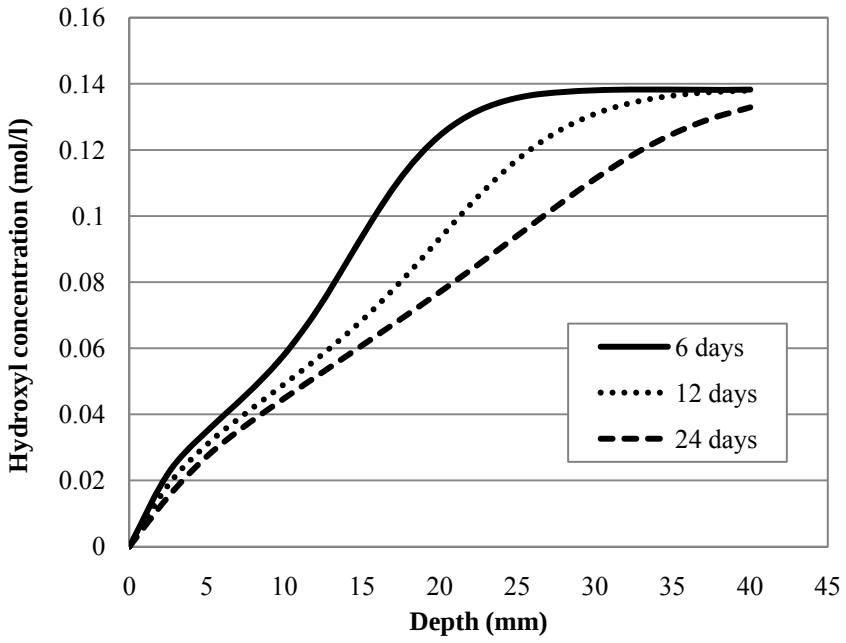

Fig. 6.4 Hydroxyl concentration profiles at T = 50 °C

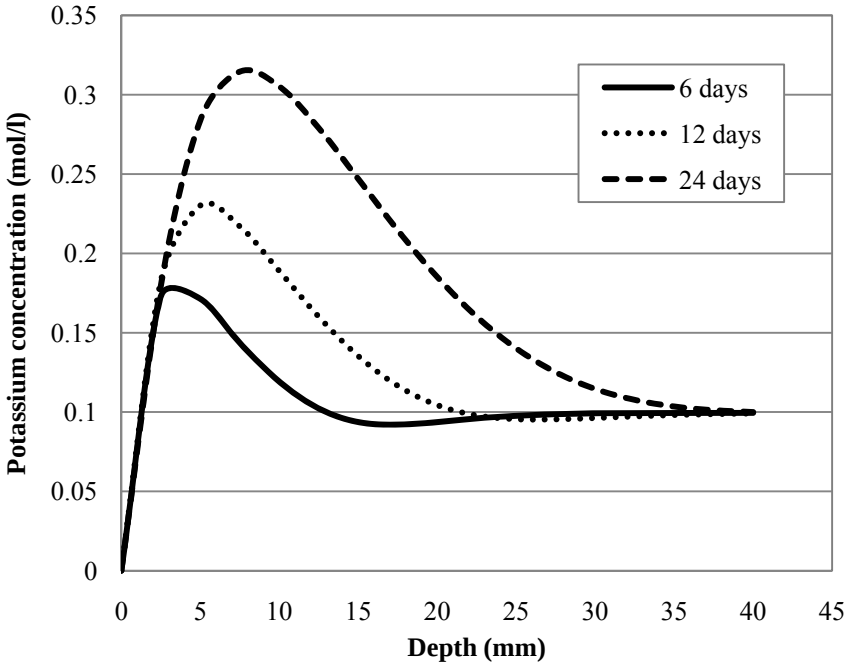

Fig. 6.5 Potassium concentration profiles at T = 50 °C

At T = 35 °C the coupled temperature effect has less influence than at T = 50 °C because of lower temperature gradient. As noticed from Figs. 6.6 and 6.7, there is no instant increase of chloride and sodium profiles at the depth close to exposed surface. Thus, at T = 35 °C, chloride and sodium concentrations decrease while Figs 6.8 and 6.9 show that hydroxyl and potassium concentrations increase with increase in the depth from exposed surface. Figs. 10 through 13 illustrate the distribution profiles of chloride, sodium, hydroxyl, and potassium ions at T = 20 °C. It is seen that the concentration profiles of these four ionic species have the same trends as obtained from T = 35 °C. The transport mechanism of four ions at T = 20 °C is diffusion and migration processes because of no temperature gradient, no coupled temperature effect taken into account. It is also noticed from Figs. 6.2 through 6.13 that the concentrations of chloride and sodium ions are higher, at any fixed temperature, with the longer period of exposure whereas the concentrations of potassium and hydroxyl ions tend to decrease, at any fixed depth, with an increase of exposure time.

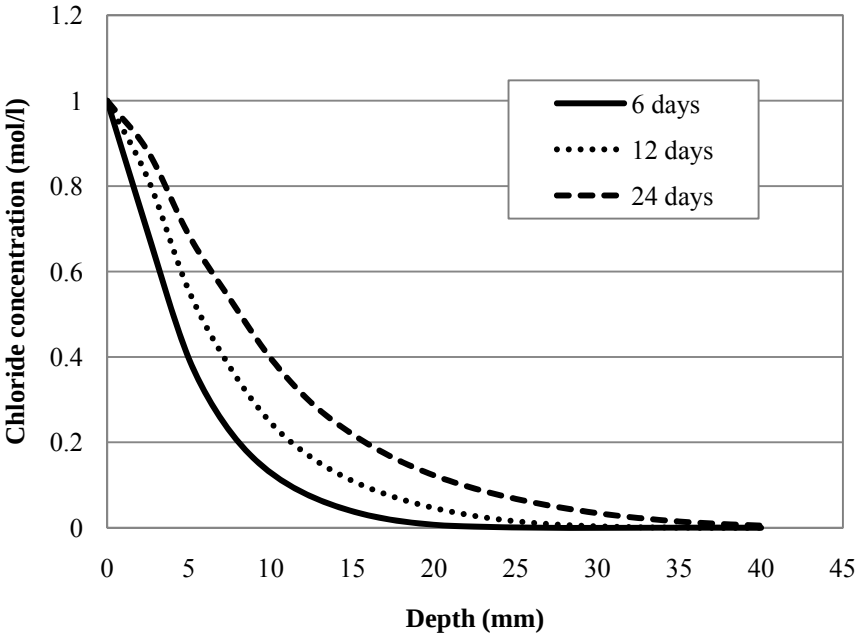

Fig. 6.6 Chloride concentration profiles at T = 35 °C

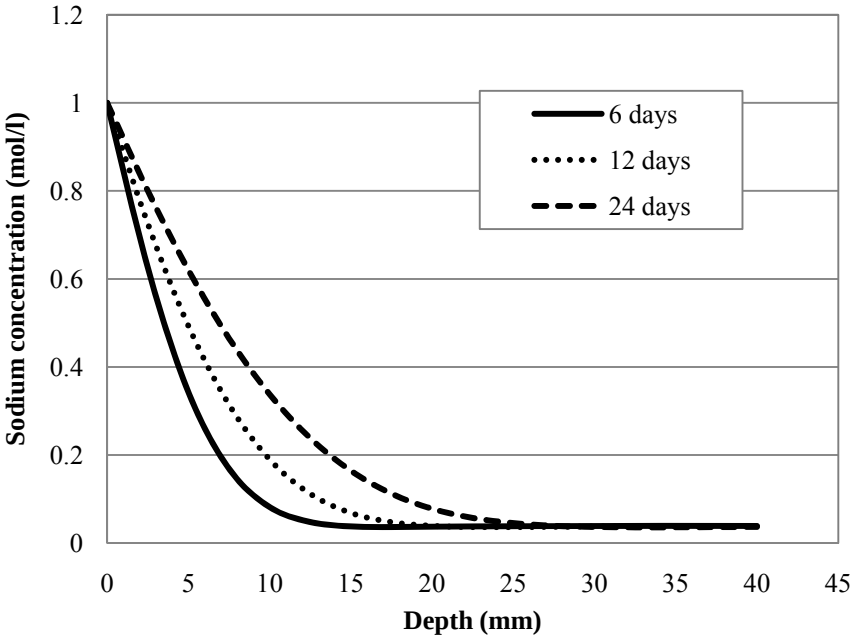

Fig. 6.7 Sodium concentration profiles at T = 35 °C

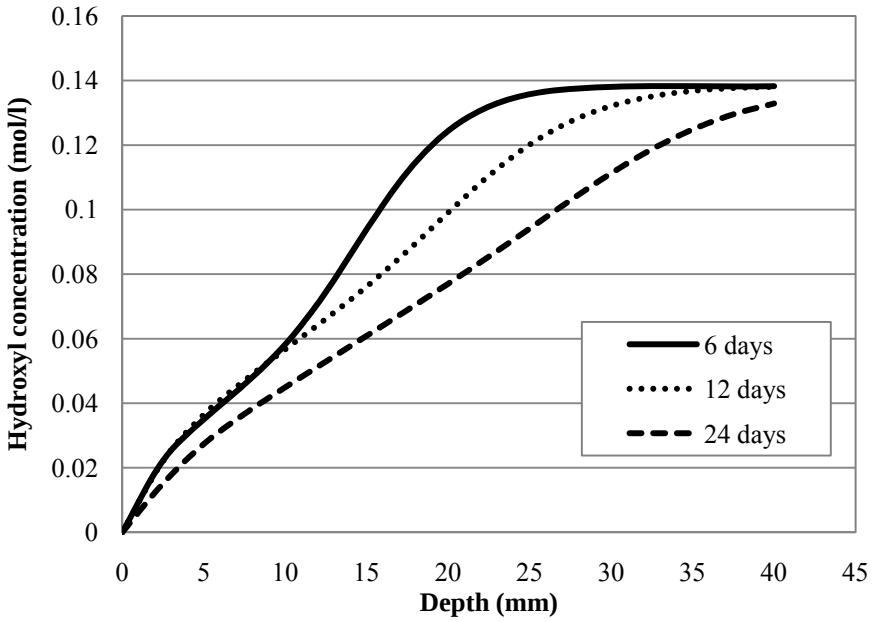

Fig. 6.8 Hydroxyl concentration profiles at T = 35 °C

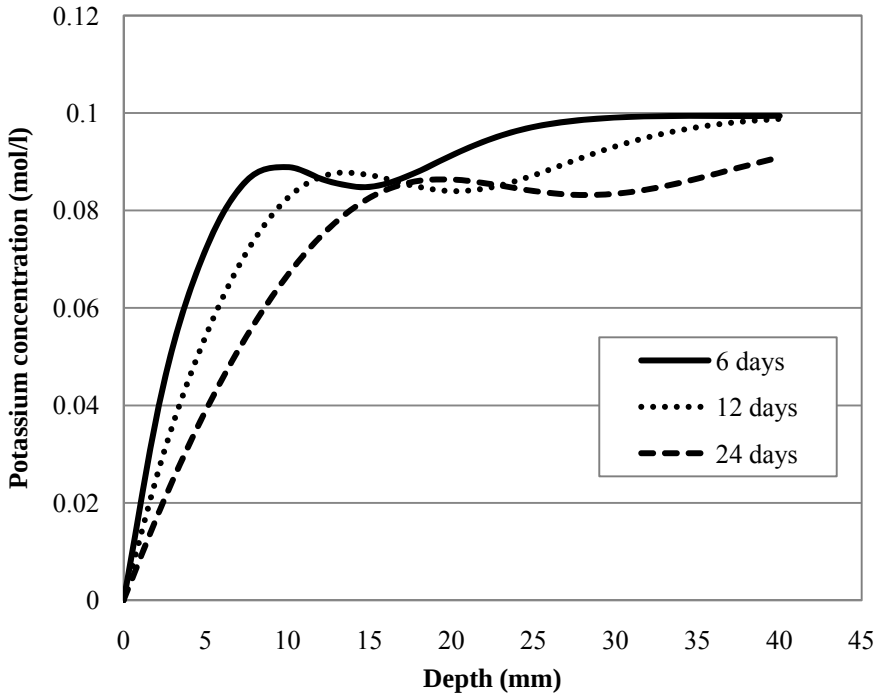

Fig. 6.9 Potassium concentration profiles at T = 35 °C

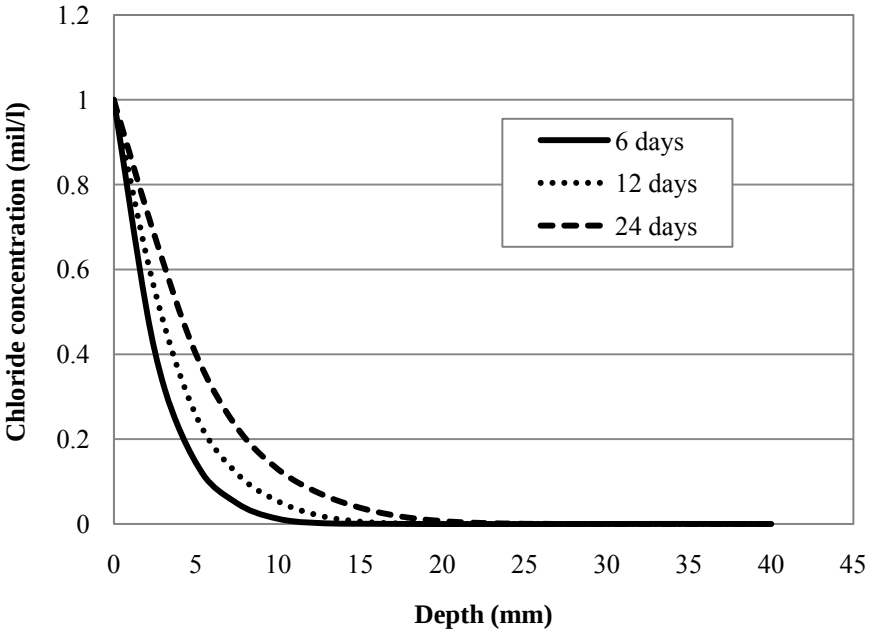

Fig. 6.10 Chloride concentration profiles at T = 20 °C

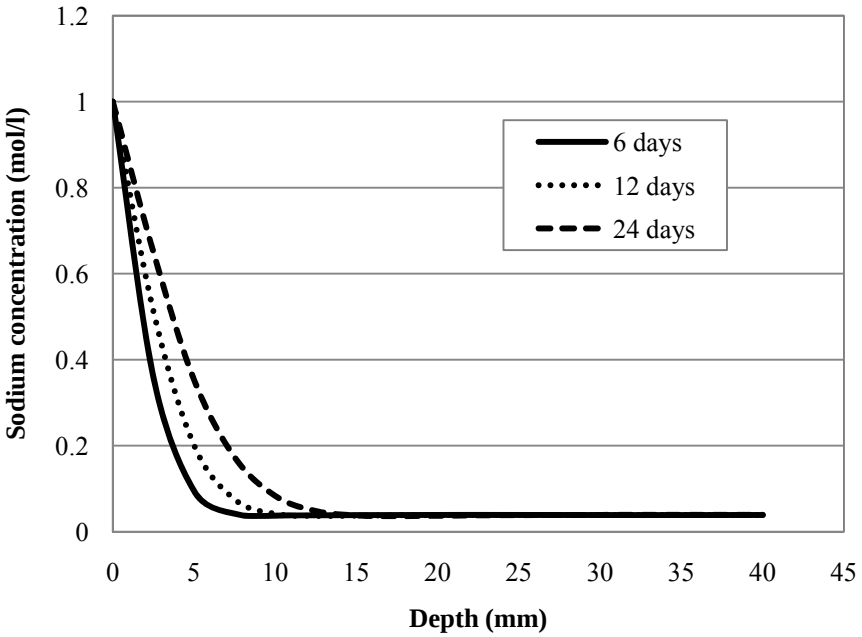

Fig. 6.11 Sodium concentration profiles at T = 20 °C

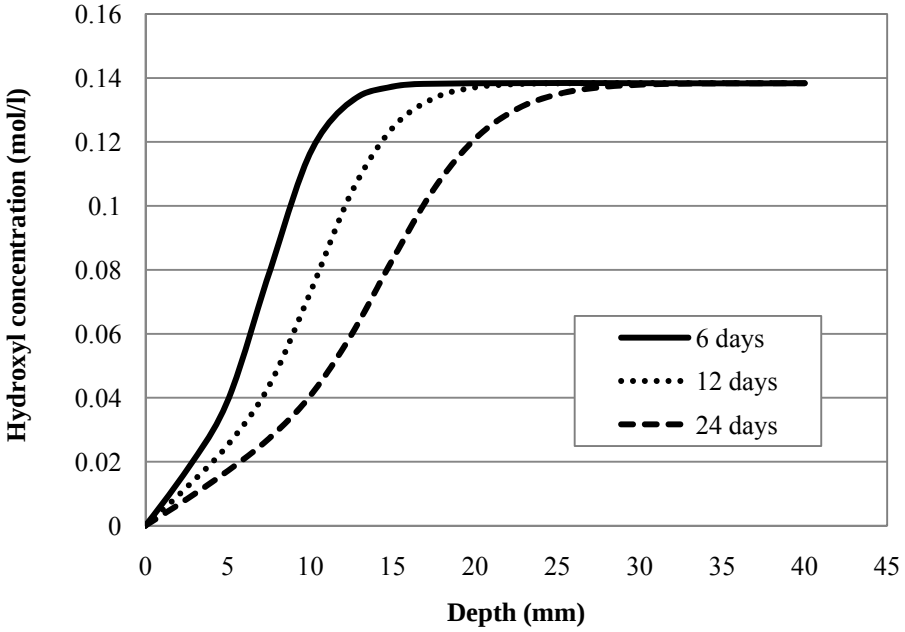

Fig. 6.12 Hydroxyl concentration profiles at T = 20 °C

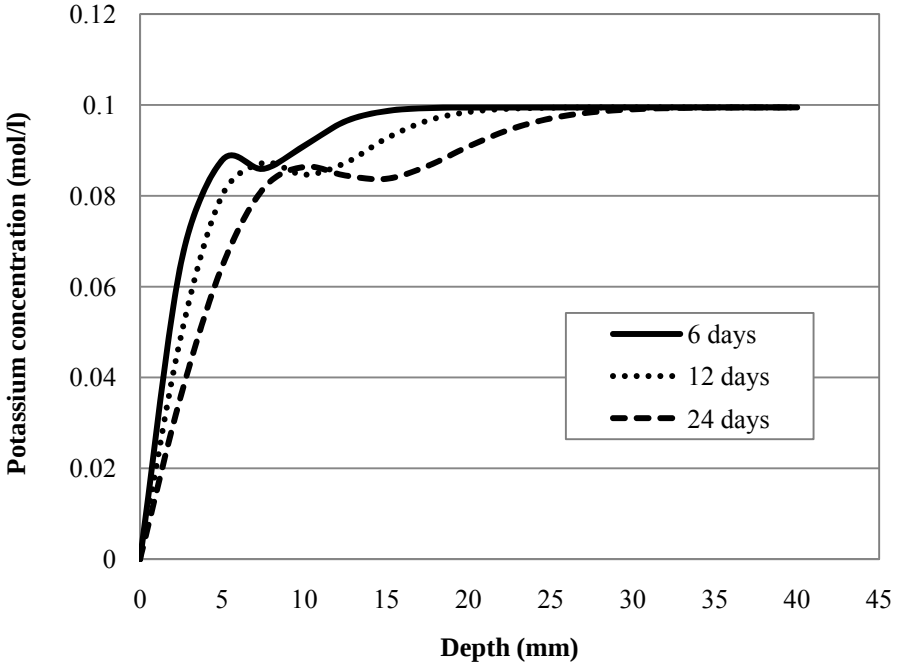

Fig. 6.13 Potassium concentration profiles at T = 20 °C

Figs 6.14 through 6.25 show the influence of temperature on ionic diffusion at different times of exposure (6, 12, and 24 days of exposure). One can see from these plots that the variations of concentration profiles of four ionic species can be observed with increasing of temperature. The higher the temperature gradient, the more significant of the coupled temperature effect. At 6, 12, and 24 days of exposure, with increasing temperature, the concentration of chloride and sodium ions increase, at any fixed depth, which is accelerated by temperature gradient. Moreover, at T = 50 °C, at any times of exposure, chloride and sodium ions are accelerated by higher temperature gradient when compared with T = 35 °C. Therefore, At T= 50 °C, hydroxyl ion diffuses faster to satisfy the electroneutrality condition with positive charge ions, Na^+ and K^+. From Figs. 16 and 24, hydroxyl concentration at T = 50 °C is slightly higher than at T = 20 °C at the depth close to exposed surface due to the electroneutrality condition. With increasing depth from this area, hydroxyl concentration at T = 20 °C is higher than both at T = 50 °C and 35 °C because the diffusion rate of hydroxyl ion is slowed down by temperature gradient. For potassium ion, when temperature increases from 20 °C to 35 °C the concentration at higher temperature is lower than the lower one, at any times of exposure. This is mainly due to the temperature flux is in the reverse direction of concentration gradient. However, when temperature reaches at T = 50 °C the concentration is higher than at T = 35 °C and 20 °C. This is because the transport mechanism of potassium is dominated by electroneutrality condition. As remarkably noticed from numerical results, we can conclude that the concentrations of four ionic species are significantly influenced by temperature.

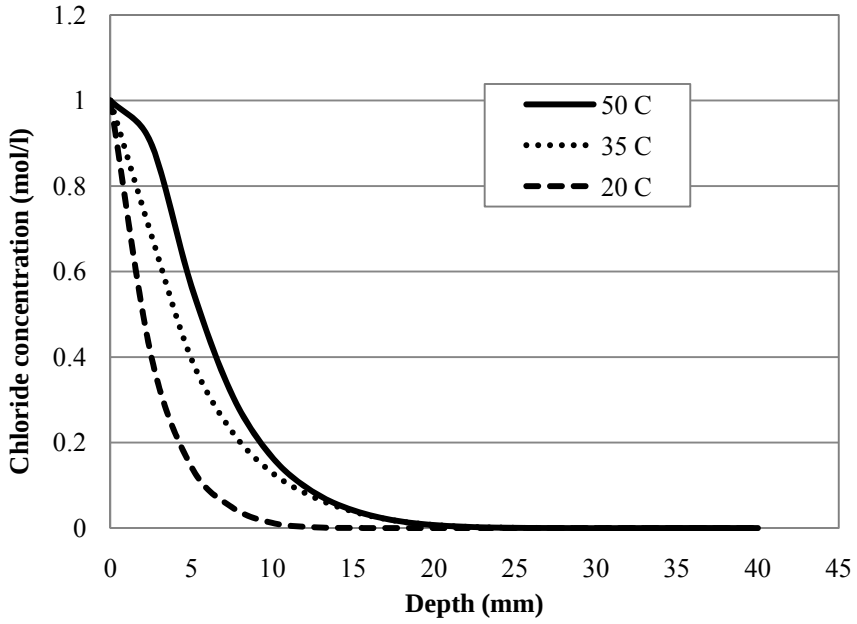

Fig. 6.14 Chloride concentration profiles exposed to 1 mol/l NaCl solution at 6 days

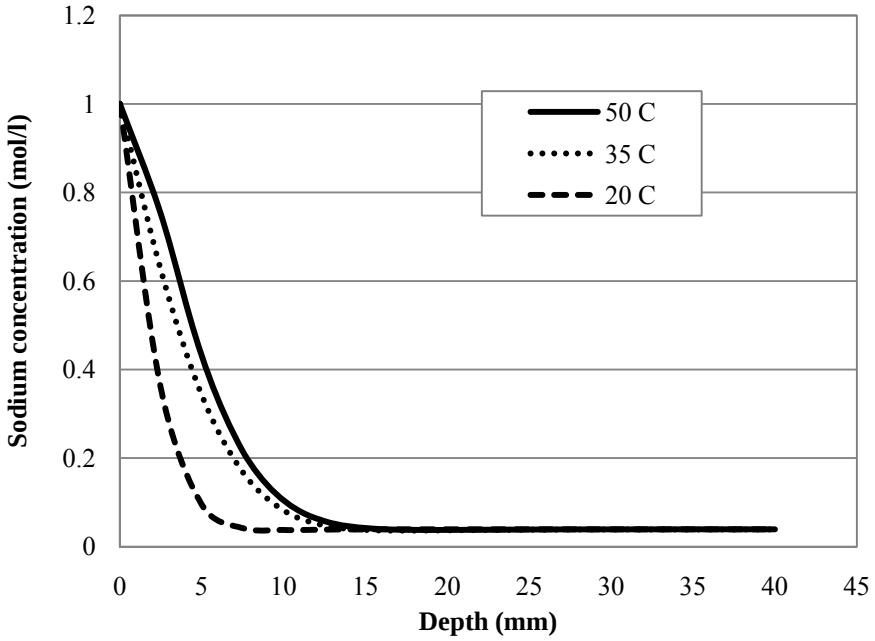

Fig. 6.15 Sodium concentration profiles exposed to 1 mol/l NaCl solution at 6 days

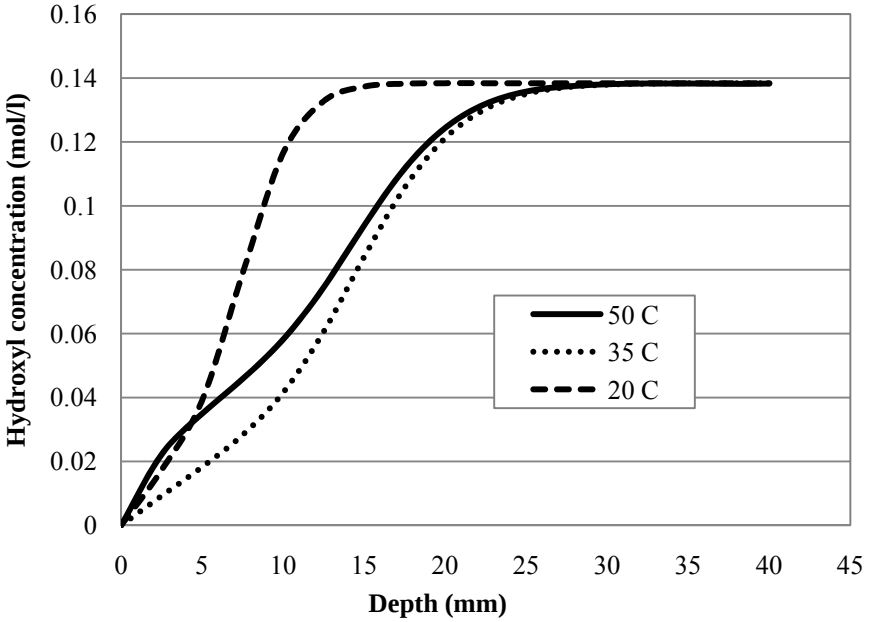

Fig. 6.16 Hydroxyl concentration profiles exposed to 1 mol/l NaCl solution at 6 days

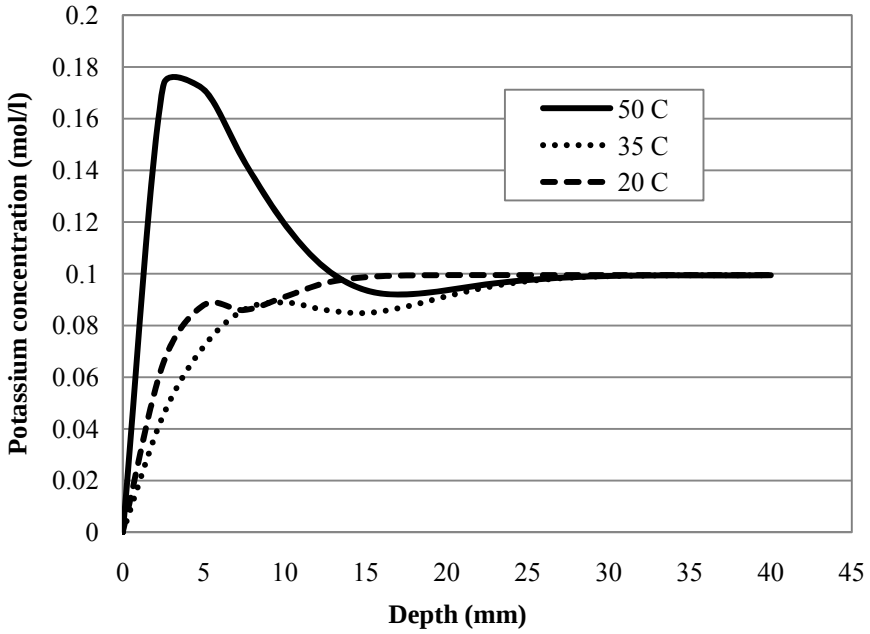

Fig. 6.17 Potassium concentration profiles exposed to 1 mol/l NaCl solution at 6 days

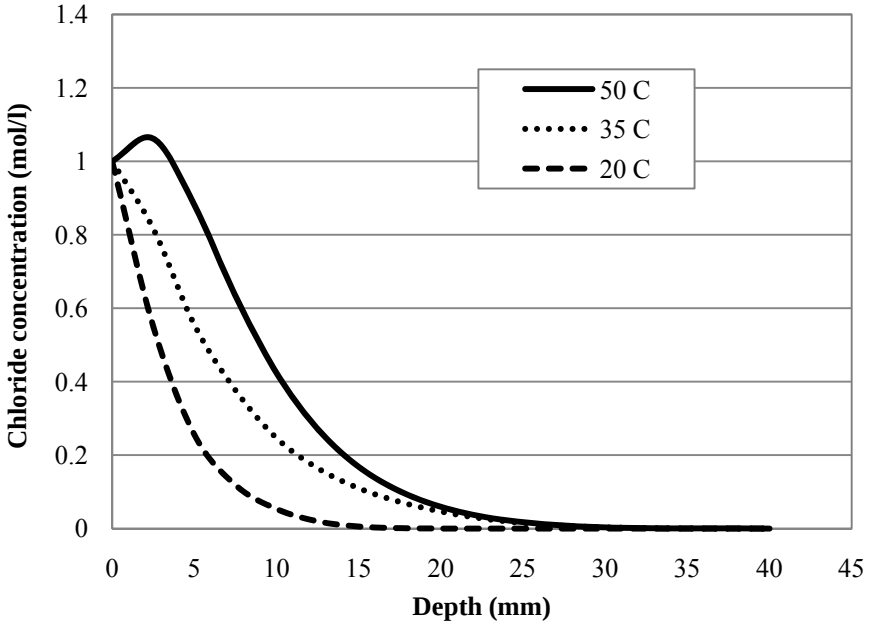

Fig. 6.18 Chloride concentration profiles exposed to 1 mol/l NaCl solution at 12 days

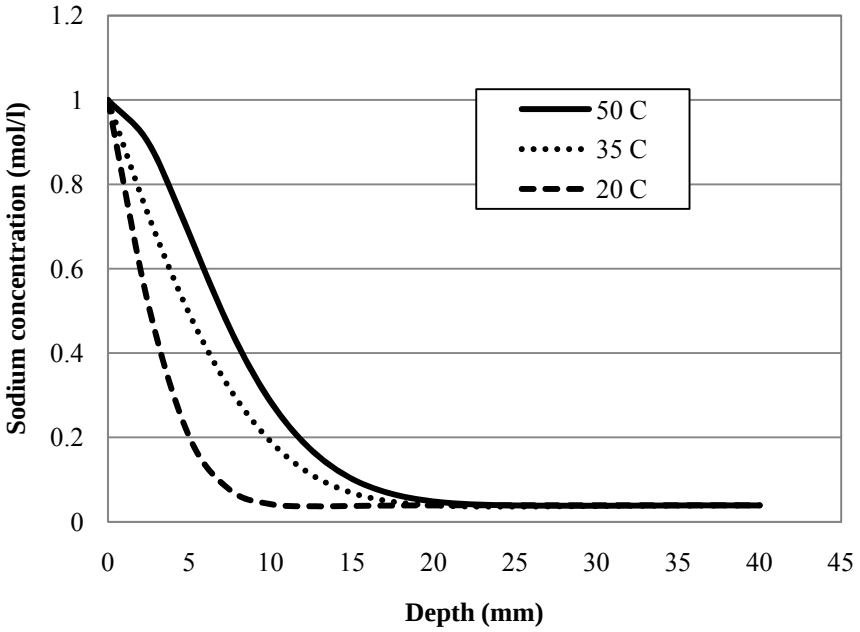

Fig. 6.19 Sodium concentration profiles exposed to 1 mol/l NaCl solution at 12 days

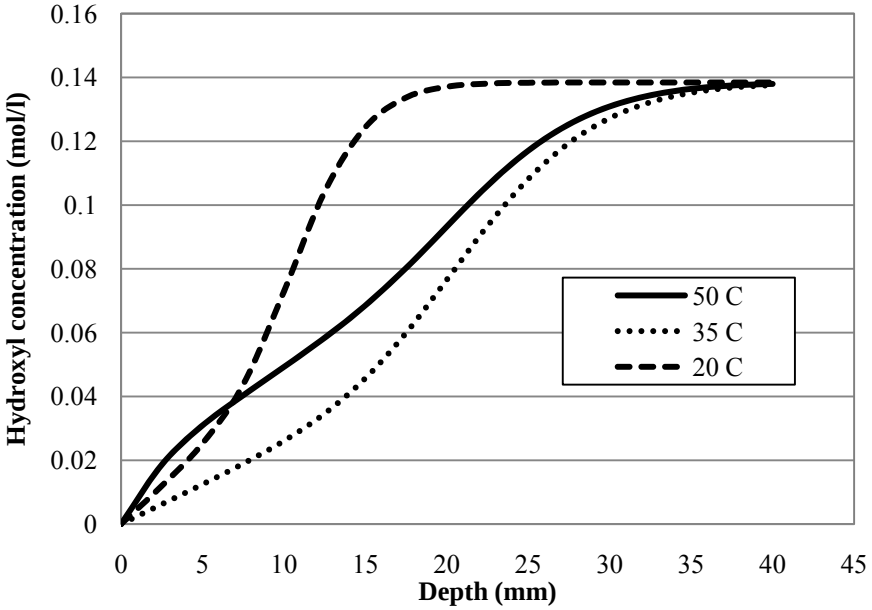

Fig. 6.20 Hydroxyl concentration profiles exposed to 1 mol/l NaCl solution at 12 days

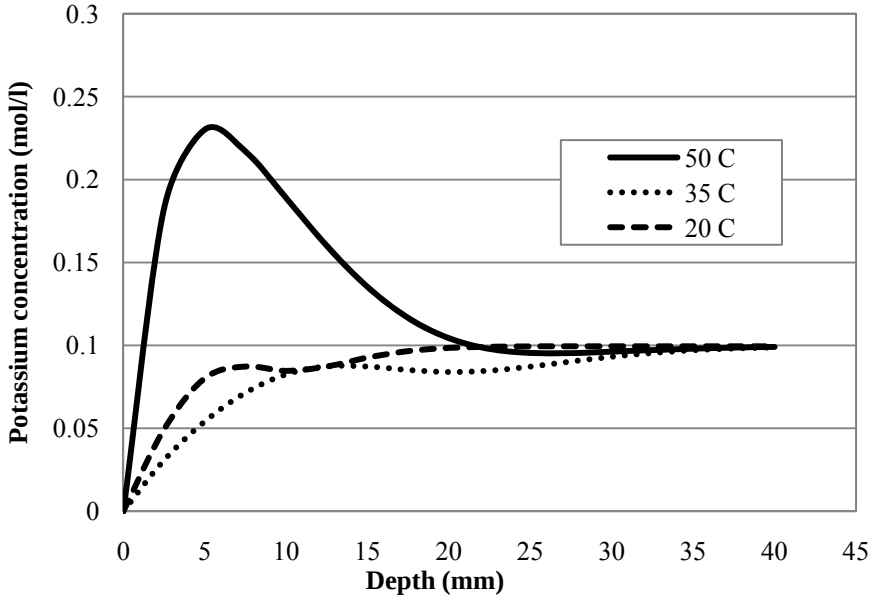

Fig. 6.21 Potassium concentration profiles exposed to 1 mol/l NaCl solution at 12 days

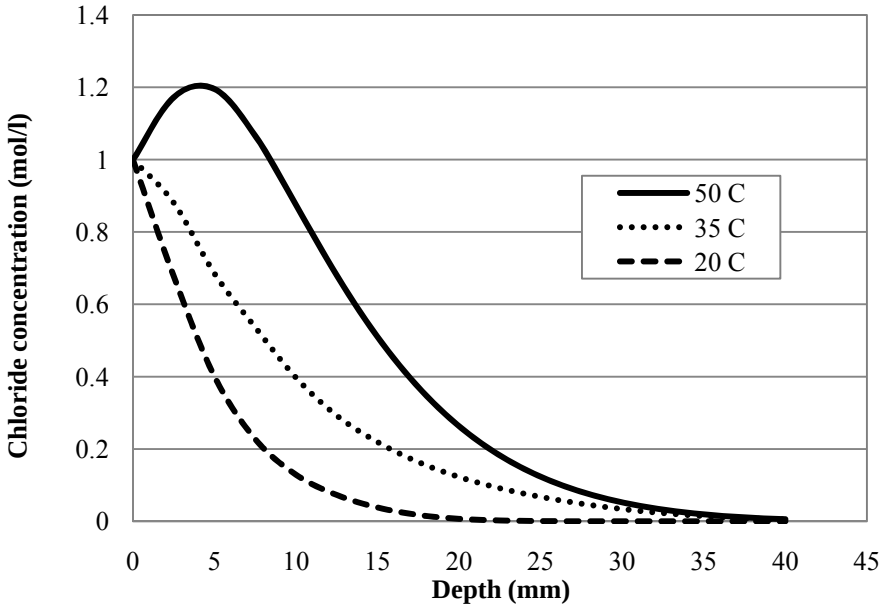

Fig. 6.22 Chloride concentration profiles exposed to 1 mol/l NaCl solution at 24 days

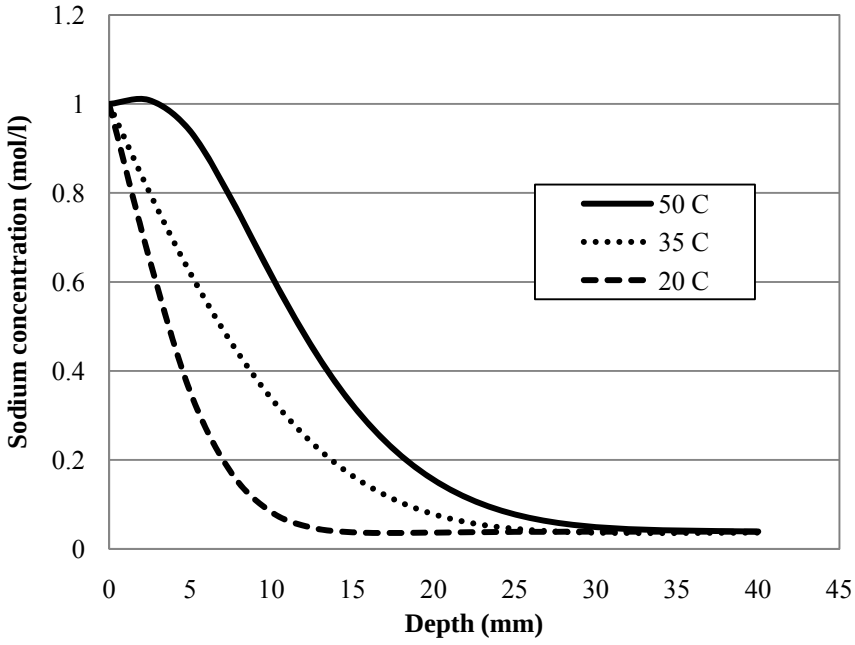

Fig. 6.23 Sodium concentration profiles exposed to 1 mol/l NaCl solution at 24 days

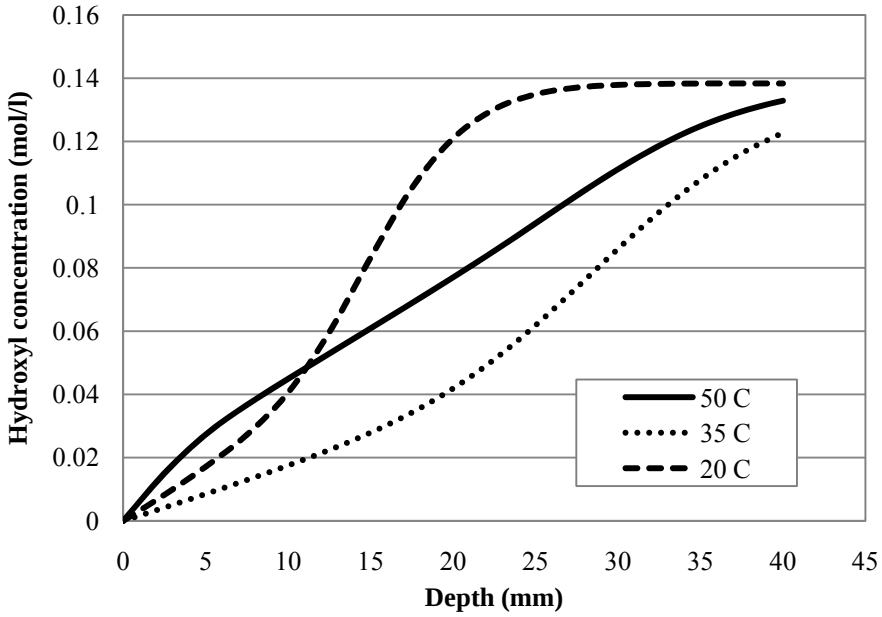

Fig. 6.24 Hydroxyl concentration profiles exposed to 1 mol/l NaCl solution at 24 days

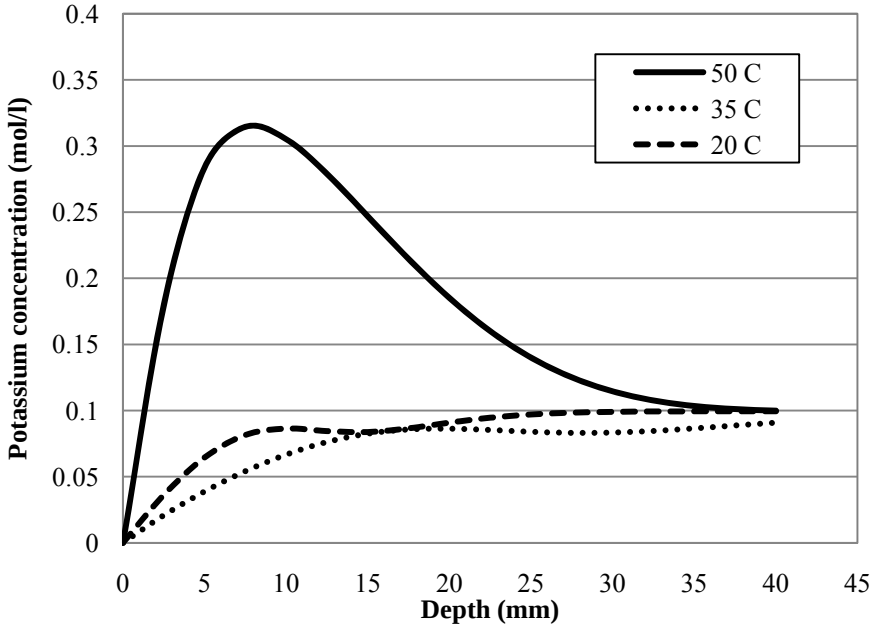

Fig. 6.25 Potassium concentration profiles exposed to 1 mol/l NaCl solution at 24 days

In this present study, the results of total chloride concentration (in gram of chloride per gram of concrete) predicted by present model are plotted and compared with the available test data obtained from Isteita (2009). The tests were conducted on chloride ponding test at different initial temperature conditions. The comparisons between numerical and experimental results exposed to 3% NaCl at T = 50 °C for 3, 6, and 12 days of exposure are shown in Figs. 6.26, 6.27, and 6.28, respectively. Figs. 6.29, 6.30, and 6.31 present the comparisons at T = 35 °C for specimens exposed to 3% NaCl for 3, 6, and 12 days of exposure, respectively. It can be seen from Figs 6.26 through 6.31, both at T = 50 °C and 35 °C, that the results obtained from the present model have a good agreement with test data. Therefore, the present comprehensive model taking into account the diffusion mechanism, ionic interaction, and the coupled temperature effect can be used to predict the chloride penetration into concrete structures not only in isothermal condition but also in non-isothermal condition.

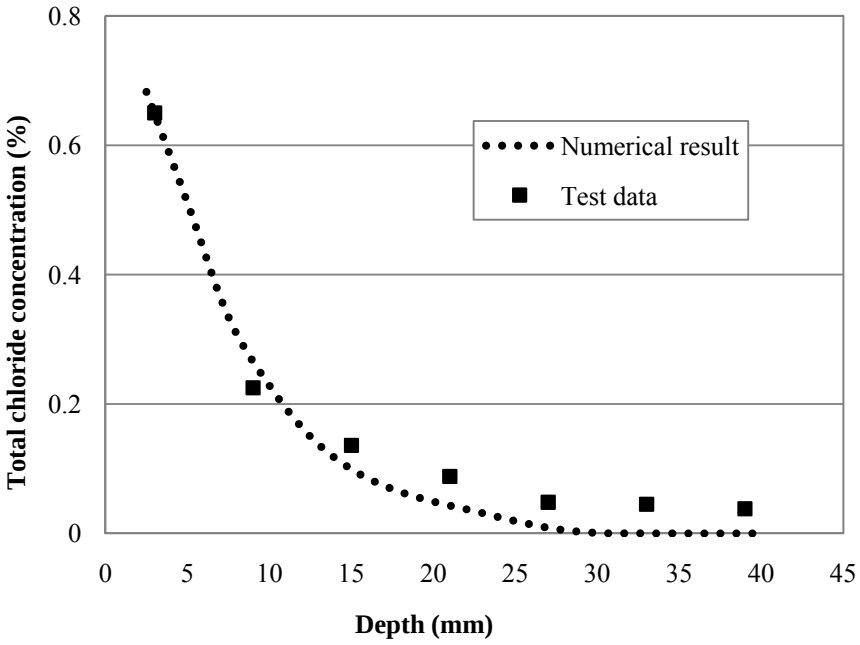

Fig. 6.26 The comparison between numerical result and test data at 3 days of specimens exposed to T = 50 °C

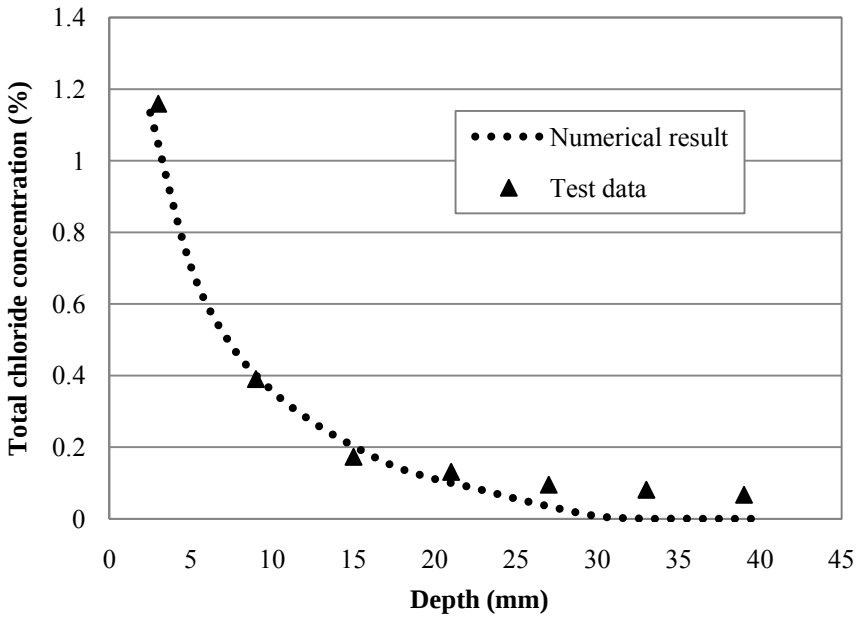

Fig. 6.27 The comparison between numerical result and test data at 6 days of specimens exposed to T = 50 °C

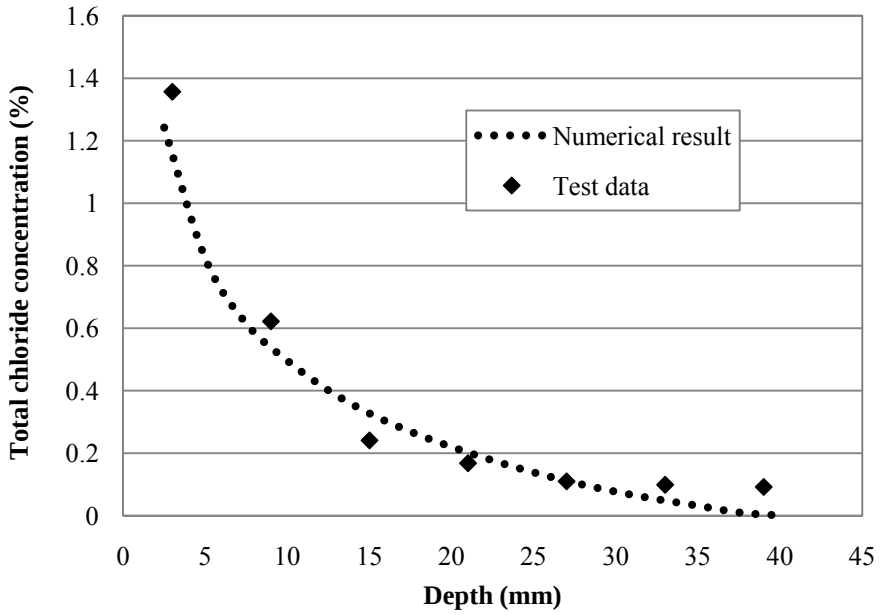

Fig. 6.28 The comparison between numerical result and test data at 12 days of specimens exposed to T = 50 °C

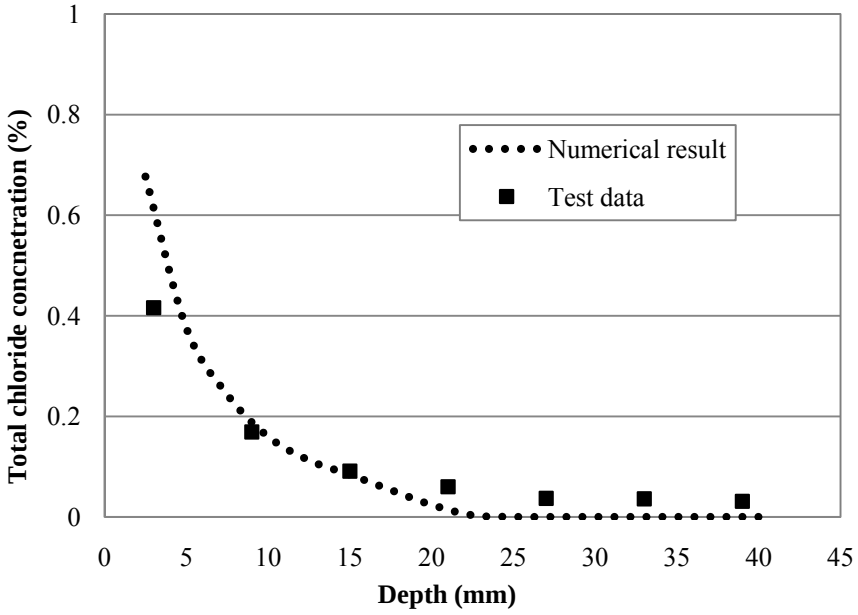

Fig. 6.29 The comparison between numerical result and test data at 3 days of specimens exposed to T = 35 °C

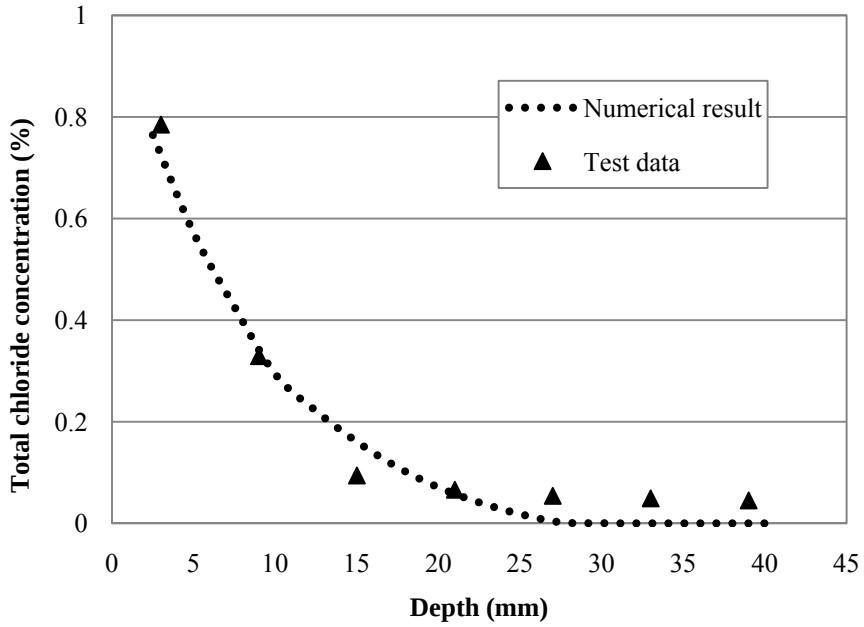

Fig. 6.30 The comparison between numerical result and test data at 6 days of specimens exposed to T = 35 °C

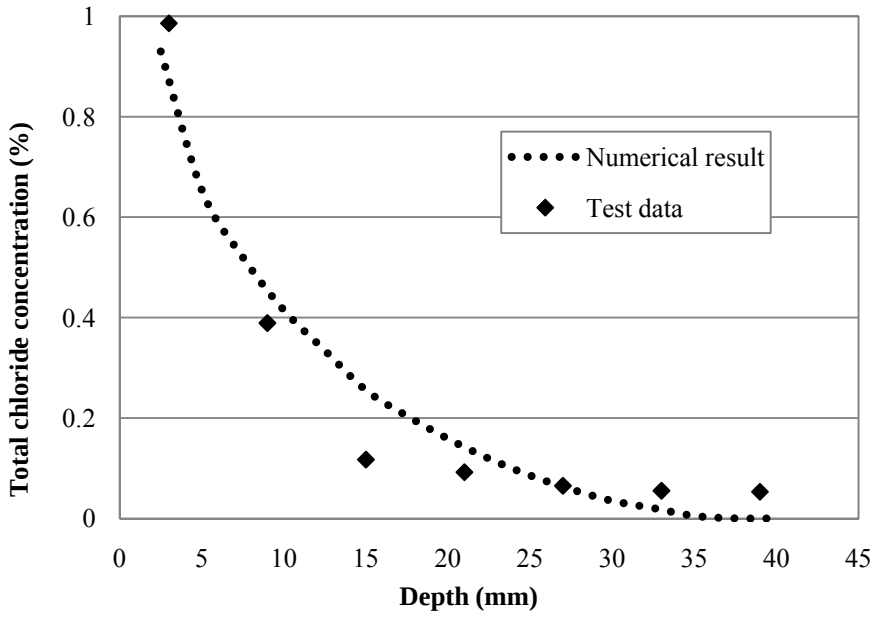

Fig. 6.31 The comparison between numerical result and test data at 12 days of specimens exposed to T = 35 °C

6.6 Conclusions

1. A mathematical model is developed to predict the chloride penetration into saturated concrete structures under non-isothermal condition. The model takes into account diffusion mechanism and ionic interaction which is formulated based on Nernst-Planck equation. The ionic fluxes are modified by incorporating the coupling term of temperature effect as an explicit term on the right-hand side of the governing equations. The ions in the pore solution (Na^+, K^+, and OH^-) are considered and the numerical simulations are performed by assuming a concrete sample exposed to chloride solution (NaCl) at different initial temperature conditions. The governing equations are solved by using finite element method.

2. The heat flow in concrete is incorporated in the model which is described by Fourier's heat conduction equation. The coupling term is proposed as an explicit term on the right-hand side of mass balance equation of each ionic species. Then, a coupling parameter is introduced which is obtained from the experimental study.

3. The numerical results show that the coupling term contributes significantly to the diffusion mechanism of four ionic species (Cl^-, Na^+, K^+, and OH^-) by accelerating the penetration rate of chloride concentration.

4. The numerical results predicted by present model are compared with the available test data. The comparison shows that the total chloride profiles obtained from the model have a good agreement with the test data.

5. The present comprehensive model can be used to predict the chloride ingress into saturated concrete structures not only isothermal but also non-isothermal conditions. It can also be used to estimate the service life and time for rehabilitation of concrete structures in temperature change condition.

CHAPTER 7

EXPERIMENTAL STUDY ON MULTI-SPECIES AGGRESSIVE CHEMICALS PENETRATION INTO CONCRETE STRUCTURES

7.1 Introduction

It has been established for several years in the research work that chloride is one of the most significant cause of corrosion of steel in reinforced concrete structures. This deleterious effect can reduce the load-bearing capacity, service life, and aesthetics of structures subjected to chloride environments such as bridge decks, parking garages, and marine/offshore structures. The degradation due to corrosion is one of the long-term durability problems for reinforced concrete structures. This study focuses on penetration of deicing salts which are considered as one of the aggressive chemicals. Deicing salts are widely used for ice and snow control on roads and bridges in North America. In some areas, one mile of four-lane roadways requires the application of more than 100 metric tons of deicing salts each year. About 15.4 million tons of road salts used annually in the U.S. for deicing of highways and roadways (Basu et al., 1999).

In each year, the U.S. spends $2.3 billion in order to keep roadways clear of snow and ice and it costs $38 million in Colorado reported by Colorado Department of Transportation (CDOT) for an average winter season (Federal Highway Administration, 2005; and O'Keefe and Shi, 2005). The most commonly used deicing salts are sodium chloride (NaCl), calcium chloride ($CaCl_2$), and magnesium chloride ($MgCl_2$). Calcium magnesium acetate (CMA), potassium acetate (KAC), sodium acetate (NaAC), and potassium formate ($KCHO_2$) (Basu et al., 1999 and

Fay et al., 2007). However, based on the survey reported by Fay et al. (2007), respondents used these acetates/formates deicers less than 25% while chloride-based deicers were still the most widely used. Over the past several years, $MgCl_2$ liquid deicer has been used by CDOT rather than NaCl salt-sand mixture because it is more effective, less toxic, and friendly to environments (Colorado Department of Transportation, 2006; Lewis 1999; and Xi and Xie, 2002). However, Levelton Consultants Limited (2007) and Trahan and Peterson (2007) found that $MgCl_2$ has more deteriorious effect on infrastructures and roadside vegetations than NaCl so that some local governments in Colorado have stopped using $MgCl_2$ and used NaCl instead as well as NaCl is the most frequently used based on the survey of respondents reported by Fay et al. (2007). Therefore, based on the above reviews, the performance of each type of deicers is still controversial. In general, different deicers are frequently used on the same areas for ice and snow control, for example, magnesium chloride solution is used before a snow storm for ice control, and calcium chloride solid salt is used during the snow storm for snow control. As a result, multiple species of deicing salts coexist on the surface and penetrate into concrete simultaneously.

The review of available literature showed that very few experimental studies were conducted on the penetration of deicing salts into concrete. This paper studies on diffusion mechanism of deicing salts but not on scaling and/or damage of concrete due to chloride attack. Although, so far, many research have been contributed on experimental study of chloride ingress into concrete these were conducted by mixing and/or immersing cement paste specimens or mortars with different types of chloride solutions. Different from our study, concrete specimens were ponded by different types of chloride-based salts that can represent the use of deicers in the

reality. This is considered as one-dimensional rather than two-dimensional diffusion which is the case of concrete samples immersed in solutions.

The studies of the effect of deicing salts and chloride solutions on concrete have been done by some researchers. Al-Hussaini et al. (1990) conducted the experimental study on the effect of free chloride ion source mixed in cement mortar. Two different types of chlorides, NaCl and $CaCl_2$, were selected in the study. They found that NaCl presented more free chloride ion than $CaCl_2$ at all concentration, from 0.5% to 2% by mass of cement, and pH of cement mortars were lower in the case of NaCl. As a result, cement mortars mixed with NaCl can accelerate the corrosion mechanism when compared with $CaCl_2$. Contrarily to Arya et al. (1990) study, $CaCl_2$ had greater effect than NaCl in terms of producing more free and bound chloride ions when mixed and immersed in specimens. Also, they found from the thin cement pate specimens immersed in 20 g/l of different types of chloride solutions that associated cation in solutions was one of the most important factors affecting on chloride binding capacity. The highest free chloride content was found from the specimens immersed in $MgCl_2$ solution and it decreased in the order of $MgCl_2$ > NaCl > Sea-water > $CaCl_2$. Similar to bound chloride content, $MgCl_2$ had the highest binding capacity and it ranked as $MgCl_2$ > $CaCl_2$ > NaCl > Sea-water. In terms of total chloride content, it can be ordered as $MgCl_2$ > $CaCl_2$ > NaCl > Sea-water.

We selected the penetration of different types of deicing salts in concrete as the focus of this study because of different performance of associated cation in chloride solutions as mentioned above. The laboratory tests were conducted to evaluate the penetration of six different groups of chloride-based deicers, i.e. 3% NaCl, 3% $CaCl_2$, 3% $MgCl_2$, 3% NaCl + 3% $CaCl_2$, 3% NaCl + 3% $CaCl_2$, and 3% $CaCl_2$ + 3% $MgCl_2$. The study was performed in terms of ponding

test. This method was chosen because, in reality, deicing salts are applied on the top surface of concrete structures and then ingress into the bottom where reinforcing steels were located.

7.2 Experimental Procedure

The mix proportions with two different water-cement ratios, 0.55 and 0.65, used in this experiment were obtained from Ababneh study (2002) and shown in Table 7.1. After 28 days of curing time, all specimens were immersed in water for 30 days to achieve saturation. The chloride ponding test in this study was conducted in saturated condition so that the effect of moisture was not considered. The compression test results for concrete specimens with dimensions of 4”x8” are shown in Table (E.1) of Appendix E. The table shows the average 28-day compressive strengths of the concrete samples for w/c = 0.65 and 0.55 are 22.06 and 24.43 kN, respectively. In addition, the Rapid Chloride Permeability Test (RCPT) was conducted standardized by ASTM C 1202 to evaluate the permeability of prepared specimens. The results of the RCPT test are shown in Table (F.1) of Appendix F and exhibit high chloride ion penetrability resulting in low chloride ion resistance.

In order to perform chloride ponding test, the ponding reservoirs were designed by using 5” tall plastic sleeves cut from PVC concrete cylinder molds with 4” diameter. Then, PVC sleeves were put on the top of concrete specimens for 2” in depth so that this created the 3” reservoir. Steel band clamps were used to tighten the PVC sleeves and concrete specimens in order to prevent leakage. A bead of silicone was added around the interface between sleeve and specimen to further prevent water leakage and create watertight compartment for chloride solution at the top of specimen as seen in Fig. 7.1.

Table 7.1 Concrete mix design

Content	Proportions	
	Mix 1	**Mix 2**
Water-cement ratio (w/c)	0.65	0.55
Weight of water (kg/m^3)	232	213
Weight of cement (kg/m^3)	356	380
Weight of sand (kg/m^3)	847	702
Weight of gravel (kg/m^3)	1031	911

Once the silicone had dried, all specimens were exposed to chloride solutions. The six different groups of chloride solutions, as mentioned above, were ponded on top of samples. The bottom face of specimen was exposed to distilled water so that there would be no moisture effect due to moisture gradient as shown in Fig. 7.2. Therefore, there were six concrete specimens of each water-cement ratio used for the test of each certain exposure time. The experimental program is summarized in Fig. 7.3. The samples were removed from the solutions after 15 and 30 days. The chloride concentration was measured by samples of concrete powder collected at various depth from the surface exposed to chloride solutions. The total chloride contents were obtained from concrete powder samples by using the rapid chloride test instrument manufactured by Germann Instruments, Inc. as described in Appendix G.

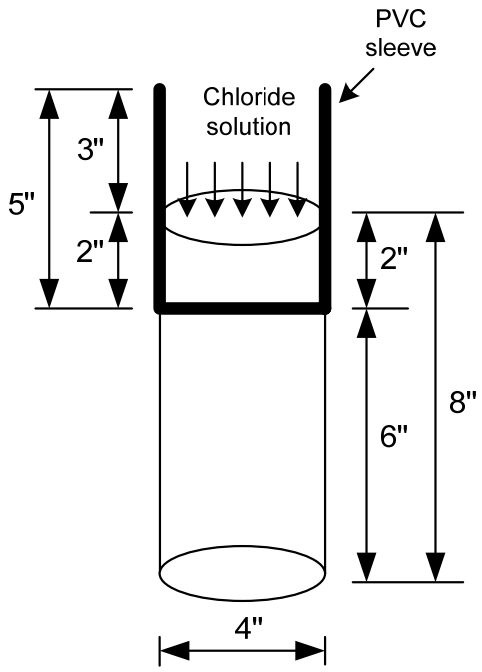

Fig. 7.1 A concrete specimen prepared for the chloride ponding test

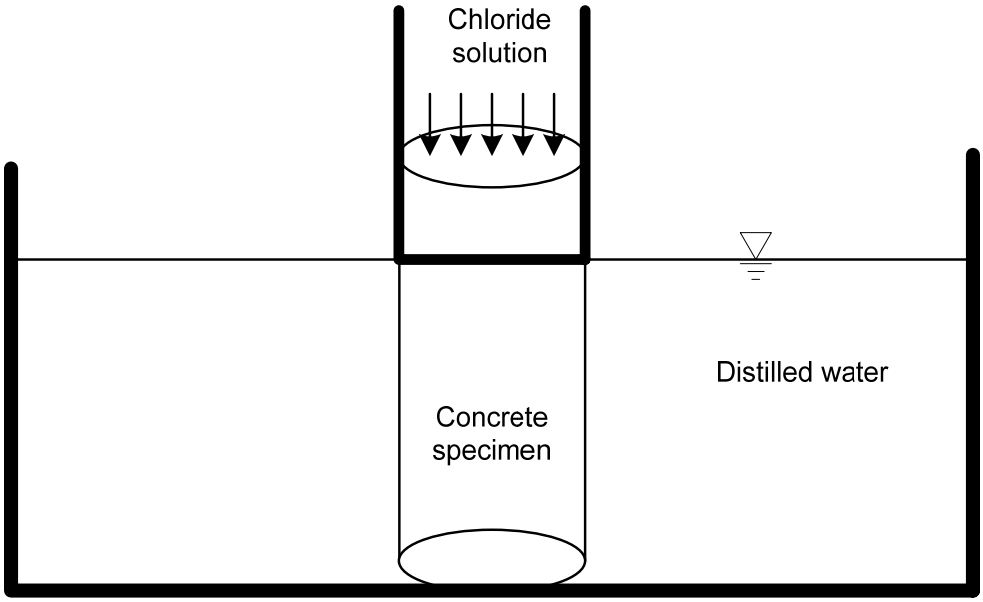

Fig. 7.2 Chloride ponding test set up

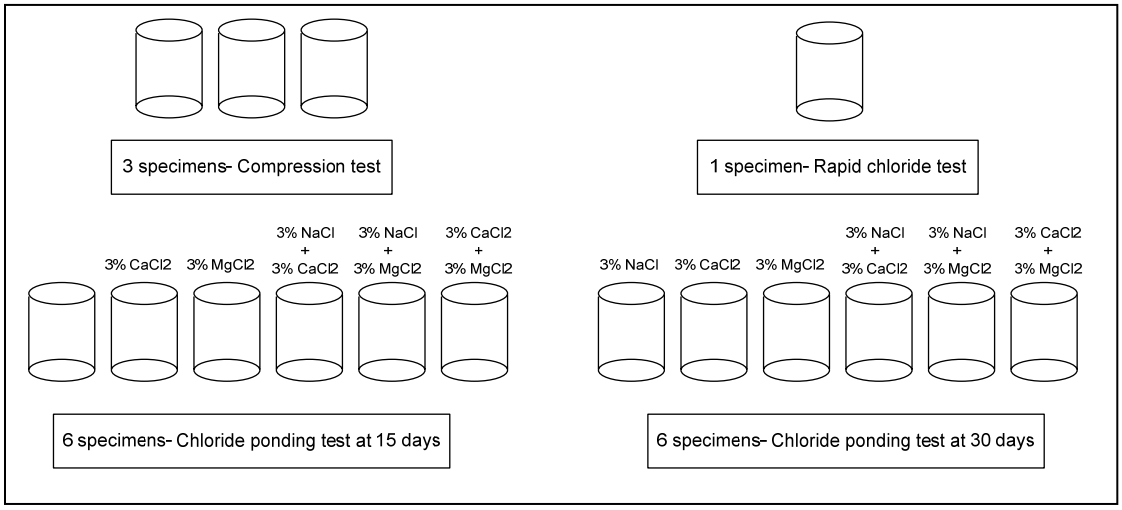

Fig. 7.3 Summarization of experimental study program

7.3 Results and Discussion

As mentioned previously, total chloride concentration is analyzed by using the Rapid Chloride Test Water-soluble (RCTW) method. The results of this electrochemical analysis were represented in mille Volt (mV). The mille Volt readings of concrete specimens at different depths from the surface exposed to different chloride solutions at 15 and 30 days of exposure are shown in Tables (G.1) and (G.3) of Appendix G. Then, by using calibration curves represented in Figs. (G.3) and (G.4), the readings are converted into chloride concentration as shown in Tables (G.5) and (G.6) of Appendix G. Total chloride profiles corresponding to Tables (G.5) and (G.6) are illustrated in Figs. 7.4 through 7.11. Figs. 7.4, 7.5, 7.8, and 7.9 are plotted for specimens with 0.55 w/c exposed to chloride solutions, and Figs. 7.6, 7.7, 7.10 and 7.11 are represented for samples with 0.65 w/c.

These plots show both 15 and 30 days of exposure and will be discussed in two cases; chloride profiles of samples exposed to different single types of salts (3% NaCl, 3% $CaCl_2$, and 3% $MgCl_2$) and combination among them (3% NaCl + 3% $CaCl_2$, 3% NaCl + 3% $CaCl_2$, and 3% $CaCl_2$ + 3% $MgCl_2$).

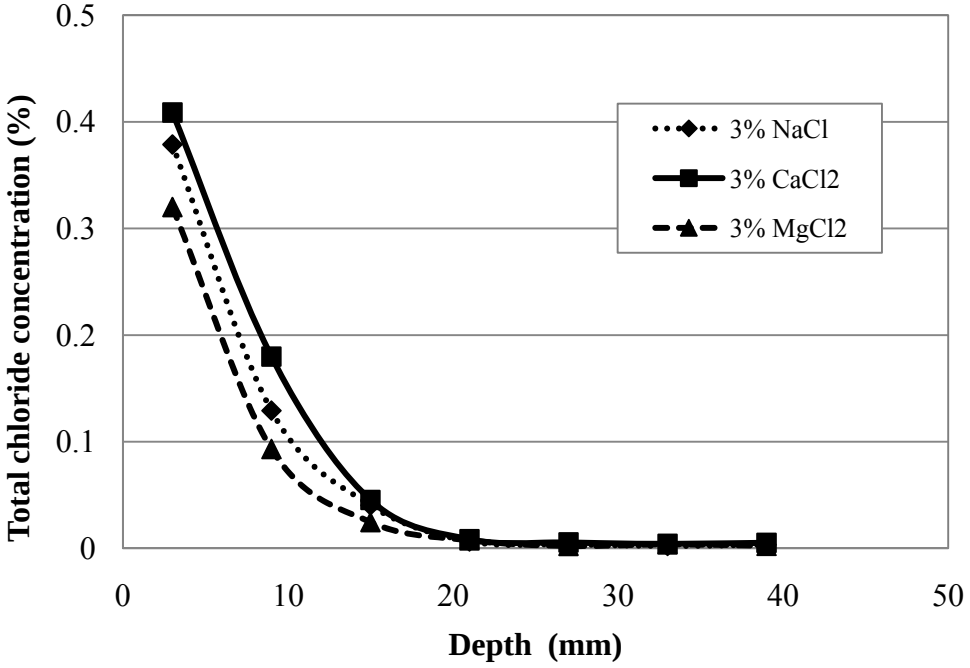

Fig. 7.4 Chloride profiles of concrete specimen at 15 days of exposure with 0.55 water-cement ratio

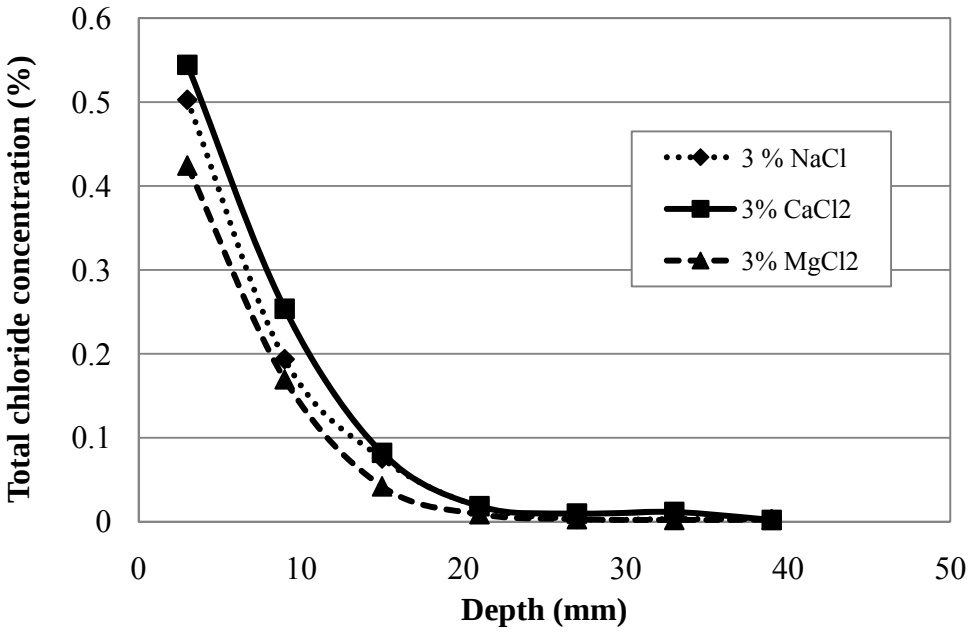

Fig. 7.5 Chloride profiles of concrete specimen at 30 days of exposure with 0.55 water-cement ratio

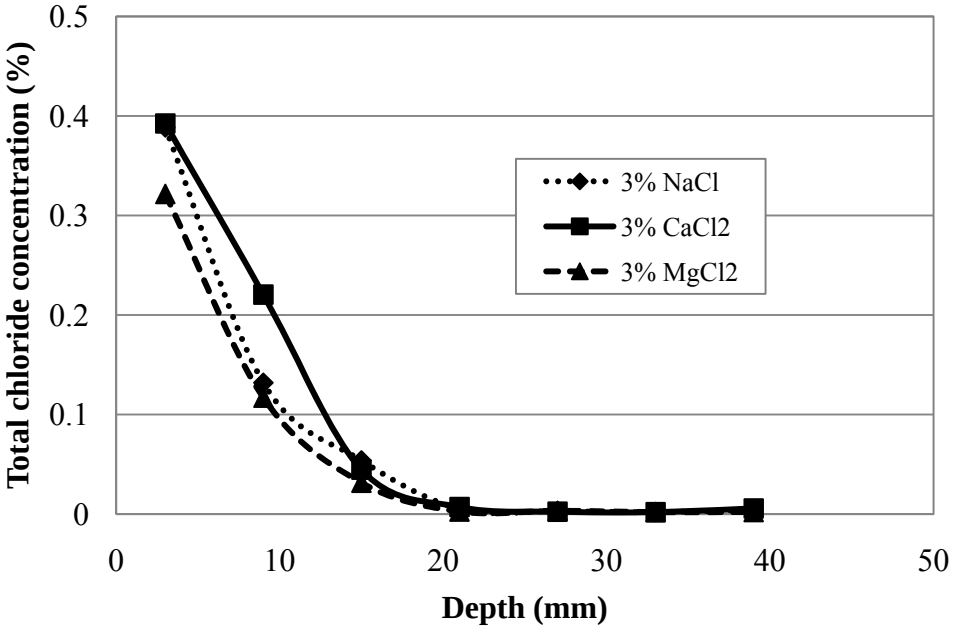

Fig. 7.6 Chloride profiles of concrete specimen at 15 days of exposure with 0.65 water-cement ratio

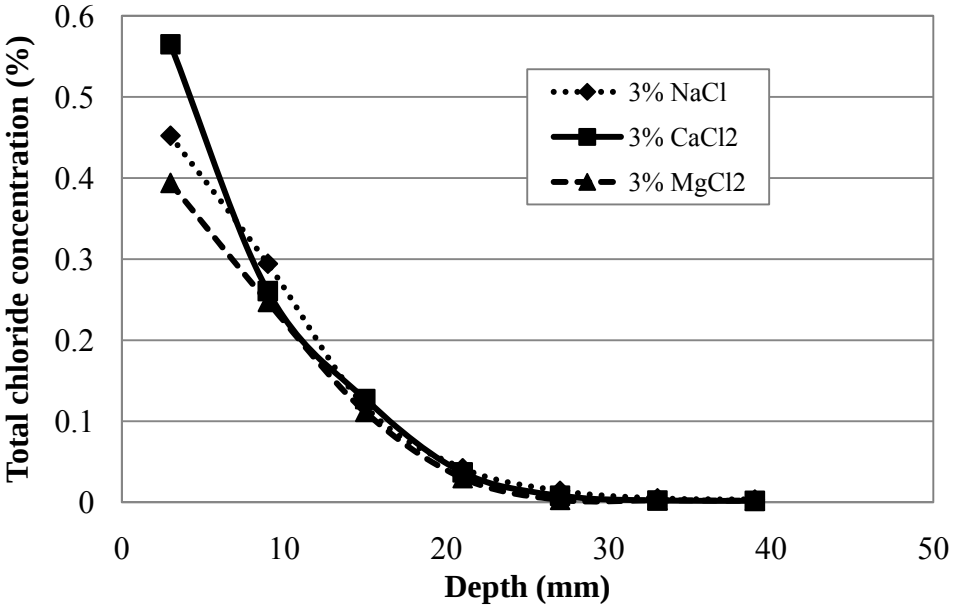

Fig. 7.7 Chloride profiles of concrete specimen at 30 days of exposure with 0.65 water-cement ratio

It can be observed from the profiles in Figs. 7.4, 7.5, 7.8, and 7.9 that the chloride concentrations contribute from 3% $CaCl_2$ solution tend to be the highest when compared with 3% NaCl and 3% $MgCl_2$, at the same location. This is because 3% solid $CaCl_2$ salt diluted in water produces higher chloride ions than 3% NaCl and 3% MgCl2. The extraction of these three chloride-based salts in solution can be described as Eqs. (7.1), (7.2), and (7.3). In order to compare the test results with numerical results, 3% NaCl, 3% $CaCl_2$, and 3% $MgCl_2$ by weight diluted in 1 liter of distilled water can be converted into mol/l as 0.513, 0.270, and 0.148, respectively. One can see from the Eqs. (7.1), (7.2), and (7.3) that 3% $CaCl_2$ can extract chloride ions higher than 3% NaCl and 3% $MgCl_2$ and 3% $MgCl_2$ produces the smallest amount of

chloride ions in solution. This means, at the fixed depth, the highest total chloride concentration is found in the case of 3% $CaCl_2$ and the lowest one occurs in the case of $MgCl_2$.

$$\begin{array}{ccccc} 3\%\,NaCl & \rightarrow & Na^{+} & + & Cl^{-} \\ (0.513\ mol/l) & & (0.513\ mol/l) & + & (0.513\ mol/l) \end{array} \tag{7.1}$$

$$\begin{array}{ccccc} 3\%\,CaCl_2 & \rightarrow & Ca^{2+} & + & 2Cl^{-} \\ (0.270\ mol/l) & & (0.270\ mol/l) & + & 2(0.270\ mol/l) \end{array} \tag{7.2}$$

$$\begin{array}{ccccc} 3\%\,MgCl_2 & \rightarrow & Mg^{2+} & + & 2Cl^{-} \\ (0.148\ mol/l) & & (0.148\ mol/l) & + & 2(0.148\ mol/l) \end{array} \tag{7.3}$$

However, there is a little difference of concentration can be observed in the case of 3% $CaCl_2$ and 3% NaCl. This is because these two salts produce almost the same amount of chloride ions and the ionic interaction among ions in pore solution, K^+ and OH^-, and ions in chloride solution has less effect on penetration mechanism. This is due to the use of low alkali cement and low concentration of chloride solutions. As discussed, in reality, not only one type of deicing salt but also the combinations of salts are frequently used in the same location. Therefore, the experimental study on the diffusion mechanism of combination of salts is investigated in this study. The three groups of mixed chloride solutions are ponded on top of concrete specimens. The chloride profiles at 15 and 30 days of exposure are shown in Figs. 7.8 and 7.9 for samples with 0.55 water-cement ratio and Figs. 7.10 and 7.11 for samples with 0.65 water-cement ratio.

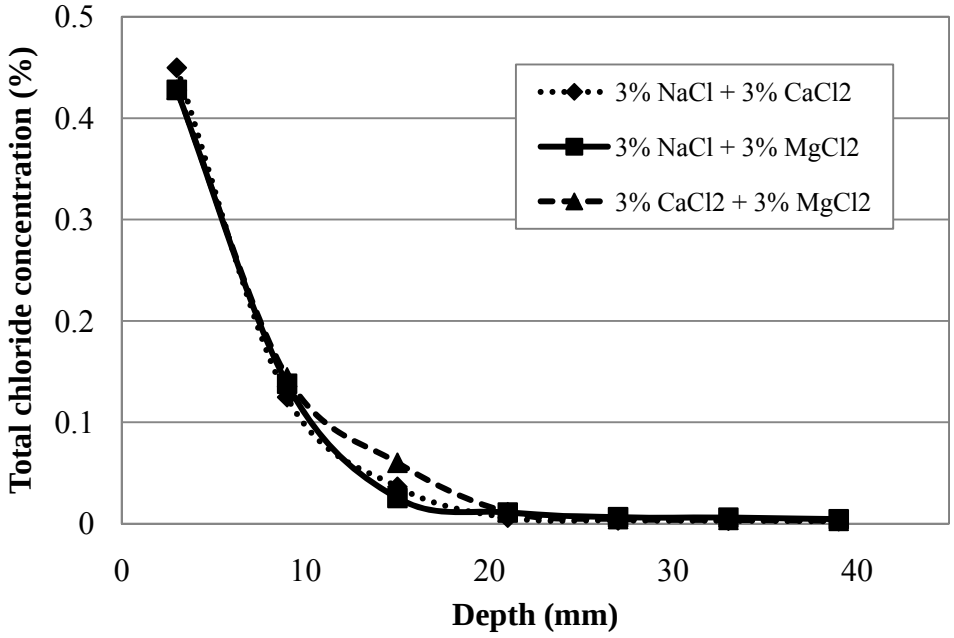

Fig. 7.8 Chloride profiles of concrete specimen exposed to a combination of chloride solutions at 15 days of exposure with 0.55 water-cement ratio

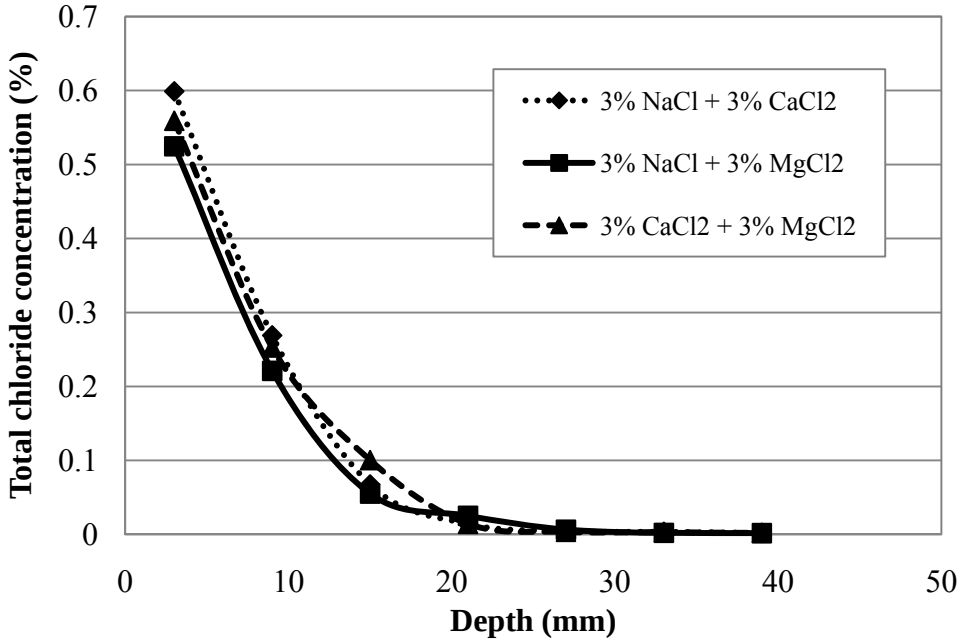

Fig. 7.9 Chloride profiles of concrete specimen exposed to a combination of chloride solutions at 30 days of exposure with 0.55 water-cement ratio

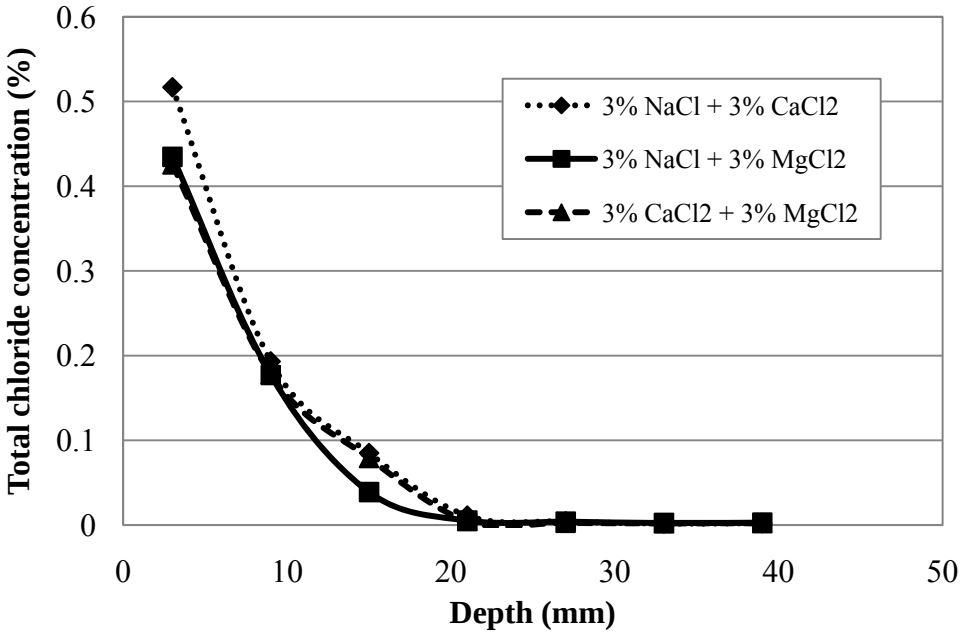

Fig. 7.10 Chloride profiles of concrete specimen exposed to a combination of chloride solutions at 15 days of exposure with 0.65 water-cement ratio

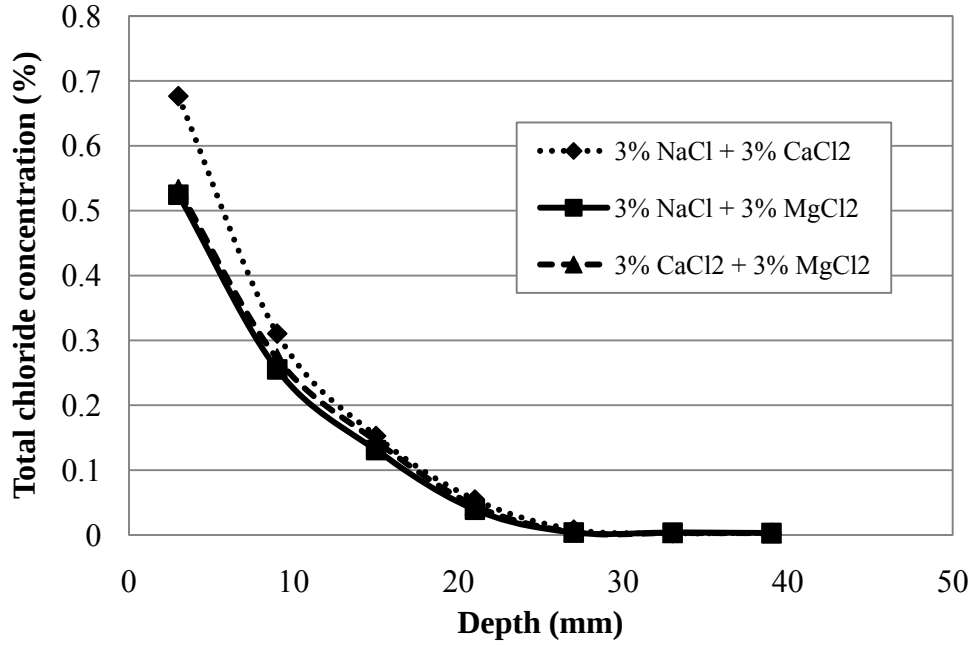

Fig. 7.11 Chloride profiles of concrete specimen exposed to a combination of chloride solutions at 30 days of exposure with 0.65 water-cement ratio

Similar to the experiment on single type of salt, the specimens exposed to combination of $CaCl_2$ with another type of salt tends to have higher concentration at the same depth, the highest concentration is found in the case of 3% NaCl + 3% $CaCl_2$ which provides the highest chloride ions in the solution as noticed in the Eq. (7.4). The specimens exposed to 3% NaCl + 3% $MgCl_2$ and 3% $CaCl_2$ + 3% $MgCl_2$ has a lower chloride concentration than 3% NaCl + 3% $CaCl_2$ due to the lower chloride ions in the solutions as shown in Eqs. (7.5) and (7.6).

$$\begin{array}{l} 3\%\ NaCl \quad + \quad 3\%\, CaCl_2 \quad \rightarrow \quad Na^+ \quad + \quad Ca^{2+} \quad + \quad 3Cl^- \\ (0.513\ mol/l) + \ (0.270\ mol/l) \ \rightarrow \ (0.513\ mol/l) + \ (0.270\, mol/l) + (1.053\, mol/l) \end{array} \tag{7.4}$$

$$\begin{array}{l} 3\%\ NaCl \quad + \quad 3\%\, MgCl_2 \quad \rightarrow \quad Na^+ \quad + \quad Mg^{2+} \quad + \quad 3Cl^- \\ (0.513\ mol/l) + \ (0.148\ mol/l) \ \rightarrow \ (0.513\ mol/l) + \ (0.148\, mol/l) \ + (0.809\, mol/l) \end{array} \tag{7.5}$$

$$\begin{array}{l} 3\%\, CaCl_2 \quad + \quad 3\%\, MgCl_2 \quad \rightarrow \quad Ca^{2+} \quad + \quad Mg^{2+} \quad + \quad 4Cl^- \\ (0.270\ mol/l) \ + \ (0.148\ mol/l) \ \rightarrow \ (0.270\ mol/l) + \ (0.148\, mol/l) \ + (0.836\, mol/l) \end{array} \tag{7.6}$$

The transport phenomena in concrete can be described based on the Nernst-Planck equation which is dependent on diffusion mechanism due to concentration gradient and migration due to ionic interaction. The flux equation of each ionic species is expressed as:

$$J_i = -D_i\left(\frac{\partial C_i}{\partial x} + \frac{z_i F}{RT}\frac{\partial \phi}{\partial x} C_i\right) \tag{7.7}$$

where C_i is the concentration, D_i is the diffusion coefficient, z_i is the charge number, F is the Faraday's constant, R is the gas constant, T is the temperature, Φ is the electrostatic potential, and index i represents for the *i-th* species.

Theoretically, the Nernst-Planck equation can be used to explain the penetration of multi-types of chloride solutions into concrete. This is because each type of salt has different associated cations that affect in the second term, migration process, of the Nernst-Planck equation. In order to verify the experiments, the test results of concrete specimens exposed to chloride solutions with 0.55 water-cement ratio at 15 and 30 days of exposure are plotted compares with the numerical results obtained by the mathematical model developed in Chapter 4 which is based on the Nernst-Planck equation. Figs. 7.12 through 7.15 show the total chloride profiles obtained from the experiment compared with the numerical results. It is noticed from these figures that the total chloride concentrations obtained from the experiment agree very well with numerical results. The present model can be used to simulate not only chloride diffusion but also other chemical species. Due to test data available for cation species, Na^+ and K^+, the concentration profiles of sodium and potassium predicted by this present model are compared with the test data obtained from concrete specimens with 0.55 water-cement ratio exposed to three different chloride solutions at 15 days of exposure as illustrated in Figs 7.16 through 7.18. As seen, the trends of sodium and potassium profiles resulting from ponding test match the prediction model. However, the concentration values of these ions deviate from the model in cases of specimens exposed to 3% $CaCl_2$ and 3% $MgCl_2$. A good agreement can be observed in case of concrete sample exposed to 3% NaCl. From the comparison point of view, it can be concluded that the cations associated in chloride solution have influence on the penetration of chloride ions into concrete structures.

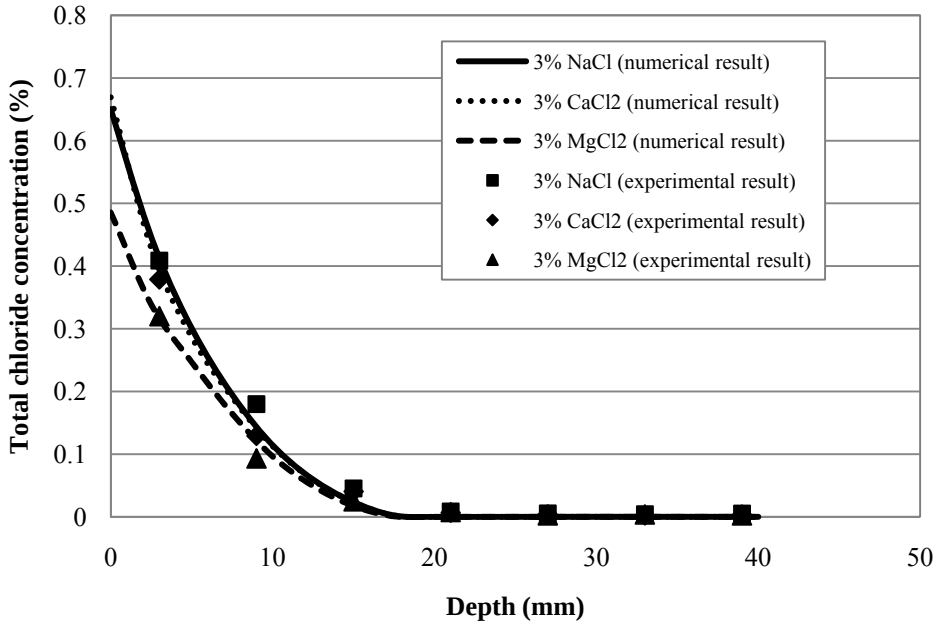

Fig. 7.12 A comparison between numerical and experimental result of specimens at 15 days of exposure

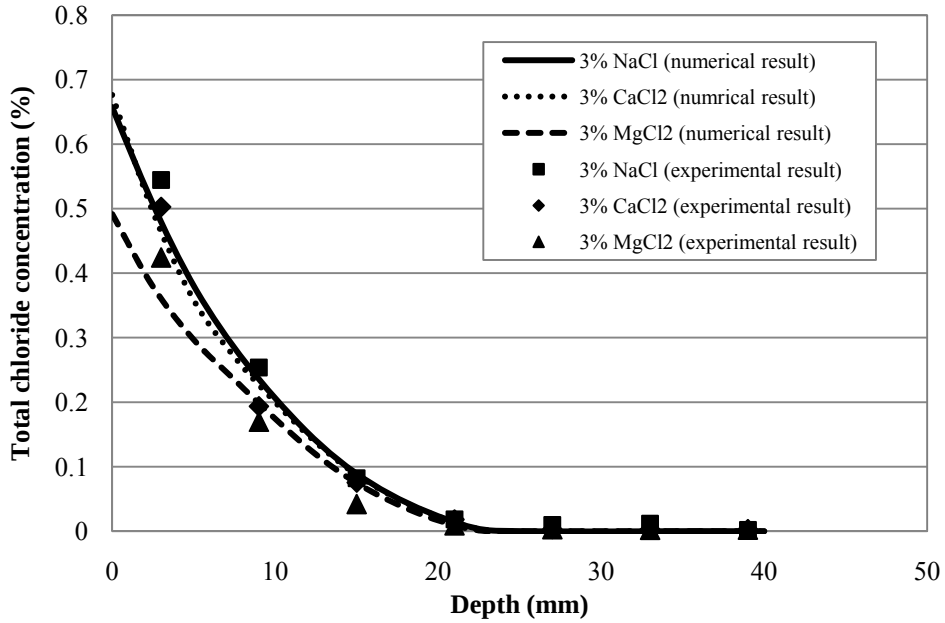

Fig. 7.13 A comparison between numerical and experimental result of specimens at 30 days of exposure

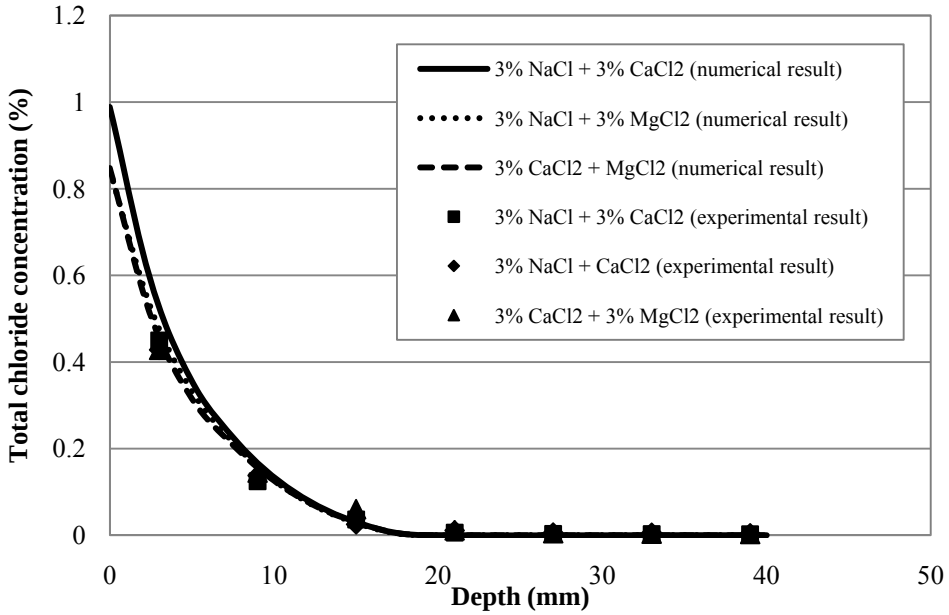

Fig. 7.14 A comparison between numerical and experimental result of specimens at 15 days of exposure

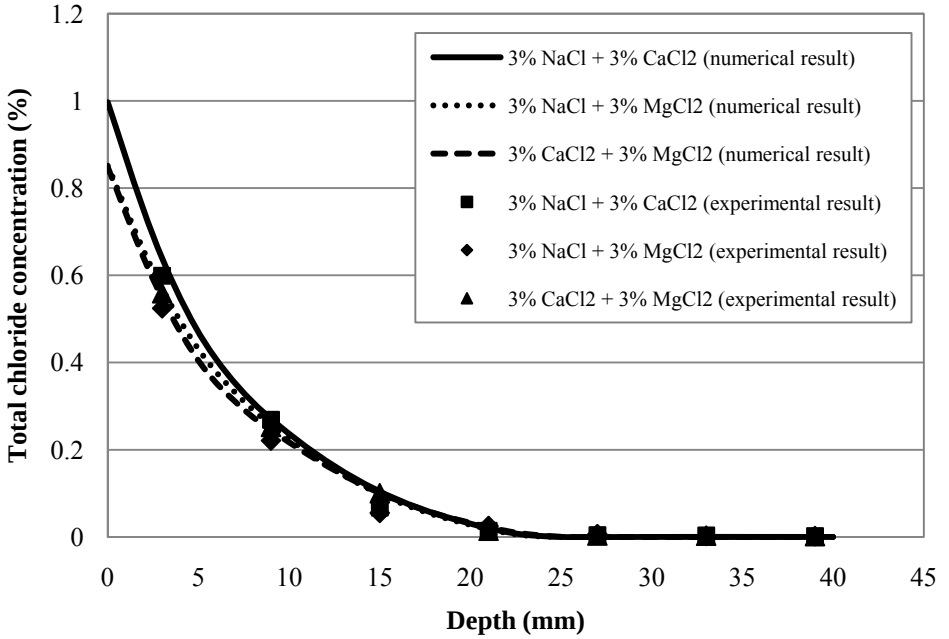

Fig. 7.15 A comparison between numerical and experimental result of specimens at 30 days of exposure

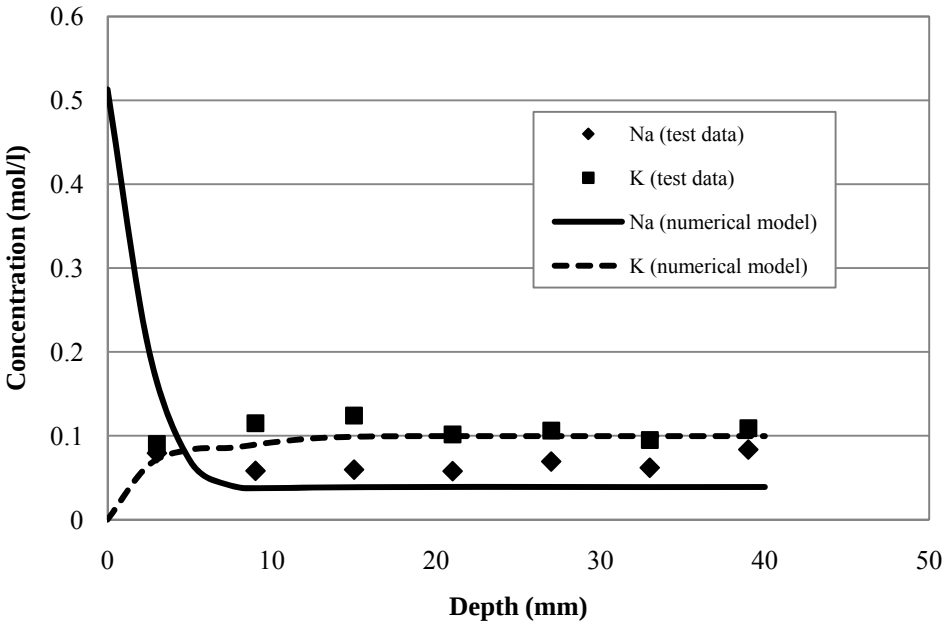

Fig. 7.16 A comparison between numerical and experimental result of specimens exposed to 3% NaCl at 15 days of exposure

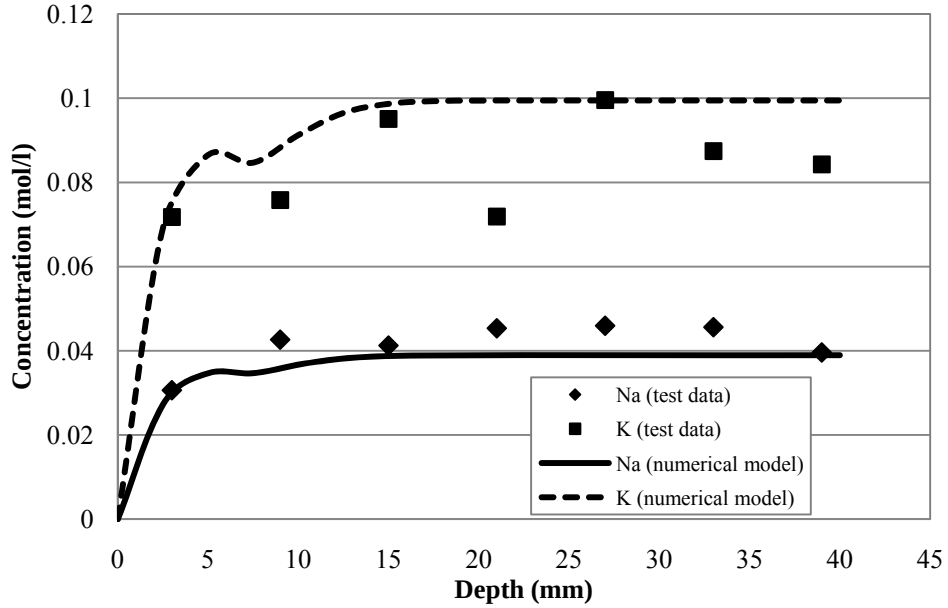

Fig. 7.17 A comparison between numerical and experimental result of specimens exposed to 3% $CaCl_2$ at 15 days of exposure

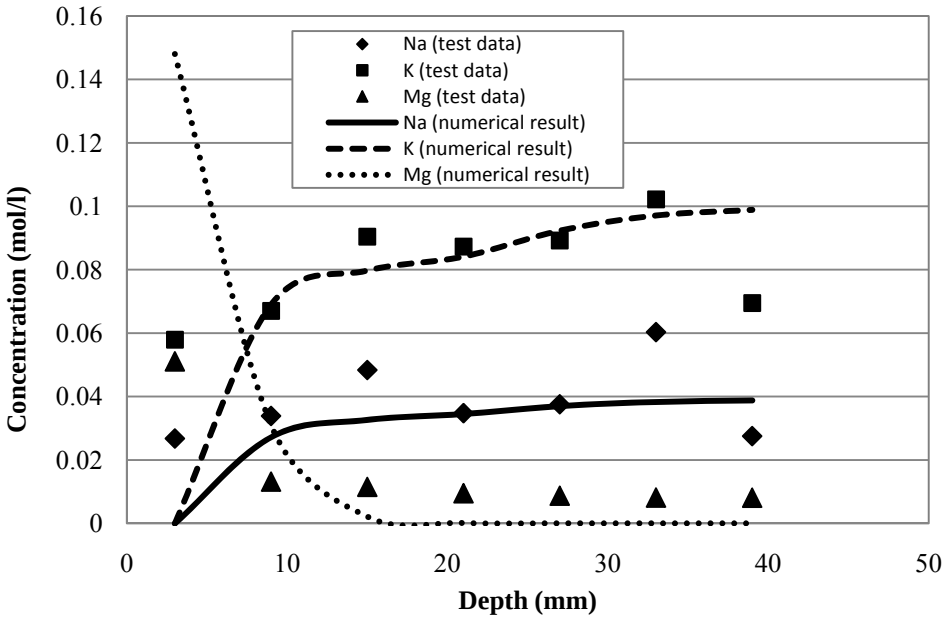

Fig. 7.18 A comparison between numerical and experimental result of specimens exposed to 3% $MgCl_2$ at 15 days of exposure

7.4 Conclusions

1. An experimental study was conducted on the penetration of various types of deicing salts into concrete. Three different types of deicers, chloride-based salts, were selected to investigate the influence of associated cations on diffusion rate of chloride solutions.

2. Concrete specimens were divided into six groups exposed to six different chloride solutions that is 3% NaCl, 3% $CaCl_2$, 3% $MgCl_2$, 3% NaCl + 3% $CaCl_2$, 3% NaCl + 3% $MgCl_2$, and 3% $CaCl_2$ + 3% $MgCl_2$.

3. In order to investigate only the diffusion mechanism of the effect of cations associated in chloride solutions, the moisture effect is neglected so that the experiment was performed in saturated condition.

4. The experimental results show that cations associated in chloride solutions have significant effect on the penetration rate of chloride ions. This can be summarized in the order of $CaCl_2$ > NaCl > $MgCl_2$ from the fastest to slowest chloride penetration. In the case of salt combinations, the diffusion rate of chloride ions can be ranked as NaCl + $CaCl_2$ > $CaCl_2$ + $MgCl_2$ > NaCl + $MgCl_2$.

5. The corrosion initiation time of reinforcing steel in reinforced concrete structures exposed to different deicers can vary due to the critical chloride content contributed from salts which produce various levels of free and bound chloride ions.

6. The experimental results are compared to the numerical results developed in Chapter 4 based on the Nernst-Planck model which accounts for the interaction between ions and a good match is obtained in a case of total chloride concentration. The good trends of sodium and potassium profiles obtained from the experiment can be observed when compared to the mathematical model.

CHAPTER 8

CONCLUSIONS AND FUTURE RESEARCH RECOMMENDATIONS

The main goal of this thesis is to investigate the penetration of multi-species aggressive chemicals into concrete structures. Aggressive chemicals can be defined as the chemicals that are harmful to concrete structures resulting in structural damages and deteriorations. These chemicals can affect the physical and mechanical properties of concrete structures by reducing load-bearing capacity, service life, and aesthetic features. The chemical causes deterioration of concrete that can be classified as alkali-silica and alkali-carbonate reactions; chloride, sulfate, and carbon dioxide attacks (Neville, 2002). The problems mentioned above can be mathematically characterized by diffusion equations of different degree of complexity.

The penetration of deicing salts into concrete structures is selected as the focus of this study because it is one of the most difficult problems encountered in the field of civil engineering. Another reason is that deicing salts are widely used for ice and snow control on roads and bridges in North America. In addition, deicing salt is one of the sources of chloride ions penetrating into reinforced concrete structures that can cause the corrosion of rebar. This problem results in structural deficiency and then maintenance and/or rehabilitation of structures is required. Frequently, different deicers are applied on the same location leading to multiple species of salts coexist on the surface and ingress into structures simultaneously. Also, in reality, concrete structures are found in non-saturated and non-isothermal conditions. Thus, challenges come from several aspects: diffusing species such as moisture and deicing chemicals are coupled

among themselves, the porous media (i.e. concrete) is not homogeneous at both large and small scale levels, and the environment conditions are highly random.

The diffusion of multi-species aggressive chemicals focusing on chloride attack in concrete through this study is mathematically modeled by two approaches. One is an empirical model based on a simple solution of one-dimensional diffusion equation which is used in Chapter 3 for statistical analysis. The other is described by the Nernst-Planck equation which is one of the physical models based on sophisticated transport theory including diffusion mechanism due to concentration gradient and migration process due to ionic interaction. This model is described in Chapter 4, 5, and 6. Both types of models require information about boundary and initial conditions and test data to validate the reliability of models. These data usually consist of measured chloride profiles obtained from structures in service or from laboratory specimens. Since the models developed in this thesis need to be validated, an experimental study is conducted in Chapter 7 to quantify the effect of multi-ionic species on chloride-based salts penetration into concrete.

8.1 Conclusions

1. In order to predict the onset of steel corrosion, a mathematical model on chloride diffusion in concrete is needed, and it is one of the most difficult diffusion problems encountered the field of civil engineering.

2. Chloride penetration into reinforced concrete structures can be mathematically characterized by two approaches. One is the empirical model based on the assumption that chloride ingress into concrete is a diffusion process due to concentration gradient, and this approach is based on Fick's law. The other is the physical model based on the sophisticated

transport theory, the Nernst-Plack equation, that penetration of chloride ions depend on the concentration gradients of the diffusing species and the migration process due to ionic-interaction-induced electrostatic potential gradient.

3. The empirical model based on Fick's law is employed in the statistical analysis for predicting the corrosion initiation time of reinforcement in concrete structures in Chapter 3. The model is developed by considering the random variables involved in nonlinear diffusion equation. An analytical probabilistic solution is derived for calculating the mean and standard deviation of the corrosion initiation time. The mean and standard deviation of the corrosion initiation time are contributed from the means and standard deviations of random variables which include concrete cover, water-cement ratio, curing time, surface chloride concentration, and chloride threshold value. Among these random variables, the variation of corrosion initiation time is mainly affected by water-cement ratio of concrete and the ratio of critical chloride concentration to surface chloride concentration.

4. The chloride penetration rate of chloride into concrete is contributed from not only the diffusion mechanism due to concentration gradients but also migration process due to electrostatic potential gradient. This can be explained by transport theory of ion in porous media (i.e. concrete) called the Nernst-Planck equation.

5. The mathematical model is developed based on the Nernst-Planck equation which can be used to formulate the diffusion of multi-ionic species in concrete. This is because, in reality, various types of deicing salts such as NaCl, $CaCl_2$, and $MgCl_2$ are frequently used in the same location for ice and snow control. As a result, multiple species of salts coexist on the surface and ingress into concrete simultaneously. The model considers the transport of not only chloride ions

but also other chemical species in concrete pore solution included sodium (Na^+), potassium (K^+), and hydroxyl (OH^-).

6. The mathematical model developed in Chapter 4 is extended to apply for non-saturated concrete structures by considering the moisture effect. The moisture transport equation is formulated and incorporated in the governing equations. The coupled effect of moisture diffusion and ion transport is included in the model. The coupling parameters are proposed and the coupling terms are incorporated in the governing equations of each ionic species and moisture. This means the coupling terms are two-way fully coupled. The numerical results are solved by the finite element method. The results show the basic trends of concentration profiles of ions and moisture. One can see from the results that the moisture gradient has significant effect on ion transport by accelerating the penetration rate of chloride and other species which ingress in the same direction. On the other hand, ions such as potassium and hydroxyl are slowed down by moisture gradient because of the reverse direction of diffusion of these two types of ions with respect to the direction of moisture diffusion. The total chloride concentrations predicted by this model agree very well with available test data. Therefore, from this study, the moisture effect cannot be negligible in the mathematical model of ion transport in concrete.

7. The extension of mathematical model by including the temperature effect is studied in Chapter 7. Based on the literature review, the influence due to temperature gradient must be taken into account in the transport mechanism of ion in concrete. The heat flow equation in concrete is described by the Fourier's law of heat conduction. The coupled effect of temperature and ion diffusion in concrete is investigated. This study considers only the contribution of temperature gradient to the rate of ion transport. This means one-way coupled effect. The coupling parameter is obtained from the experimental study by Isteita (2009). The parameter is

developed for the temperature effect on chloride diffusion in concrete based on multifactor method taken into account the influence of chloride concentration, curing time of concrete, and temperature. The coupling term is incorporated in the governing equations for not only chloride ion but also other species based on the assumption that temperature can accelerate or slow down the diffusion rate of other ions in the same way as chloride ions. The results obtained from numerical analysis show that the temperature has remarkable influence on ion transport in concrete. The prediction of this proposed model has a good agreement with available test data. Thus, the coupled effect due to temperature must be included in the ion transport phenomena in non-isothermal concrete.

8. The experimental study in Chapter 7 presents the penetration of different types of chloride-based deicing salts into concrete. Theoretically, the Nernst-Planck equation can be used to explain the results obtained from the experiment that the diffusion rate of chloride ion depends on the cations associated in chloride solutions. This phenomenon can be described by the second term of the Nernst-Planck equation that induces the electrostatic potential gradient. Based on this finding, the chloride diffusion coefficient should be included a factor due to cations associated in solution. This means the chloride diffusion coefficient should have different values for different chloride solutions. The experimental results can also be used to validate the mathematical model developed in Chapter 4.

8.2 Future Research Recommendations

1. The mathematical model of multi-species aggressive chemicals transport in concrete can be further extended to include the mechanical model such as damage models related to the corrosion-induced cracking of concrete cover.

2. The incorporation of the coupling effects among moisture, temperature, and ion transport, Hygro-Thermo-Chemo diffusion, needs to be considered in the experimental and numerical studies of multi-species transport in concrete.

3. The coupling parameters of moisture diffusion and ion transport; and temperature and ion transport in concrete need to be further developed based on the theoretical or experimental studies.

4. One more parameter, i.e. the influence of cations associated in chloride solutions must be incorporated in the multifactor equation of chloride diffusion coefficient. Also, the diffusion coefficients of other species such as sodium, potassium, calcium, and hydroxyl ions need to be developed based on the theoretical or experimental studies. These coefficients should be considered as inconstant values depending on multifactor such as the influences of water-cement ratio, curing time, volume fraction of aggregates, ion concentration, temperature, and moisture. This can be performed by using the frame work of the derivation of chloride diffusion coefficient.

5. The further development of experimental and numerical studies are needed on the effect of mineral additives such as fly ash, silica fume, and ground blast furnace slag on chloride penetration and ion transport in concrete.

BIBLIOGRAPHY

Ababneh, A. (2002). "The Coupled Effect of Moisture Diffusion Chloride Penetration and Freezing-Thawing on Concrete Durability." Ph.D. Dissertation of the University of Colorado at Boulder.

Ababneh, A. and Xi, Y. (2002). "An Experimental Study on the Effect of Chloride Penetration on Moisture Diffusion in Concrete." *Materials and Structures*, 35, 659-664.

Ababneh, A., Benboudjema, F., and Xi, Y. (2003). "Chloride Penetration in Nonsaturated Concrete." *Journal of Materials in Civil Engineering, ASCE*, 15(2), 183-191.

Abarr, L. (2005). "The Effect of Moisture Diffusion on Chloride Penetration." M.S. Thesis of the University of Colorado at Boulder.

Adler, P.M. (1992). Porous media - Geometry and transports, Butterworth-Heinemann, Boston.

Adler, R.J. (1981). The geometry of random fields, John Wiley, Chichester, U.K.

Andrade, C. (1993). "Calculation of Chloride Diffusion Coefficient in Concrete from Ionic Migration Measurements." *Cement and Concrete Research*, 23(3), 724-742.

Andrade, C. and Sanjuan, M.A. (1994). "Experimental Procedure for the Calculation of Chloride Diffusion Coefficients in Concrete from Migration Tests." *Advances in Concrete Research*, 6(23), 127-134.

Barbarulo, R., Marchand, J., Snyder, K.A. and Prene, S. (2000). "Dimensional analysis of ionic transport problems in hydrated cement systems: Part I, theoretical consideration." *Cement and Concrete Research*, 30, 1955-1960.

Basu, R., Breshears, J.S., and Clausen, E.C. Calcium Magnesium Acetate at Lower Production Cost: Production of CMA Deicer from Biomass, *Report No. FHWA-RD-98-055*, Federal Highway Administration, Virginia. (1999).

Bazant, Z.P. and Chern, J-C. (1981). "Finite Element Program for Moisture and Heat Transfer in Heated Concrete." *Nuclear Engineering and Design*, 68, 61-70.

Bazant, Z.P. and Najjar, L.J. (1972). "Nonlinear Water Diffusion of Nonsaturated Concrete." *Materials and Structures*, 5(25).

Benjamin, J.R. and Cornell, C.A. (1970). Probability, Statistics, and Decision for Civil Engineers, McGraw-Hill, New York.

Bentz, E.C. (2003). "Probabilistic modeling of service life for structures subjected to Chlorides." *ACI Materials Journal*, 100, 391-397.

Bertolini, L., Elsener, B., Pedeferri, P., and Polder, R. (2004). Corrosion of Steel in Concrete. Wiley-VCH Verlag GmbH & Co. KGaA, Weinheim, Germany.

Boddy, A., Bentz, E., Thomas, M.D.A. and Hooton, R.D. (1999). "An overview and sensitivity study of a multi-mechanistic chloride transport model." *Cement and Concrete Research*, 29, 827-837.

Braunstein, J. (1971). Statistical thermodynamics of molten salts and concentrated aqueous electrolytes. In: Petrucci, S. (ed.): Ionic Interactions Vol.1. Academic Press, New York, 180-261.

Buenfeld, N.R., Shurafa-Daoudi, M.T. and McLoughlin, I.M. (1997). "Chloride transport due to wick action in concrete. In: Nilsson, L.O. and Ollivier, J.P. (eds.): Chloride Penetration into Concrete." *Proceedings of the International RILEM Workshop*, St-Remy-les-Chevreuse, France, 315-324.

Chatterji, S. (1994). "Transportation of Ions through Cement Based Materials, Part I: Fundamental Equations and Basic Measurement Techniques." *Cement and Concrete Research*, 24(5), 907-912.

Christensen, R.M. (1979). Mechanics of Composite Materials. Wiley Interscience, New York.

Clegg, S.L. and Pitzer, K.S. (1992). "Thermodynamics of multi-component, miscible, ionic solutions: generalized equations for symmetric electrolytes." *Journal of Physics Chemistry*, 96, 3513-3520.

Clifton, J.R. (1993). "Predicting the service life of concrete." *ACI Materials Journal*, 90, 611–617.

Collepardi, M., Marciall, A., and Turriziani, R. (1972). "Penetration of Chloride Ions in Cement Pastes and Concrete." *Journal of American Ceramic Society*, 55(10), 534-535.

Costa, A. and Appleton, J. (1999). "Chloride Penetration into Concrete in Marine Environment – Part II: Prediction of Long Term Chloride Penetration." *Materials and Structures (RILEM)*, 32, 354-359.

Daigle, L., Lounis, Z., and Cusson, D. (2004). "Numerical prediction of early-age cracking and corrosion in high performance concrete bridges – case study." *2004 Annual Conference of the Transportation Association of Canada on the Innovation in Bridge Engineering Session*. Quebec City, Quebec.

Dunker, K.F. and Rabbat, B.G (1993). "Why America's Bridges Are Crumbling." *Scientific American*, 268, 66-72.

Duprat, F. (2007). "Reliability of RC beams under chloride-ingress." *Construction and Building Materials*, 21, 1605-1616.

Engelund, S. and Sorensen, J.D. (1998). "A probabilistic model for chloride-ingress and initiation of corrosion in reinforced concrete structures." *Structural Safety*, 20, 69-89.

Engelund, S., Sorensen, J.D., and Krenk, S. (1995) "Estimation of the time to initiation of corrosion in existing uncracked concrete structures." *In: M. Lemaire, J.L. Favre and A. Mebarki (editors): Application of statistics and probability, ICASP7 Proceedings*, Paris, Balkema, 501-506.

Federal Highway Administration (2000). "Our nation's highways – selected figures and facts." U.S. Department of Transportation.

Frank, H. and Thompson, P.T. (1959). In: Hamer, W. (ed.): Structure of Electrolytic Solution. Wiley-Sons, New York, 113-134.

Freeze, R.A. and Cherry, J.A. (1979). Groundwater: Englewood Cliffs. New Jersey, Prentice-Hall, Inc.

Garrabrants, A.C., Sanchez, F., and Kosson, D.S. (2004). "Changes in constituent equilibrium leaching and pore water characteristics of a Portland cement mortar as a result of carbonation. *Waste Management*, 24, 19-36.

Gharaibeh, E.S., Hanai, T., Kong, J.S., Xi, Y., and Frangopol, D.M. (2000). "Effect of uncertainties on chloride renetration in saturated concrete." *8th ASCE Specialty Conference on Probabilistic Mechanics and Structural Reliability*. 1-6.

Hall, C. (1989). "Water sorptivity of mortars and concretes: a review." *Magazine of Concrete Research*, 41, 51-61.

Harned, S. and Owen, B.B. (1958). The Physical Chemistry of Electrolytis Solutions. Reinhold Book Corporation, New York.

Hoffman, P.C. and Weyers, R.E. (1994). "Predicting critical chloride levels in concrete bridge decks." *In: Schueller G.I., Shinozuka, M. and Yao, J.T.P. (eds.): Structural Safety and Reliability. Proceedings of ICOSSAR'93*, A.A. Balkema, Rotterdam, 957-959.

Huang, C.L. D., Siang, H. H., and Best, C. H. (1978). "Heat and Moisture Transfer in Concrete Slabs." *Heat Mass Transfer*, 22, 257-266.

Hudson, L. R. (1987). Calcium Magnesium Acetate from Low Grade Biomass, Energy from Biomass and Wastes, Institute of Gas Technology, Orlando, Florida.

Jennings, H.M. and Tennis, P.D. (1994). "A Model for the Developing Microstructure in Portland Cement Paste." *Journal of American Ceramic Society*, 77(2), 3161-3172.

Jennings, H.M. and Xi, Y. (1993). "Microstructurally Based Mechanisms for Modeling Shrinkage of Cement Paste at Multiscale Levels." *Proc. of the 5th Int. Conf. on Creep and Shrinkage of Concrete*, Barcelona, Spain, September.

Jennings, H.M., Xi, Y., Bazant, Z.P., and Ming Y. (1994). "Constitutive Characterizations of Cementitious Materials Based on Microstructural Models." *Proc. of NATO/RILEM workshop on the Modeling of Microstructure and its Potential for Studying Transport Properties and Durability*, St. Remy-les-Chevreuse, France, July 10-13.

Johannesson, B., Yamada, K., Nilsson, L.O., and Hosokawa, Y. (2007). "Multi-species ionic diffusion in concrete with account to interaction between ions in the pore solution and cement hydrates." *Materials and Structures*, 40, 651-665.

Kempers, L.J.T.M. (2001). "Multiplicity of Solutions Induced by Thermosolutal Convection in a Square Porous Cavity Heated from Below and Submitted to Horizontal Concentration Gradient in the Presence of Soret Effect." *Journal of Chemical Physics*, 115, 6330-6341.

Kirkpatrick, T.J., Weyers, R.E., Anderson-Cook, C.M., and Sprinkel, M.M. (2002). "Probabilistic model for the chloride-induced corrosion service life of bridge decks." *Cement and Concrete Research*, 32, 1943-1960.

Kirkpatrick, T.J., Weyers, R.E., Sprinkel, M.M., and Anderson-Cook, C.M. (2002). "Impact of specification changes on chloride-induced corrosion service life of bridge deck." *Cement and Concrete Research*, 32, 1189–1197.

Kong, J.S., Ababneh, A.N., Frangopol, D.M., and Xi, Y. (2002). "Reliability analysis of chloride penetration in saturated concrete." *Probabilistic Engineering Mechanics*, 17, 305–315.

Li, L., Damrongwiriyanupap, N., and Xi, Y. (2010). "A Probabilistic Prediction Model for the Corrosion Initiation Time of Steel Reinforcement in Concrete Structures." *International Journal of Modelling, Identification, and Control* (In press).

Li, L.Y. and Page, C.L. (2000). "Finite element modeling of chloride removal from concrete by an electrochemical method." *Corrosion Science*, 42, 2145-2165.

Li, L.Y. and Page, C.L. (1998). "Modeling of electrochemical chloride extraction from concrete: influence of ionic activity coefficients." *Computational Materials Science*, 9, 303-308.

Lounis, Z. and Amleh, L. (2003). "Reliability-based prediction of chloride ingress and reinforcement corrosion of aging concrete bridge decks." *Proc. of the 3rd International IABMAS Workshop on Life-Cycle Cost Analysis and Design of Civil Infrastructure Systems*. Lausanne, Switzland, 139-147.

Lounis, Z. (2003). "Probabilistic modeling of chloride contamination and corrosion of concrete bridge structures." *Proc. of Int. Symp. on Uncertainty Modelling and Analysis, College Park, MD.*, September 21-24, 447-451.

Mansour, A.,Amahmid, A., Hasnaoui, M., and Bourich, M. (2006). "Multiplicity of Solutions Induced by Thermosolutal Convection in a Square Porous Cavity Heated from Below and Submitted to Horizontal Concentration Gradient in the Presence of Soret Effect." *Numerical Heat Transfer, Part A: Applications*, 49, 69-94.

Marchand, J. (2001). "Modeling the behavior of unsaturated cement systems exposed to aggressive chemical environments." *Materials and Structures*, 34, 195-200.

Marchand, J., Samson, E., Maltais, Y., and Beaudoin, J.J. (2002). "Theoretical analysis of the effect of weak sodium sulfate solutions on the durability of concrete. Cement & Concrete Composites, 24, (2002) 317-329.

Martin-Perez, B., Zibara, H., Hooton, R.D., and Thomas, M.D.A. (2000). "A study of the effect of chloride binding on service life predictions." *Cement and Concrete Research*, 30, 1215-1223.

Martys, N.S., Torquato, S., and Bentz, D.P. (1994). "Universal Scaling of Fluid Permeability for Sphere Packings." *Phys. Rev.*, E, 50(1), 403-408.

McGrath, P. (1996). "Development of Test Methods for Predicting Chloride Penetration into High Performance Concrete." Department of Civil Engineering, University of Toronto.

Moran, V.M. (1992). "A Comparison of Conventional and Alternate Deicers: An Environmental Impact Perspective." *in Chemical Deicers and the Environment, F.M. D'Itri (Editor)*, Lewis Publishers, Chelsea, MI, USA. (1992).

Mortimer, R.G. and Eyring, H. (1980). "Elementary Transition State Theory of the Soret and Dufour Effects." *Proceedings of the National Academy of Sciences*, 77, 1728-1731.

Nakhi, A. (2004). "Damage Impace on Chloride Diffusion through Concrete: Experimental, Theoretical, and Numerical Studies." Ph.D. Dissertation of the University of Colorado at Boulder.

Newman, J.S. (1973). Electrochemical Systems. Prentice-Hall, Englewood Cliffs, NJ.

Nguyen, T.Q., Baroghel-Bouny, V., and Dangla, P. (2006). "Prediction of chloride ingress into saturated concrete on the basis of multi-species model by numerical calculations." *Computers and Concrete*, 3(6), 401-422.

Nguyen, T.Q., Petkovic, J., Dangla, P., and Baroghel-Bouny, V. (2008). "Modelling of coupled ion and moisture transport in porous building materials." *Construction and Building Materials*, 22, 2185-2195.

Nilsson, L.O. (2005). "Concepts in chloride ingress modeling." *Proc. 3rd International RILEM Workshop on Testing and Modeling Chloride Ingress into Concrete*, RILEM Publications, Cachan, France, 29-48.

Nilsson, L.O. (2006). "Present limitations of models for predicting chloride ingress into reinforced concrete structures." *Journal of Physics IV France*, 136, 123-130.

Oberholster, R. and Davies, G. (1986). "An accelerated method for testing the potential reactivity of siliceous aggregates." *Cement and Concrete Research*, 16, 181-189.

Page, C.L., Short, N.R., and El Tarras, A. (1981). "Diffusion of Chloride Ions in Hardened Cement Paste." *Cement and Concrete Research*, 11(3), 395-406.

Perez, B.M., Zibara, H., Hooton, R.D., and Thomas, M.D.A. (1999). "A study of the effect of chloride binding on service life prediction." *ACI Materials Journal*, 96.

Philip, J.R. (1969). "Theory of infiltration." *Advance Hydroscience*, 5, 215-296.

Pielou, E.C. (1977). Mathematical Ecology, A Wiley-Interscience Publication, John Wiley & Sons, New York.

Platten, J.K. (2006). "The Soret Effect: A Review of Recent Experimental Results." *Journal of applied mechanics*, 73, 5-15.

Poirier, J.C. (1966). In: Conway, B.E. and Barrados (eds.): Chemical Physics of Ionic Solutions. Wiley-Sons, New York, 9-27.

Probstein, R.F. (1989). Physicochemical Hydrodynamics. Butterworth Publishers, New York.

Resibois, P.M.V. (1966). Electrolyte Theory, Harper and Row. New York.

Saetta, A.V., Scotta, R.V., and Vitaliani, R.V. (1993). "Analysis of Chloride Diffusion into Partially Saturated Concrete." *ACI Materials Journal*, 90(5), 441-451.

Samson, E. and Marchand, J. (2007). "Modeling the transport of ions in unsaturated cement-based materials." *Computers and Structures*, 85, 1740-1756.

Samson, E. and Marchand, J. (1999). "Numerical Solution of the Extended Nernst-Planck Model." *Journal of Colloid and Interface Science*, 215, 1-8.

Samson, E., Lemaire, G., Marchand, J., and Beaudoin, J.J. (1999). "Modeling chemical activity effects in strong ionic solutions." *Computational Materials Science*, 15, 285-294.

Samson, E., Marchand, J., Robert, J.L., and Bournazel, J.P. (1999). "Modelling ion diffusion mechanisms in porous media." *International Journal for Numerical Methods in Engineering*, 46, 2043-2060.

Sergi, G., Walker, R.J., and Page, C.L. (1996). "Mechanism and criteria for the realkalisation of concrete, corrosion of reinforcement in concrete construction." *In: Page, C.L., Bamforth, P.B. and Figg, J.W. (eds.): Royal Society of Chemistry*, Cambridge, 491-500.

Sergi, G., Yu, S.W., and Page, C.L. (1992). "Diffusion of chloride and hydroxyl ions in cementitious materials exposed to a saline environment." *Magazine of Concrete Research*, 44, 63-72.

Serra, J. (1982). Image Analysis and Mathematical Morphology, Vol. 1, Academic Press, London.

Serra, J. (1988). Image analysis and Mathematical Morphology, Vol. 2: Theoretical Advances, Academic Press, Harcourt Brace Jovanovich, Publishers, London.

Snyder, K.A. and Marchand, J. (2001). "Effect of speciation on the apparent diffusion coefficient in non-reactive porous systems." *Cement and Concrete Research*, 31, 1837-1845.

Stanish, K.D., Hooton, R.D., and Thomas, M.D.A (1997). "Testing the Chloride Penetration Resistance of Concrete: A Literature Review." Department of Civil Engineering, University of Toronto.

Stix, G. (1993), "Concrete solutions." *Scientific American,* 268(4), 102-112.

Streicher, P.E. and Alexander, M.G. (1995). "A Chloride Conduction Test for Concrete." *Cement and Concrete Research*, 25(6), 1284-1294.

Suwito, A. and Xi, Y. (2004). "Service Life of Reinforced Concrete Structures with Corrosion Damage due to Chloride Attack." *In: Frangopol, D.M., Bruhwiler, E., Faber, M.H. and Adey, B. (eds): Life-Cycle Performance of Deteriorating Structures: Assessment, Design and Management,* Special Publication of ASCE, 207-218.

Suwito, X.-C. Cai, and Y. Xi (2006). "Parallel Finite Element Method for Coupled Chloride Penetration and Moisture Diffusion in Concrete." *International Journal of Numerical Analysis and Modeling*, 3(4), 481-503.

Swaddiwudhipong, S, Wong, S.F., Wee, T.H., and Lee, S.L. (2000). "Chloride Ingress in Partially Saturated and Fully Saturated Concretes." *Concrete Science and Engineering*, 2, 17-31.

Tang, L. and Nilsson, L.O. (1992). "Chloride Diffusivity in High Strength Concrete." *Nordic Concrete Research*, 11, 162-170.

Taylor, H.F.W. (1987). "A method for predicting alkali ion concentration in cement pore solution." *Advances in Cement Research*, 1, 5-17.

Thomas, M.D.A. and Jones, M.R. (1996). "A critical review of service life modeling of concretes exposed to chlorides." *In: Dhir, R.K. and Hewlett, P.C. (eds.): Concrete in Service of Mankind: Radical Concrete Technology. E. & F.N.Spon, Lomdon*, 723-736.

Torquato, S. (1992). "Connection between Morphology and Effective Properties of Heterogeneous Materials, in Applied Mechanics Division, ASCE, AMD-Vol. 147, Macroscopic Behavior of Heterogeneous Materials from the Microstructure.

Torquato, S. (1986). "Microstructure Characterization and Bulk Properties of Disordered Two-Phase Media." *Journal of Statistical Physics*, 45(5,6), 843-873.

Torquato, S. (1991). "Random heterogeneous media: Microstructure and improved bounds on effective properties." *Appl. Mech. Rev.*, 44(2), Feb., 37-76.

Vu, K.A.T. and Stewart, M.G. (2000). "Structural reliability of concrete bridges including improved chloride-induced corrosion models." *Structural Safety*, 22, 313-333.

Wang, H.F. and Anderson, M.P. (1982). Introduction to Groundwater Modeling: Finite Difference and Finite Element Methods. W.H. Freeman and Company.

Wang, Y., Li, L.Y. and Page, C.L. Modeling of chloride ingress into concrete from a saline environment. Building and Environment 40, (2005)1573-1582.

Wang, Y., Li, L.Y., and Page, C.L. A two-dimensional model of electrochemical chloride removal from concrete. Computational Materials Science, 20, (2001) 196-212.

Wee, T.H., Wong, S.F., Swadiwudhipong, S., and Lee, S.L. (1997). "A Prediction Method for Long-Term Chloride Concentration Profiles in Hardened Cement Matrix Materials." *ACI Materials Journal*, 94(6), 565-576.

Whiting, D. (1981). "Rapid Determination of the Chloride Permeability of Concrete." Federal Highway Administration, Report No. FHWA/RD-81/119, Washington, DC.

Williamson, G.S., Weyers, R.E., Brown, A.R., and Sprinkel, M.M. (2008). "Validation of probability-based chloride-induced corrosion service-life model." *ACI Materials Journal*, 105(4), 375-380.

Xi, Y. (1995a). "A Model for Moisture Capacities of Composite Materials, Part I: Formulation." *Computational Materials Scien*ce, 4, 65-77.

Xi, Y. (1995b). "A Model for Moisture Capacities of Composite Materials, Part II: Application to Concrete." *Computational Materials Science*, 4, 78-92.

Xi, Y. (1996). "Analysis of Internal Structures of Composite Materials by Second Order Property of Mosaic Patterns." *Materials Characterization*, Jan., 11-25.

Xi, Y. and Bazant, Z. (1999). "Modeling Chloride Penetration in Saturated Concrete." *Journal of Materials in Civil Engineering*, ASCE, 11(1), 58-65.

Xi, Y., Bazant, Z.P., and Jennings, H.M. (1995a). “Moisture Diffusion in Cementitious Materials: Adsorption Isotherm." *Journal of Advanced Cement-Based Materials*, 1, 248-257.

Xi, Y., Bazant, Z.P., and Jennings, H.M. (1995b). “Moisture Diffusion in Cementitious Materials: Moisture Capacity and Diffusivity." *Journal of Advanced Cement-Based Materials*, 1, 258-266.

Xi, Y., Jennings, H.M., and Tennis, P. (1996). “Mathematical Modeling of Cement Paste Microstructure by Mosaic Pattern Part I: Theory.” *Journal of Materials Research*, 11(8), 1943--1952.

Xi, Y., Willam, K., and Frangopol, D. (2000). “Multiscale Modeling of Interactive Diffusion Process in Concrete.” *Journal of Materials in Civil Engineering, ASCE*, 126(3), 258-265.

Zhang, M.H. and Gjorv, O.E. (1991). “Permeability of high strength lightweight concrete.” *ACI Materials Journal*, 88, 463-469.

APPENDIX A

DIFFERENTIAL OF THE INVERSE OF THE COMPLEMENTARY ERROR FUNCTION

Consider the following complementary error function

$$y = erfc(x) = 1 - erf(x) = \frac{2}{\sqrt{\pi}} \int_{x}^{\infty} e^{-t^2} dt \tag{A.1}$$

The inverse of equation (A-1) thus is expressed as,

$$x = erfc^{-1}(y) \tag{A.2}$$

The differential of equation (A-1) is given as follows,

$$\frac{dy}{dx} = -\frac{2}{\sqrt{\pi}} e^{-x^2} \tag{A.3}$$

Hence, the differential of equation (A-2) is given by,

$$\frac{dx}{dy} = \frac{d}{dy}\left[erfc^{-1}(y)\right] = -\frac{\sqrt{\pi}}{2} e^{x^2} = -\frac{\sqrt{\pi}}{2} \exp\left[\left(erfc^{-1}(y)\right)^2\right] \tag{A.4}$$

APPENDIX B

THE DERIVIATION OF CORROSION INITIATION TIME WITH RESPECT TO WATER-CEMENT RATIO AND CURING TIME

Since we have,

$$t_{corr} = \frac{d^2\left(1+\frac{C_{b,th}}{C_{f,th}}\right)}{4D_a\left[erfc^{-1}\left(\frac{C_{f,th}}{C_0}\right)\right]^2} = \frac{d^2\left(1+C_1\right)}{4D_a\left[erfc^{-1}\left(C_2\right)\right]^2} \tag{B.1}$$

when

$$D_a = \left\{\left[\frac{1}{4}+\frac{28-t_0}{300}\right](w/c)^{6.55}+\frac{(28-t_0)}{62,500}\right\}.\frac{2\left[1-(V_p-V_p^c)\right]}{S^2}\left(V_p-V_p^c\right)^f\left[1-k_{ion}(C_f)^m\right] \tag{B.2}$$

$$\frac{\partial t_{corr}}{\partial(w/c)} = \frac{\partial t_{corr}}{\partial D_a}\frac{\partial D_a}{\partial(w/c)} \tag{B.3}$$

$$\frac{\partial t_{corr}}{\partial t_0} = \frac{\partial t_{corr}}{\partial D_a}\frac{\partial D_a}{\partial t_0} \tag{B.4}$$

$$\frac{\partial t_{corr}}{\partial D_a} = -\frac{t_{corr}}{D_a} = -\frac{t_{corr}}{\left\{\left[\frac{1}{4}+\frac{28-t_0}{300}\right](w/c)^{6.55}+\frac{(28-t_0)}{62,500}\right\}.\frac{2\left[1-(V_p-V_p^c)\right]}{S^2}\left(V_p-V_p^c\right)^f\left[1-k_{ion}(C_f)^m\right]} \tag{B.5}$$

$$\frac{\partial D_a}{\partial (w/c)} = \left\{ (6.55)\left[\frac{1}{4} + \frac{28 - t_0}{300} \right] (w/c)^{5.55} \right\} . \frac{2\left[1 - (V_p - V_p^c) \right]}{S^2} \left(V_p - V_p^c \right)^f \left[1 - k_{ion} (C_f)^m \right] \tag{B.6}$$

$$\frac{\partial D_a}{\partial t_0} = -\left[\frac{(w/c)^{6.55}}{300} + \frac{1}{62,500} \right] . \frac{2\left[1 - (V_p - V_p^c) \right]}{S^2} \left(V_p - V_p^c \right)^f \left[1 - k_{ion} (C_f)^m \right] \tag{B.7}$$

Substituting (B.5) and (B.6) into (B.3), yields

$$\frac{\partial t_{corr}}{\partial (w/c)} = \frac{-6.55 t_{corr} \left\{ \left[\frac{1}{4} + \frac{28 - t_0}{300} \right] (w/c)^{5.55} \right\}}{\left\{ \left[\frac{1}{4} + \frac{28 - t_0}{300} \right] (w/c)^{6.55} + \frac{(28 - t_0)}{62,500} \right\}} \tag{B.8}$$

Also, substituting (B.5) and (B.7) into (B.4), yields

$$\frac{\partial t_{corr}}{\partial t_0} = \frac{t_{corr} \left[\frac{(w/c)^{6.55}}{300} + \frac{1}{62,500} \right]}{\left\{ \left[\frac{1}{4} + \frac{28 - t_0}{300} \right] (w/c)^{6.55} + \frac{(28 - t_0)}{62,500} \right\}} \tag{B.9}$$

APPENDIX C

ADSORPTION ISOTHERMS AND MOISTURE CAPACITIES OF CEMENT PASTE AND AGGREGATE

The adsorption isotherm of porous media is described as the relationship between moisture content and relative humidity at a constant temperature which can be explained by the BSB model (Brunauer et al., 1969).

$$w = \frac{CkV_m H}{(1-kH)[1+(C-1)kH]} \tag{C.1}$$

The moisture capacity can be obtained in the form of derivative of the adsorption isotherm, Eq. (C.1), with respect to relative humidity, H, as follows:

$$\frac{dw}{dH} = \frac{CkV_m + wk[1+(C-1)kH] - wk[(C-1)(1-kH)]}{(1-kH)[1+(C-1)kH]} \tag{C.2}$$

in which V_m is the monolayer capacity which is the mass of adsorbate required to cover the adsorbent with a single molecular layer, C, is the net heat of adsorption which is a function of temperature, and k represents the degree of saturation of the pores. These three material parameters can be evaluated by using adsorption test data of the material.

Adsorption Isotherm and Moisture Capacity of Cement Paste

The adsorption isotherm and moisture capacity of cement paste can be calculated by using Eqs. (C.1) and (C.2). The three parameters, V_m, C, and k, can be obtained by Xi study (1995b) as follows:

$$V_m = \left(0.068 - \frac{0.22}{t}\right)\left(0.85 + 0.45\frac{w}{c}\right)V_{ct} \quad t > 5 \ days, \quad 0.3 < \frac{w}{c} < 0.7 \tag{C.3}$$

where t is the time in days, w/c is the water-to-cement ratio, and V_{ct} is the type of cement which V_{ct} = 0.9, 1.0, 0.85, and 0.6 for type I, II, III, and IV cements, respectively. The parameter C can be calculated as:

$$C = \exp\left(\frac{C_0}{T}\right) \tag{C.4}$$

in which T is the temperature in Kelvin, and C_0 = 855. The parameter k is expressed as:

$$k = \frac{(1 - 1/n)C - 1}{C - 1} \tag{C.5}$$

in which n is the number of the adsorbed layers in the pore and it is a function of time (in days), water-cement ratio (w/c), and type of cement (N_{ct} = 1.1, 1.0, 1.15, and 1.5 for type I, II, III, and IV cements, respectively):

$$n = \left(2.5 + \frac{15}{t}\right)\left(0.33 + 2.2\frac{w}{c}\right)N_{ct} \qquad t > 5 \ \ days, \quad 0.3 < \frac{w}{c} < 0.7 \tag{C.6}$$

Adsorption Isotherm and Moisture Capacity of Aggregate

The adsorption isotherm and moisture capacity of aggregates can be evaluated based on the same BSB theory, and thus Eqs. (C.1), (C.2), (C.4) and (C.5) are still valid, but the monolayer capacity, V_m, and the number of the adsorbed layers, n, are different. The parameters V_m and n of aggregates can be calculated based on the model proposed by Xi (1995b):

$$V_m = 0.0647 V_{agg} \tag{C.7}$$

$$n = 4.063 n_{agg} \tag{C.8}$$

where V_{agg} and n_{agg} depend on the pore structure of aggregates. For dense aggregates, V_{agg} ranges from 0.05 to 0.1 and from 1.0 to 1.5 for n_{agg}. For porous aggregates, V_{agg} is between 0.01 to 0.04 and from 1.7 to 2.0 for n_{agg}. It should be noted that V_{agg} is larger and nag is smaller for dense aggregates because of their small size of pores and high surface area. Some examples of dense aggregates are Dolomite, granite, crushed limestone, and river gravel. Lightweight aggregates and river sand are considered as porous aggregates (Ababneh, 2002).

APPENDIX D

VOLUME PERCENTAGES OF DIFFERENT HYDRATION PRODUCTS

The model proposed by Jennings and Tennis (1994) is used in this present study which considers five different phases of cement paste: anhydrous, inner hydration product, outer hydration product, capillary pores, and calcium hydroxide (CH and other AFm phases). The volume of C-S-H gel is the sum of the inner and outer hydration products.

$$V_{C-S-H} = V_{inner} + V_{outer} \tag{D.1}$$

The volume fraction of C-S-H gel is:

$$f_{C-S-H} = \frac{V_{C-S-H}}{V_{total}} = \frac{V_{total} - V - V_{cp}}{V_{total}} = 1 - f_1 - f_{cp} \tag{D.2}$$

where V_{total} is the total volume and assumed to be a constant, V_{cp} and f_{cp} are the volume and volume fraction of capillary pores, and V_1 and f_1 are the volume and volume fraction of anhydrous cores of cement grains and of all the crystalline phases such as CH and ettringite. The volume fraction of capillary pores can be express as:

$$f_{cp} = \left(\left(1 - c\right) - c\Omega\right)p \tag{D.3}$$

in which, parameters c and p are dependent on the water-cement ratio, w/c, and the densities of cement, ρ_c, and water, ρ_w, as follows:

$$c = \frac{1}{1+(w/c)} \tag{D.4}$$

$$p = \frac{(1+(w/c))\rho_c}{1+(w/c)(\rho_c/\rho_w)} \tag{D.5}$$

The parameter Ω is related to degree of hydration which can be written as follows:

$$\Omega = 0.437\alpha_{C3S}W_{C3S} + 0.503\alpha_{C2S}W_{C2S} + 0.379\alpha_{C3A}W_{C3A} + 0.136\alpha_{C4AF}W_{C4AF} \tag{D.6}$$

in which W_{C3S}, W_{C2S}, W_{C3A}, W_{C4AF} are the initial weight percentages of the compounds of the cement. And, α_{C3S}, α_{C2S}, α_{C3A}, α_{C4AF} are the degree of hydration of the compounds of cement. The initial percentages of the cement compounds, W_i (i = C_3S, C_2S, C_3A, and C_4AF) depends on the type of cement. The degree of hydration of cement compounds, α_i (i = C_3S, C_2S, C_3A, and C_4AF) can be calculated as:

$$\alpha_i = 1 - e^{-a_i(t-b_i)^{C_i}} \tag{D.7}$$

where a_i, b_i, and c_i (i = C_3S, C_2S, C_3A, and C_4AF) are constants determined experimentally (Taylor et al., 1987) as shown in Table (D.1).

Table D.1 Parameter related to the hydration of different compounds of cement

Compond	a_i	b_i	c_i
C_3S	0.25	0.90	0.70
C_2S	0.46	0.00	0.12
C_3A	0.28	0.90	0.77
C_4AF	0.26	0.90	0.55

Also, f_1 is the volume percentage of the anhydrous cores of cement particles, calcium hydroxide (CH) crystals and ettringite as follows:

$$f_1 = f_{core} + f_{CH} + f_{AFm} \tag{D.8}$$

The volume fraction of the anhydrous cores of cement particles can be determined by the following equation:

$$f_{core} = c\left(\frac{1-\psi}{\rho_c}\right)p \tag{D.9}$$

in which c and p can be obtained from Eqs. (D.4) and (D.5), ρ_c is the density of cement and ψ is a factor depending on the degree of hydration of the compounds of the cement and can be evaluated based on the weight average as follows:

$$\psi = \alpha_{C3S} W_{C3S} + 0\alpha_{C2S} W_{C2S} + 0\alpha_{C3A} W_{C3A} + \alpha_{C4AF} W_{C4AF} \quad \text{(D.10)}$$

The volume fraction of CH crystals and AFm phase can be determined by:

$$f_{CH} = c(0.189\alpha_{C3S} W_{C3S} + 0.058\alpha_{C2S} W_{C2S}) p \quad \text{(D.11)}$$

$$f_{AFm} = c(0.849\alpha_{C3A} W_{C3A} + 0.472\alpha_{C4AF} W_{C4AF}) p \quad \text{(D.12)}$$

The volume fraction of the other two phases can be calculated as:

$$f_3 = [0.706(w/c) + 0.131](1 - f_1 - f_{cp}) + f_{cp} \quad \text{(D.13)}$$

$$f_2 = 1 - f_1 - f_3 \quad \text{(D.14)}$$

APPENDIX E

COMPRESSION TEST RESULTS

Concrete cylinders of 4”x8” were cast and used through the experimental study. The specimens were de-molded after 28 days and cured in a moisture room with RH = 100% for 28 days. After curing, all specimens were capped and tested according to ASTM C39. The compression test of concrete cylinders was performed using a universal MTS loading machine, with maximum capacity of 484 kN (110 kips). The test was set up by applying a compressive axial load on concrete specimens at a rate of 2 kN/sec until failure. The maximum loads were recorded and the compressive strength can be calculated by dividing the average maximum loads by the cross-sectional area of specimen. Table (E.1) as shown below are the compression test results of concrete specimens prepared from the mix used in the experimental study.

Table E.1 Compression test results

Specimen #	**Maximum load (kN)**	
	w/c = 0.65	**w/c = 0.55**
1	203.86	187.76
2	155.95	232.91
3	176.91	172.72
Average	178.91	197.80
f_c' (MPa)	22.06	24.43

APPENDIX F

RAPID CHLORIDE PERMEABILITY TEST (RCPT)

This test was conducted by following ASTM C 1202. The apparatus used in this study based on requirements of ASTM standard was commercially produced by *Prove-It Instruments*. The specimens were prepared by using water-cooled diamond saw to cut the faces of specimens in 50 mm thick and 100 mm diameter as shown in Fig. (F.1). In order to prevent fluid from leaking through the sidewalls of the disc and to create linear flow of electrical current, the cylinder walls of specimens were sealed with a coating of silicone and allowed to dry for 12 hours. After drying, they were then vacuumed for 3 hours. De-aerated water was filled into container to cover the specimens and vacuum pump was maintained to run for one additional hour. The specimens were allowed to submerge in water for 18 hours. Each specimen was then immediately loaded into apparatus, which can be seen as Fig. (F.2). When loaded, solutions were added to the two chambers: one with 3% solution of NaCl and the other with 0.3 NaOH. Chloride ion penetrability was measured by using supplied software and interface hardware. Once the test cycle started, a 60 Volt applied DC voltage was imposed across the concrete specimens for six hours. The capability of chloride ion passed through faces of concrete specimens was measured in terms of the impedance in Coulombs over the total time of the test.

Fig. F.1 Concrete specimens for Rapid Chloride Permeability Test

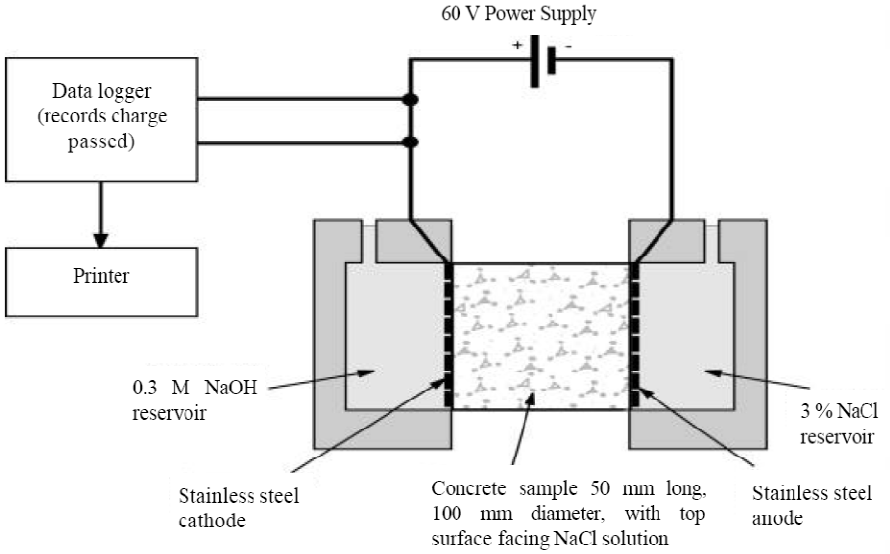

Fig. F.2 Rapid Chloride Permeability Test Set Up (Stanish et al., 1997)

Test Results of RCPT

The results of Rapid Chloride Permeability Test of concrete specimens prepared from the mix used in the experimental study are shown in Table (F.1). It is found that the total charge passed through the concrete specimens is in high rate of chloride ion permeability when compared with ASTM standard shown in Table (F.2). Therefore, it can be concluded that these concrete specimens have high chloride ion penetrability. As a result, the specimens are considered as low chloride ion resistance.

Table F.1 RCPT Test Results

Mix 1 (w/c = 0.65)	**Coulombs**	**Chloride ion penetrability (compared with ASTM C 1202)**
Sample# 1	5108	High
Sample# 2	9680	High
Mix 2 (w/c = 0.55)	**Coulombs**	**Chloride ion penetrability (compared with ASTM C 1202)**
Sample# 1	5613	High
Sample# 2	7219	High

Table F.2 RCPT Concrete Permeability Ratings (ASTM C 1201)

Charge Passed (Coulombs)	Chloride Ion Penetrability
> 4000	High
2000 – 4000	Moderate
1000 – 2000	Low
100 -1000	Very Low
< 100	Negligible

APPENDIX G

EXPERIMENTAL PROCEDURE FOR OBTAINING CHLORIDE PROFILES

After each certain exposure period (15 and 30 days) the samples were removed from the solutions and cleaned by removing salts, and then dried at room temperature for one day. Since the specimens had dried the surface were cleaned from salt deposit on top surface by using a wire brush.

Collecting Concrete Dust Samples

The concrete dust samples were collected using a drill press shown in Fig. (G.1). The drilling started from the top surface exposed to the chloride solution and extended at ¼" (≈ 6 mm) depth increments.

Electro-Chemical Analysis

In order to obtain chloride profiles, concrete dust samples were analyzed by the Rapid Chloride Test Water-soluble (RCTW) method. The results from this analysis represented in a profile of total chloride concentration as a weight percentage of concrete weight. The RCTW test kit was manufactured by *Germann Instruments, Inc*. and the items used from this test kit to analyze the powder samples included; the chloride electrode, the electrometer for mV (mille Volt) readings, the calibration liquids (0.005%, 0.020%, 0.050% and 0.500%), the chloride ion extraction liquid, the

electrode wetting agent, distilled water, and cleaning tissues as shown below in Fig. (G.2).

Fig. G.1 Drilling of concrete sample (Isteita, 2009)

Fig. G.2 Items used for chloride concentration measurement (Isteita, 2009)

The electro-chemical analysis procedure is summarized as follows:

1. The chloride electrode was filled with the electrode wetting agent and cleaned with distilled water.
2. The electrode was submerged into a vial containing the 0.005% calibration solution and the voltage reading (mV) displayed by the electrometer was recorded. This procedure was repeated for the remaining three calibration liquids and the readings from the four solutions were used to plot the 'before' calibration curve.
3. The electrode was cleaned by spraying with distilled water and wiping after each use.
4. 10 ml of chloride extraction liquid was added to a vile containing 1.5 grams of the collected dust sample.
5. The vials containing the concrete dust and the extraction liquid were secured with lids and shaken for 5 minutes.
6. The electrode was submerged next day into the vials containing the concrete dust and extraction liquid and the measured mV-readings were recorded.
7. After taking the readings from all of the samples the electrode was calibrated again, using the method explained above in Step 2. These readings were then used to plot the 'after' calibration curve.
8. The measured mV-readings were converted to total chloride concentration by using the 'before' and 'after' calibration curves and finding the average of the two conversions.

The followings are the results of electro-chemical analysis.

Table G.1 The mV readings after 15 days of exposure

Specimen	Depth Range (mm)						
	0-6	6-12	12-18	18-24	24-30	30-36	36-42
3% NaCl (w/c = 0.55)	2.3	18.4	45.4	78.1	86.8	91.9	88.0
3% $CaCl_2$ (w/c = 0.55)	3.8	24.9	47.7	83.6	93.7	104.8	96.4
3% $MgCl_2$ (w/c = 0.55)	7.1	31.3	57.4	80.7	104.3	94.2	103.6
3% NaCl + 3%$CaCl_2$ (w/c = 0.55)	0.4	25.5	49.7	85.5	97.2	99.8	103.4
3% NaCl + 3% $MgCl_2$ (w/c = 0.55)	1.4	23.6	56.9	73.2	84.2	85.4	91.3
3% $CaCl_2$ + 3% $MgCl_2$ (w/c = 0.55)	1.4	22.7	39.9	72.6	90.6	94.8	100.4
3% NaCl (w/c = 0.65)	3.1	14.4	45.7	81.5	102.9	106.4	85.9
3% $CaCl_2$ (w/c = 0.65)	3.3	26.8	42.0	87.4	98.1	105.6	89.3
3% $MgCl_2$ (w/c = 0.65)	7.0	24.4	52.5	101.5	96.6	106.8	105.4
3% NaCl + 3% $CaCl_2$ (w/c = 0.65)	-2.3	17.0	33.1	73.0	91.4	108.1	104.0
3% NaCl + 3% $MgCl_2$ (w/c = 0.65)	1.1	18.7	48.4	87.3	93.0	101.3	99.2
3% $CaCl_2$ + 3% $MgCl_2$ (w/c = 0.65)	1.5	18.6	34.5	89.6	100.6	105.8	103.6

Table G.2 The mV readings for the calibration associated with Table G.1

% Cl	mV Before	mV After
0.005	76.2	76.0
0.02	65.6	65.3
0.05	54.6	54.2
0.5	-5.1	-5.4

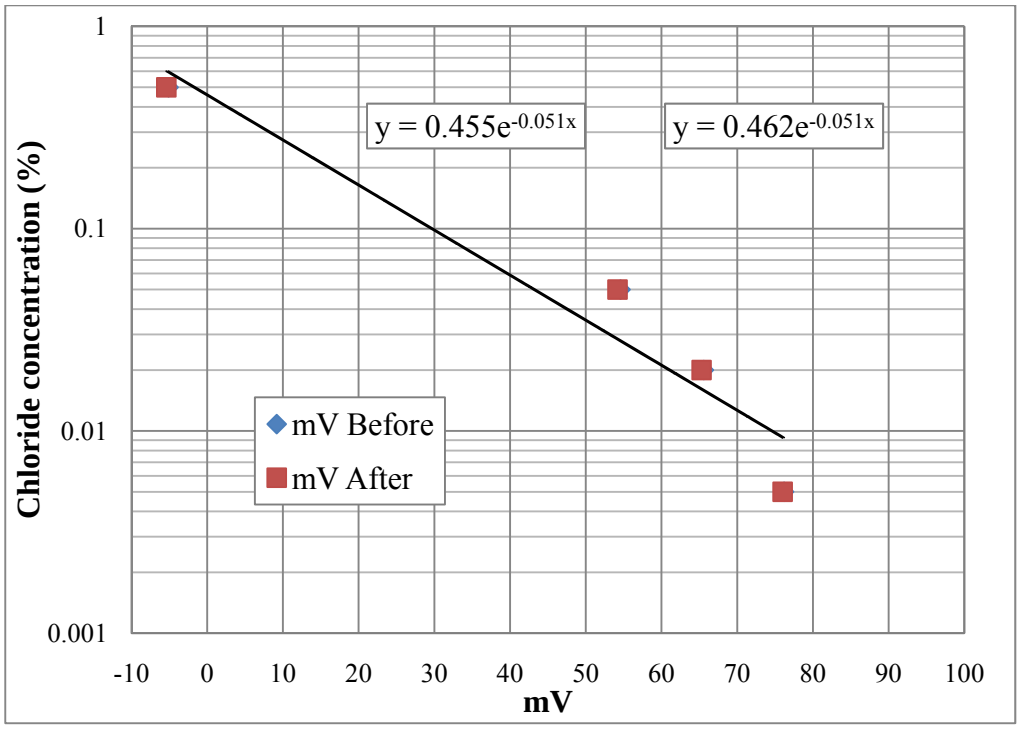

Fig. G.3 Calibration curve for obtaining chloride concentrations

(associated with Tables G.1 and G.2)

Table G.3 The mV readings after 30 days of exposure

Specimen	Depth Range (mm)						
	0-6	6-12	12-18	18-24	24-30	30-36	36-42
3% NaCl (w/c = 0.55)	-2.3	12.1	33.4	61.6	73.7	70.4	102.9
3% $CaCl_2$ (w/c = 0.55)	-0.8	17.2	35.0	61.9	94.3	94.5	95.4
3% $MgCl_2$ (w/c = 0.55)	2.4	19.7	46.0	75.3	95.6	102.9	100.5
3% NaCl + 3%$CaCl_2$ (w/c = 0.55)	-4.1	11.0	37.0	66.6	88.3	93.0	103.6
3% NaCl + 3% $MgCl_2$ (w/c = 0.55)	-1.6	14.7	40.9	55.7	81.3	102.6	105.5
3% $CaCl_2$ + 3% $MgCl_2$ (w/c = 0.55)	-2.8	12.2	29.6	66.5	93.3	96.0	104.6
3% NaCl (w/c = 0.65)	-3.0	11.6	25.1	48.4	76.7	100.1	103.8
3% $CaCl_2$ (w/c = 0.65)	1.2	9.3	26.5	46.0	66.4	85.8	93.0
3% $MgCl_2$ (w/c = 0.65)	3.8	12.6	27.6	52.4	95.3	98.3	104.0
3% NaCl + 3% $CaCl_2$ (w/c = 0.65)	-6.4	8.3	21.7	41.1	76.8	97.8	95.2
3% NaCl + 3% $MgCl_2$ (w/c = 0.65)	-1.6	12.0	24.6	47.5	91.6	91.8	94.8
3% $CaCl_2$ + 3% $MgCl_2$ (w/c = 0.65)	-1.9	10.8	22.7	44.7	90.0	96.1	98.7

Table G.4 The mV readings for the calibration associated with Table G.3

% Cl	mV Before	mv After
0.005	73.7	74.2
0.02	65.7	65.2
0.05	54.2	54.0
0.5	-4.1	-4.1

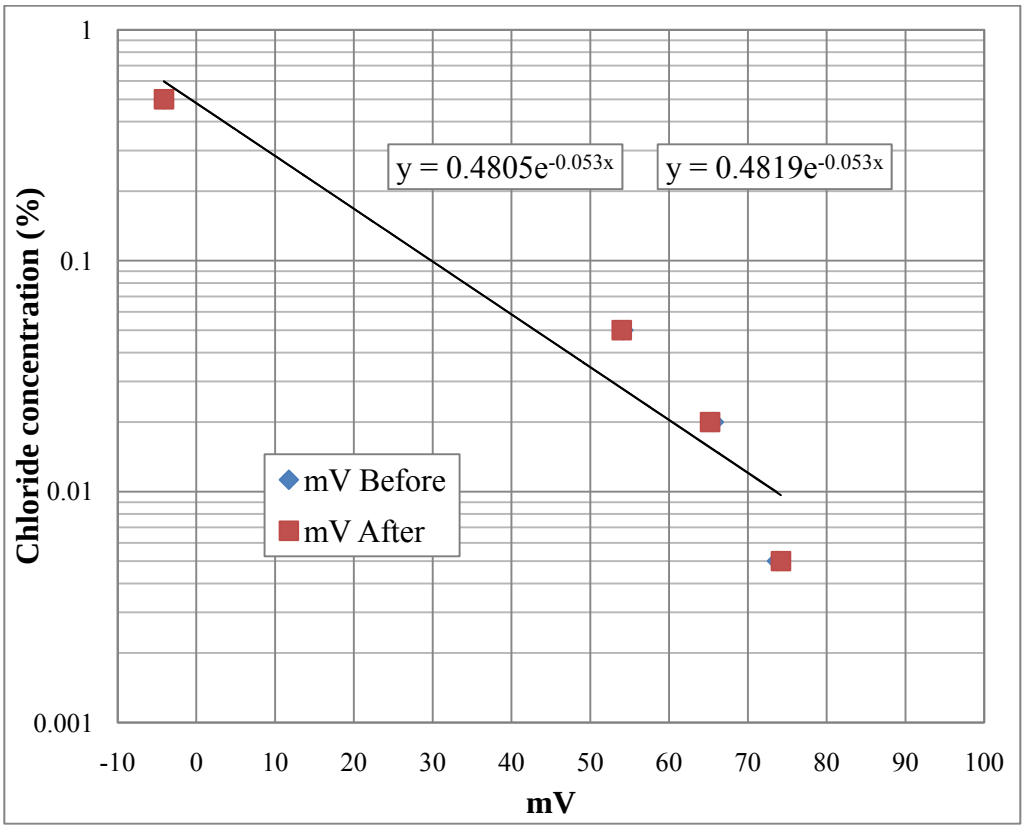

Fig. G.4 Calibration curve for obtaining chloride concentrations

(associated with Tables G.3 and G.4)

Table G.5 Total chloride concentration after 15 days of exposure

Specimen	Depth Range (mm)						
	0-6	6-12	12-18	18-24	24-30	30-36	36-42
3% NaCl (w/c = 0.55)	0.409	0.180	0.045	0.009	0.005	0.004	0.005
3% $CaCl_2$ (w/c = 0.55)	0.379	0.129	0.040	0.006	0.004	0.002	0.003
3% $MgCl_2$ (w/c = 0.55)	0.320	0.093	0.025	0.007	0.002	0.004	0.002
3% NaCl + 3%$CaCl_2$ (w/c = 0.55)	0.450	0.125	0.036	0.006	0.003	0.003	0.002
3% NaCl + 3% $MgCl_2$ (w/c = 0.55)	0.428	0.138	0.025	0.011	0.006	0.006	0.004
3% $CaCl_2$ + 3% $MgCl_2$ (w/c = 0.55)	0.428	0.144	0.060	0.011	0.005	0.004	0.003
3% NaCl (w/c = 0.65)	0.392	0.221	0.045	0.007	0.002	0.002	0.006
3% $CaCl_2$ (w/c = 0.65)	0.388	0.117	0.054	0.005	0.003	0.002	0.005
3% $MgCl_2$ (w/c = 0.65)	0.322	0.132	0.032	0.003	0.003	0.002	0.002
3% NaCl + 3% $CaCl_2$ (w/c = 0.65)	0.517	0.193	0.085	0.011	0.004	0.002	0.002
3% NaCl + 3% $MgCl_2$ (w/c = 0.65)	0.435	0.177	0.039	0.005	0.004	0.003	0.003
3% $CaCl_2$ + 3% $MgCl_2$ (w/c = 0.65)	0.426	0.178	0.079	0.005	0.003	0.002	0.002

Table G.6 Total chloride concentration after 30 days of exposure

Specimen	Depth Range (mm)						
	0-6	6-12	12-18	18-24	24-30	30-36	36-42
3% NaCl (w/c = 0.55)	0.544	0.254	0.082	0.018	0.010	0.012	0.002
3% $CaCl_2$ (w/c = 0.55)	0.503	0.194	0.075	0.018	0.003	0.003	0.003
3% $MgCl_2$ (w/c = 0.55)	0.424	0.170	0.042	0.009	0.003	0.002	0.002
3% NaCl + 3%$CaCl_2$ (w/c = 0.55)	0.599	0.269	0.068	0.014	0.004	0.003	0.002
3% NaCl + 3% $MgCl_2$ (w/c = 0.55)	0.525	0.221	0.055	0.025	0.006	0.002	0.002
3% $CaCl_2$ + 3% $MgCl_2$ (w/c = 0.55)	0.559	0.252	0.100	0.014	0.003	0.003	0.002
3% NaCl (w/c = 0.65)	0.565	0.261	0.127	0.037	0.008	0.002	0.002
3% $CaCl_2$ (w/c = 0.65)	0.452	0.294	0.118	0.042	0.014	0.005	0.003
3% $MgCl_2$ (w/c = 0.65)	0.394	0.247	0.112	0.030	0.003	0.003	0.002
3% NaCl + 3% $CaCl_2$ (w/c = 0.65)	0.677	0.310	0.153	0.055	0.008	0.003	0.003
3% NaCl + 3% $MgCl_2$ (w/c = 0.65)	0.525	0.255	0.131	0.039	0.004	0.004	0.003
3% $CaCl_2$ + 3% $MgCl_2$ (w/c = 0.65)	0.533	0.272	0.145	0.045	0.004	0.003	0.003

APPENDIX H

FINITE ELEMENT FORMULATION

Finite element method is an effective tool to solve several physical problems in engineering and science which are explained in terms of partial differential equations. And, these problems such as heat transfer, fluid flow, and mass diffusion can be solved approximately by finite element. From civil engineering point of view, finite element method is widely used to predict the behavior of structures, soils, and fluid flow. By applying finite element method, chloride diffusion and ion transport in concrete which the governing equation is described by partial differential equation can be solved numerically. Finite element formulation of multi-ionic species diffusion in concrete based on the Nernst-Planck equation will be presented. In order to develop the finite element program, first, the space domain, Ω, is discretized into a number of small regions called finite elements (Suwito, 2005) or often called elements (Fish and Belytschko, 2007). Second, the function of problem is defined within the element using the nodal values of element. Third, the shape function interpolation related to the unknowns in an element is introduced. Finally, the defined function against nodal unknowns is determined for stationary condition. If the problem is time dependent, it is considered as ordinary differential equation and time need to be discretized. If not, the problem will be solved algebraically.

Ion Transport in Concrete

The mechanisms of ion diffusion in concrete can be explained by the Nernst-Planck equation. Not only diffusion mechanism due to concentration gradient but also the electrical coupling between the different ions presented in an ideal solution is accounted for the Nernst-Planck equation.

Governing Equation

The ionic flux of each species is described by the Nernst-Planck equation as follow:

$$J_i = -D_i \nabla C_i - z_i D_i \left(\frac{F}{RT} \nabla \phi \right) C_i \qquad \text{(H.1)}$$

where J_i is the flux, D_i is the diffusion coefficient, C_i is the concentration, z_i is the charge number, F is the Faraday's constant, R is the gas constant, T is the temperature, Φ is the electrostatic potential, and index i represents for *i-th* species.

The mass balance equation can be expressed as:

$$\frac{\partial C_i}{\partial t} = -\nabla J_i \qquad \text{(H.2)}$$

Substituting Eq. (H.1) into Eq. (H.2), leading to

$$\frac{\partial C_i}{\partial t} = \nabla \left(D_i \nabla C_i + z_i D_i \left(\frac{F}{RT} \nabla \phi \right) C_i \right) \qquad \text{(H.3)}$$

The Poisson's equation is selected to solve the electrostatic potential according to spatial distribution of the electric charges which can be written as:

$$\nabla^2\phi + \frac{\rho}{\varepsilon} = 0 \qquad \text{(H.4)}$$

in which ρ is the electrical charge density and ε is the dielectric constant of the surrounding medium expressed as:

$$\rho = F(\sum z_i C_i + w) \qquad \text{(H.5)}$$

Finite Element Formulation

By applying method of weighted residual, the weak form can be written as:

$$W = \int_{\Omega} \lfloor \delta_1 \ \delta_2 ..... \rfloor \begin{Bmatrix} R_1 \\ R_2 \\ M \end{Bmatrix} d\Omega = 0 \qquad \text{(H.6)}$$

where R_i's = the residual functions associated to each of equations.

δ_i's = the weighting functions.

For each of ionic species, the residual functions are represented as Eqs. (H.7) and (H.8) :

$$R_i = \frac{\partial C_i}{\partial t} - div\left(-D_i \left(grad(C_i) + \frac{z_i F}{RT} C_i grad(\phi) \right) \right) \tag{H.7}$$

$$R_v = \nabla^2 \phi - \frac{F}{\varepsilon} (\sum z_i C_i + w) \tag{H.8}$$

Applying Galerkin's method to the residual functions, yields

$$W = \int_{\Omega} N^T \left(\frac{\partial C_i}{\partial t} - div\left(-D_i \left(grad(C_i) + \frac{z_i F}{RT} C_i grad(\phi) \right) \right) \right) d\Omega = 0 \tag{H.9}$$

$$W = \int_{\Omega} N^T \left(\nabla^2 \phi - \frac{F}{\varepsilon} (\sum z_i C_i + w) \right) d\Omega = 0 \tag{H.10}$$

Before formulating the finite element from Eqs. (H.9) and (H.10), the relation between concentration and electrostatic potential in an element, C and Φ; and element nodal concentration and electrostatic potential, C^e and Φ^e, are defined by using the shape function interpolation as follow:

$$C_i = N C_i^{\,e} \tag{H.11}$$

$$grad(C_i) = BC_i^{\ e} \tag{H.12}$$

$$\phi \ = N\phi^{\ e} \tag{H.13}$$

$$grad(\phi) = B\phi^e \tag{H.14}$$

Rewriting the residual function, Eq. (H.9), we have

$$\begin{aligned} W = &\int_\Omega N^T \frac{\partial C_i^e}{\partial t} N d\Omega + \int_\Omega div\left(N^T D_i grad(C_i^e)\right) d\Omega + \int_\Omega \frac{\partial N^T}{\partial x} D_i C_i^e \frac{\partial N}{\partial x} d\Omega \\ &+ \int_\Omega div\left(N^T D_i \frac{z_i F}{RT} grad(\phi) \right) d\Omega + \int_\Omega \frac{\partial N^T}{\partial x} D_i \frac{z_i F}{RT} C_i^e \phi \frac{\partial N}{\partial x} d\Omega = 0 \end{aligned} \tag{H.15}$$

when

$$\int_\Omega div\left(N^T D_i grad(C_i^e)\right) d\Omega = \int_\Gamma N^T D_i \frac{\partial C_i^e}{\partial x} d\Gamma \tag{H.16}$$

$$\int_\Omega div\left(N^T D_i \frac{z_i F}{RT} grad(\phi) \right) = \int_\Gamma N^T D_i \frac{z_i F}{RT} \frac{\partial \phi}{\partial x} d\Gamma \tag{H.17}$$

Rearranging Eq. (H.15), leads to,

$$\int_{\Omega} N^T \frac{\partial C_i^e}{\partial t} N d\Omega + \int_{\Omega} \frac{\partial N^T}{\partial x} D_i C_i^e \frac{\partial N}{\partial x} d\Omega + \int_{\Omega} \frac{\partial N^T}{\partial x} D_i \frac{z_i F}{RT} C_i^e \phi \frac{\partial N}{\partial x} d\Omega = - \int_{\Gamma} N^T D_i \frac{\partial C_i^e}{\partial x} d\Gamma - \int_{\Gamma} N^T D_i \frac{z_i F}{RT} \frac{\partial \phi}{\partial x} d\Gamma \tag{H.18}$$

Similar to another residual function based on Poisson's equation, it can be rewritten as:

$$W = \int_{\Omega} \frac{\partial}{\partial x}\left(N^T \frac{\partial \phi}{\partial x} \right) d\Omega - \int_{\Omega} \frac{\partial N^T}{\partial x} \frac{\partial \phi}{\partial x} d\Omega - \int_{\Omega} N^T \frac{F}{\varepsilon} z_i C_i^e N d\Omega - \int_{\Gamma} N^T \frac{F}{\varepsilon} w d\Gamma = 0 \tag{H.19}$$

when

$$\int_{\Omega} \frac{\partial}{\partial x}\left(N^T \frac{\partial \phi}{\partial x} \right) d\Omega = \int_{\Gamma} N^T \frac{\partial \phi}{\partial x} d\Gamma \tag{H.20}$$

Rearranging Eq. (H.19), we obtain

$$- \int_{\Omega} \frac{\partial N^T}{\partial x} \frac{\partial \phi}{\partial x} d\Omega - \int_{\Omega} N^T \frac{F}{\varepsilon} z_i C_i^e N d\Omega = \int_{\Gamma} N^T \frac{F}{\varepsilon} w d\Gamma - \int_{\Gamma} N^T \frac{\partial \phi}{\partial x} d\Gamma \tag{H.21}$$

Applying Eqs. (H.11) through (H.14) into Eqs. (H.18) and (H.21); and combining these two equations, we have

$$\int_{\Omega} N^T \frac{\partial C_i^e}{\partial t} N d\Omega + \int_{\Omega} B^T D_i C_i^e B d\Omega + \int_{\Omega} B^T D_i \frac{z_i F}{RT} C_i^e \phi B d\Omega - \int_{\Omega} B^T \phi B d\Omega$$
$$- \int_{\Omega} N^T \frac{F}{\varepsilon} z_i C_i^e N d\Omega = \int_{\Gamma} N^T \frac{F}{\varepsilon} w d\Gamma - \int_{\Gamma} N^T \frac{\partial \phi}{\partial x} d\Gamma - \int_{\Gamma} N^T D_i \frac{\partial C_i^e}{\partial x} d\Gamma - \int_{\Gamma} N^T D_i \frac{z_i F}{RT} \frac{\partial \phi}{\partial x} d\Gamma \tag{H.22}$$

Transient Mass Diffusion

In this formulation, we assume that there are 2 ionic species in the system and it can be easily extended to more species. After element assembly, the system equation is given by

$$M \dot{d} + Kd = F \tag{H.23}$$

where

$$d = \begin{Bmatrix} C_1 \\ C_2 \\ \phi \end{Bmatrix} \tag{H.24}$$

$$\dot{d} = \begin{Bmatrix} \dot{C}_1 \\ \dot{C}_2 \\ \dot{\phi} \end{Bmatrix} \tag{H.25}$$

$$M = \int_{\Omega} N^T M_C N d\Omega \tag{H.26}$$

$$M_C = \begin{bmatrix} 1 & 0 & 0 \\ 0 & 1 & 0 \\ 0 & 0 & 0 \end{bmatrix} \tag{H.27}$$

$$K = \int_{\Omega} B^T K_D B d\Omega + \int_{\Omega} B^T K_P B d\Omega \tag{H.28}$$

$$K_D = \begin{bmatrix} D_1 & 0 & \dfrac{D_1 z_1 F}{RT} C_1 \\ 0 & D_2 & \dfrac{D_2 z_2 F}{RT} C_2 \\ 0 & 0 & 1 \end{bmatrix} \tag{H.29}$$

$$K_P = \begin{bmatrix} 0 & 0 & 0 \\ 0 & 0 & 0 \\ -\dfrac{F}{\varepsilon} z_1 & -\dfrac{F}{\varepsilon} z_2 & 0 \end{bmatrix} \tag{H.30}$$

$$F = F_f + F_e \tag{H.31}$$

in which

F_f = Flux on the boundaries of an element

F_e = External force due to the fixed charge density (w)

$$F_f = -\int_{\Gamma} N^T D_i \frac{\partial C}{\partial x} d\Gamma - \int_{\Gamma} N^T D_i \frac{z_i F}{RT} \frac{\partial \phi}{\partial x} d\Gamma - \int_{\Gamma} N^T \frac{\partial \phi}{\partial x} d\Gamma \tag{H.32}$$

$$F_e = -\int_{\Gamma} N^T \frac{F}{\varepsilon} w d\Gamma \tag{H.33}$$

Initial and Boundary Conditions

To solve the governing equation and perform finite element method, the initial and boundary conditions need to be specified. The initial conditions for two ionic species and electrostatic potential can be expressed as:

$$C1(x, t=0) = C1_0(x) \qquad x \in (\Omega \bigcup \Gamma) \tag{H.34}$$

$$C2(x, t=0) = C2_0(x) \qquad x \in (\Omega \bigcup \Gamma) \tag{H.35}$$

$$\phi(x, t=0) = \phi_0(x) \qquad x \in (\Omega \bigcup \Gamma) \tag{H.36}$$

Boundary conditions can be generally classified into three types which are:

1) The first kind or Dirichlet's boundary condition on Γ_{C1}, Γ_{C2}, and Γ_{Φ}

$$C_1(x,t) = \overline{C_1}(x,t) \qquad x \in \Gamma_{C1} \tag{H.37}$$

$$C_2(x,t) = \overline{C_2}(x,t) \qquad x \in \Gamma_{C2} \tag{H.38}$$

$$\phi(x,t) = \bar{\phi}(x,t) \qquad x \in \Gamma_{\phi} \tag{H.39}$$

where $\overline{C_1}(x,t)$, $\overline{C_2}(x,t)$, and $\bar{\phi}(x,t)$ are prescribed values of first species, second species, and electrostatic potential on Γ_{C1}, Γ_{C2}, and Γ_{Φ}, respectively.

2) The second kind or Neumann's boundary condition on Γ^q_{C1}, Γ^q_{C2}, and Γ^q_{Φ}

$$\left(D_1 \nabla C_1 + z_1 D_1 \left(\frac{F}{RT} \nabla \phi \right) C_1 + D_2 \nabla C_2 + z_2 D_2 \left(\frac{F}{RT} \nabla \phi \right) C_2 \right) \vec{n} = \overline{q_{C1}}(x,t) \qquad x \in \Gamma^q_{C1} \tag{H.40}$$

$$\left(D_1 \nabla C_1 + z_1 D_1 \left(\frac{F}{RT} \nabla \phi \right) C_1 + D_2 \nabla C_2 + z_2 D_2 \left(\frac{F}{RT} \nabla \phi \right) C_2 \right) \vec{n} = \overline{q_{C2}}(x,t) \qquad x \in \Gamma^q_{C2} \tag{H.41}$$

$$\left(D_1 \nabla C_1 + z_1 D_1 \left(\frac{F}{RT} \nabla \phi \right) C_1 + D_2 \nabla C_2 + z_2 D_2 \left(\frac{F}{RT} \nabla \phi \right) C_2 \right) \vec{n} = \overline{q_{\phi}}(x,t) \qquad x \in \Gamma^q_{\phi} \tag{H.42}$$

in which $\overline{q_{C1}}(x,t)$, $\overline{q_{C2}}(x,t)$, and $\overline{q_{\phi}}(x,t)$ are boundary fluxes of first species, second species, and electrostatic potential, respectively. $\vec{n}$ is the unit normal vector pointing outward from boundary.

3) The third kind or Cauchy's (mixed) boundary condition on Γ^{c}_{C1}, Γ^{c}_{C2}, and Γ^{c}_{Φ}:

$$\left(D_1\nabla C_1 + z_1 D_1\left(\frac{F}{RT}\nabla\phi\right)C_1 + D_2\nabla C_2 + z_2 D_2\left(\frac{F}{RT}\nabla\phi\right)C_2\right)\vec{n} = \beta_{C1}(C_1(x,t) - C_{1_\infty}) \quad x \in \Gamma^{c}_{C1} \qquad \text{(H.43)}$$

$$\left(D_1\nabla C_1 + z_1 D_1\left(\frac{F}{RT}\nabla\phi\right)C_1 + D_2\nabla C_2 + z_2 D_2\left(\frac{F}{RT}\nabla\phi\right)C_2\right)\vec{n} = \beta_{C2}(C_2(x,t) - C_{2_\infty}) \quad x \in \Gamma^{c}_{C2} \qquad \text{(H.44)}$$

$$\left(D_1\nabla C_1 + z_1 D_1\left(\frac{F}{RT}\nabla\phi\right)C_1 + D_2\nabla C_2 + z_2 D_2\left(\frac{F}{RT}\nabla\phi\right)C_2\right)\vec{n} = \beta_{\phi}(\phi(x,t) - \phi_\infty) \quad x \in \Gamma^{c}_{\phi} \qquad \text{(H.45)}$$

where β_{C1} , β_{C2} , β_{ϕ} are the convective coefficient of first species, second species, and electrostatic potential, respectively; and C_{1_∞} , C_{2_∞} , and ϕ_∞ are the environmental concentration of first species, second species, and electrostatic potential, respectively.

The union of Γ_{Ci}, Γ^{q}_{Ci}, and Γ^{c}_{Ci} forms a complete boundary for each species; and the union of Γ_{Φ}, Γ^{q}_{Φ}, and Γ^{c}_{Φ} forms a complete boundary for electrostatic potential where index i represents for *i-th* species.